

Spring 5-22-2015

Investigations of Thioether Generation for S-D-Ribosyl-L-homocysteine Synthesis

Brendan Corcoran
brendanjcorcoran.1@gmail.com

Follow this and additional works at: <https://repository.usfca.edu/thes>

 Part of the [Organic Chemistry Commons](#)

Recommended Citation

Corcoran, Brendan, "Investigations of Thioether Generation for S-D-Ribosyl-L-homocysteine Synthesis" (2015). *Master's Theses*. 268.
<https://repository.usfca.edu/thes/268>

This Thesis is brought to you for free and open access by the Theses, Dissertations, Capstones and Projects at USF Scholarship: a digital repository @ Gleeson Library | Geschke Center. It has been accepted for inclusion in Master's Theses by an authorized administrator of USF Scholarship: a digital repository @ Gleeson Library | Geschke Center. For more information, please contact repository@usfca.edu.

Investigations of Thioether Generation for *S*-D-Ribosyl-L-homocysteine Synthesis

A Thesis Presented to the Faculty of the Department of Chemistry at the University of San Francisco in
Partial Fulfillment of the Requirements for the Degree of Master of Science in Chemistry

Written by

Brendan J. Corcoran

Bachelor of Arts

Saint Mary's University of Minnesota

May 2007

Investigations of Thioether Generation for *S*-D-Ribosyl-L-homocysteine Synthesis

Thesis written by Brendan Corcoran

This thesis is written under the guidance of the Faculty Advisory Committee, and approved by all its members, and has been accepted in partial fulfillment of the requirements for the degree of

**Master of Science in Chemistry
at the University of San Francisco**

Thesis Committee

Megan Bolitho, Ph.D.
Research Advisor

Claire Castro, Ph.D.
Professor of Chemistry

Janet Yang, Ph.D.
Assistant Professor of Chemistry

Marcelo Camperi, Ph.D.
Dean, College of Arts and Sciences

Acknowledgements

I had a wonderful advisor in Megan Bolitho. I would like to thank her for helping me shake off the rust and for patiently polishing me into a chemist. I appreciate the guidance, conversation, and intellect she shared with me on a daily basis.

Many thanks to the University of San Francisco faculty development fund and chemistry department for their support and to the members of the chemistry department community. My special appreciation to Deidre Shymanski, Angela Qin, and my fellow student researchers for all of their help and friendship. Thank you to Chad Schwietert for endless stimulating conversation and assistance. Thank you to Andy Huang for his enthusiastic teaching of the things you can't find in the textbooks. Thank you to Emily Showell-Rouse for her mentorship, continued discussions, and clear interruptions when I was about to make irreversible mistakes.

My sincere gratitude to the members of my thesis committee. Claire Castro and Janet Yang provided great insights for this thesis and much encouragement throughout my graduate research. I thank them for their time and support.

Thank you to those who shaped my love for chemistry: my godfather Dean Schrandt, my mentors Jim Vogel and Brett Bodsgard, and my family.

Unending love and appreciation to my lovely wife Amanda. She encourages, supports, and loves me in an unconditional way.

Table of Contents

Chapter 1. Targeting Bacterial Quorum Sensing as an Anti-Infective Strategy	1
1.1 Autoinducer-2 and System Two QS	3
1.1.1 Biosynthesis, Detection, and Function of AI-2 <i>in vivo</i>	5
1.1.1.1 Discerning a Target Option in System Two QS	6
1.1.1.2 Molecular Role of AI-2 <i>in vivo</i>	7
1.1.2 Targeting and Suppressing System Two QS	8
1.2 Competitive Inhibition of LuxS Using SRH Analogues	9
1.2.1 The LuxS Mechanism	9
1.2.2 Ellman's Bioassay for LuxS Activity	11
1.3 Chemical Synthesis of SRH	12
1.3.1 Routes to Thioether Generation	12
1.3.2 Groundwork SRH Thioether Generation by Bimolecular Nucleophilic Substitution	15
1.3.3 Radical Generation of Thioethers	18
1.4 Project Summary	19
Chapter 2. Preparation of the SRH Thioether by Bimolecular Nucleophilic Substitution	21
2.1 Previously Reported Generation of SRH-Related Thioethers by S _N 2	21
2.1.1 Previously Reported SRH Generation	23
2.1.2 Previously Reported SRH Analogues	23
2.2 General Features of the Bimolecular Nucleophilic Substitution Mechanism	24
2.3 New S _N 2 Conditions for Preparing the SRH Thioether	25
2.3.1 S _N 2 Retrosynthesis "A": Nucleophilic Homocysteine	27
2.3.1.1 Reaction Condition Selection: Base and Solvent	27
2.3.1.2 Electrophile Screen for Efficient Coupling	28
2.3.1.3 Protecting Group Strategy	32

2.3.1.4 Summary of SRH Thioether Generation by S _N 2 Approach “A”	33
2.3.2 S _N 2 Retrosynthesis “B”: Nucleophilic Thioribose	34
2.3.2.1 Preparation of Amino Acid Derived Electrophile	35
2.3.2.2 Nucleophilic Thioribose Preparation	36
2.4 Summary, Conclusions, and Future Directions of S _N 2 Thioether Generation	37
Chapter 3: Preparation of the SRH Thioether Bond by Thiol-Ene Coupling	39
3.1 Previously-Reported TEC Preparations of Thioether Bonds in Small Biomolecules	39
3.2 General Features of the TEC Mechanism	41
3.2.1 Conditions Used in TEC Reactions	42
3.2.1.1 Reaction Effects from the Alkene Substituent	42
3.2.1.2 Reactivity of the Thiol Substituent	43
3.3 Identification of TEC Strategies for Preparation of the SRH Thioether	43
3.4 TEC Retrosynthesis “A”: Carbohydrate as the Alkene Substituent	45
3.4.1 Generation of the Erythrofuranoside Olefin	45
3.4.2 TEC Strategy “A” for the Synthesis of SRH	46
3.4.2.1 Definitive Identification of Major Product as the SRH-like Diastereomer	47
3.4.2.2 Three Dimensional Modeling of SRH Diastereomers	50
3.4.3 Summary of TEC Coupling Strategy “A”	52
3.5 TEC Retrosynthesis “B”: Vinylglycine as the Alkene Substituent	52
3.5.1 Preparation of Vinyl Glycine by Grieco Elimination	53
3.5.2 Preparation of D-Thioribose Derivative	55
3.5.3 Formal Synthesis of SRH by TEC	55
3.6 Summary and Future Directions	57
3.6.1 Proposed Synthesis for an Alkylated Vinyl Glycine Suitable for TEC Coupling	58

3.6.2 Proposed Synthesis for an Alkylated Homoserine Derivative for S _N 2 Coupling	59
3.6.3. Additional LuxS Inhibition Targets	60
Experimental	61
References	77
Supporting Information	83

Abstract

Creation of the thioether linkage is a fundamental step for the chemical preparation of the bacterial quorum sensing molecule *S*-D-ribosyl-L-homocysteine (SRH). Although previous preparations of SRH and its analogues have been reported in the literature, they employ assorted methods with varied results. Therefore, a reassessment of the methodology used for synthetic preparation of the thioether bond in SRH-like molecules is here considered. This work examines four methods of thioether generation following two mechanisms, bimolecular nucleophilic substitution (S_N2) and radical-initiated thiol-ene coupling, in an attempt to generate SRH in a more efficient and reproducible manner. Both mechanisms address key objectives for SRH preparation: consistent production of the target compound in an analytically pure form, synthesis from easily obtained commodity materials, and improved understanding of each variable involved in creating the thioether bond in this molecule. One application of the thiol-ene coupling reaction generates the SRH thioether at a trial scale with a much-improved yield (93% over 70%) when compared to the most successful reported method to date. Other observations include improved understanding of steric effects involved in both mechanisms, optimization of conditions, assessment of electrophile choice, and the synthesis of a diastereomer of SRH, which may be considered for use in competitive inhibition assays.

Chapter 1. Targeting Bacterial Quorum Sensing as an Anti-Infective Strategy

Antibiotic resistance is a major health issue worldwide. Certain strains of bacteria are no longer responding to long-used treatments, and infections that were once easily cured are becoming difficult to manage. The Infectious Diseases Society of America reports that bacterial evolution against conventional therapies is far outpacing the rate of new drug development.¹ Meanwhile, an estimated two million infections developed annually in the United States are caused by antibiotic-resistant pathogens, resulting in at least 23,000 deaths each year.² The most well-known representation of this health crisis may be the emergence of methicillin-resistant *Staphylococcus aureus* (commonly known as MRSA). During the mid-1900's, *S. aureus* began to develop resistance to penicillin and other related β -lactam antibiotics. Evolving over time, some more recent strains have begun to show resistance to even some of the “last resort” therapies such as vancomycin.³

While bacteria adapt in order to defend themselves against conventional antibiotic treatments, the scientific community continues to explore new molecular pathways as avenues to treat infections. Bacterial quorum sensing (QS) is one enticing target option. QS is a molecular signaling system in which bacteria secrete small organic molecules called autoinducers (AI's) into their environment. When a microbial population grows sufficiently large, the resulting concentration of secreted AI's surpasses a threshold value that is correlated to an optimal cell density (Figure 1). Once that signal threshold level is achieved, each individual member of the community of bacteria is able to detect the AI, resulting in the collective regulation of gene expression that enables the colony members to behave in concert.⁴⁻⁶

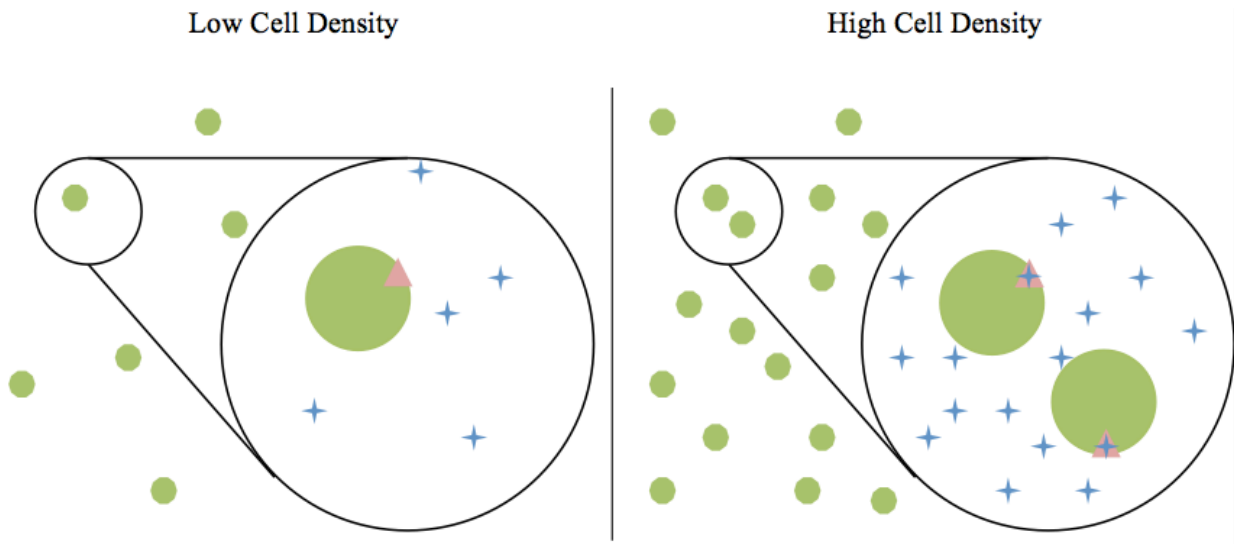


Figure 1. Bacterial AI biosynthesis and quorum sensing AI's (blue crosses) are biosynthesized and secreted by bacteria (green circles) into the surrounding environment. After a certain concentration of AI's has accumulated in proportion to cell density, a receptor (pink triangles) located at the surface (depicted above, i.e., LuxN, LsrB) or within the cytoplasm (not depicted, i.e., LuxR) of each bacterium is able to detect the AI's. In QS-active species, this detection triggers a regulation in gene expression and associated behavioral changes throughout the colony.⁷

Both Gram-negative and Gram-positive species utilize AI's for QS, and various bacterial behaviors have been tied to AI-regulated activity. While some bacteria use QS circuits for benign behaviors such as bioluminescence, others commonly regulate virulence factor expression. Table 1 lists a selection of QS-regulated traits observed across the bacterial kingdom.

Table 1. Behaviors associated with QS in Gram-positive and Gram-negative species

Organism	Gram Identity	Regulated Behavior ⁷
<i>Bacillus thuringiensis</i>	Positive	Sporulation ⁸
<i>Enterococcus faecalis</i>	Positive	Conjugation & Adhesion ⁹
<i>Escherichia coli</i>	Negative	Motility & Acid Resistance ¹⁰
<i>Pantoea stewartii</i>	Negative	Adhesion ¹¹
<i>Salmonella Typhimurium</i>	Negative	Virulence & Motility ¹²
<i>Staphylococcus aureus</i>	Positive	Exotoxins & Biofilm ¹³
<i>Streptococcus pneumoniae</i>	Positive	Competence ¹⁴
<i>Vibrio cholerae</i>	Negative	Biofilm & Virulence ¹⁵
<i>Vibrio harveyi</i>	Negative	Bioluminescence ¹⁶

Targeting QS as a new anti-infective strategy against associated virulent behaviors is attractive particularly due to its potential for the development of a new class of non-lethal antibiotics. Upon blocking the QS signal, it is reasonable to predict that the expression of virulent traits may be disrupted without actually killing the bacteria, as QS-regulated behaviors are not generally critical to survival.⁷ This non-lethal approach to treatment could subdue infection without “selecting for” chemically resistant strains that possess an incentive to evolve antibiotic resistant traits.¹⁷ In fact, development of resistance to an anti-cooperative treatment (i.e., resisting the prevention of activity induced by QS) could actually prove disadvantageous to a bacterium expending its resources in an otherwise competitive environment.¹⁸

1.1 Autoinducer-2 and System Two QS

While many AI's are species-specific (i.e., operate among only one species of bacteria), the system two QS signaling molecule, autoinducer-2 (AI-2), facilitates interspecies cell-to-cell communication.¹⁹

Hundreds of publications have reviewed and studied system two signaling, and behaviors in dozens of bacterial species (several of which are virulent) have been attributed to AI-2 induction.²⁰ For this reason, it is believed that system two QS could act as something of a broad spectrum target for a potential therapy. It is worth noting that AI-2 has been shown to operate in concurrence with other factors to regulate behavior changes, suggesting that targeting AI-2 alone may not eliminate a particular phenotype. For example, *Vibrio harveyi* requires three individual signaling molecules, AI-2, CAI-1, and HAI-1, to act synergistically in order to elicit its maximum bioluminescence response.²¹ A list of representative behaviors affected by AI-2 activated gene expression is summarized in Table 2.^{5,7,20}

Table 2. Selected traits affected by AI-2 regulated gene expression

Bacterial Species	Phenotype Affected by AI-2 ^{5,20}
<i>Actinobacillus pleuropneumoniae</i>	Formation of Biofilm, Adhesion ²²
<i>Borrelia burgdorferi</i>	Lipoprotein Expression ²³
<i>Clostridium perfringens</i>	Toxin Production ²⁴
<i>Escherichia coli</i> (EHEC)	Motility, Toxic Protein Production, Attachment ²⁵
<i>Helicobacter pylori</i>	Motility ²⁶
<i>Pseudomonas aeruginosa</i>	Virulence Factor Expression ²⁷
<i>Salmonella enterica</i> Typhimurium	Virulence Factor Expression ²⁸
<i>Staphylococcus aureus</i>	Capsule Structure ²⁹
<i>Streptococcus intermedius</i>	Biofilm Production, Antibiotic Susceptibility ³⁰
<i>Vibrio cholerae</i>	Biofilm Production, Virulence factors, Competence ³¹

Development of an anti-infective treatment directed at a particular component involved in the AI-2 circuit could proceed in a number of ways. Targets include cellular factors involved in the synthesis or the detection of the QS signal. The following section provides a brief overview of the production and activity of AI-2.

1.1.1 Biosynthesis, Detection, and Function of AI-2 *in vivo*

AI-2 is biosynthesized *in vivo* (Figure 2A) as a catabolite within a variation of the activated methyl cycle (AMC) that is specific to bacteria. Universally, demethylation of the methyl donor *S*-adenosylmethionine (SAM) results in the production of the toxic intermediate *S*-adenosylhomocysteine (SAH).^{19,20} Eukaryotes and some bacteria then break down SAH in a single step using the enzyme SAH hydrolase. This enzyme cleaves SAH into adenosine (Ado) and L-homocysteine (L-HCys), which can then be reused as cellular metabolites.⁵

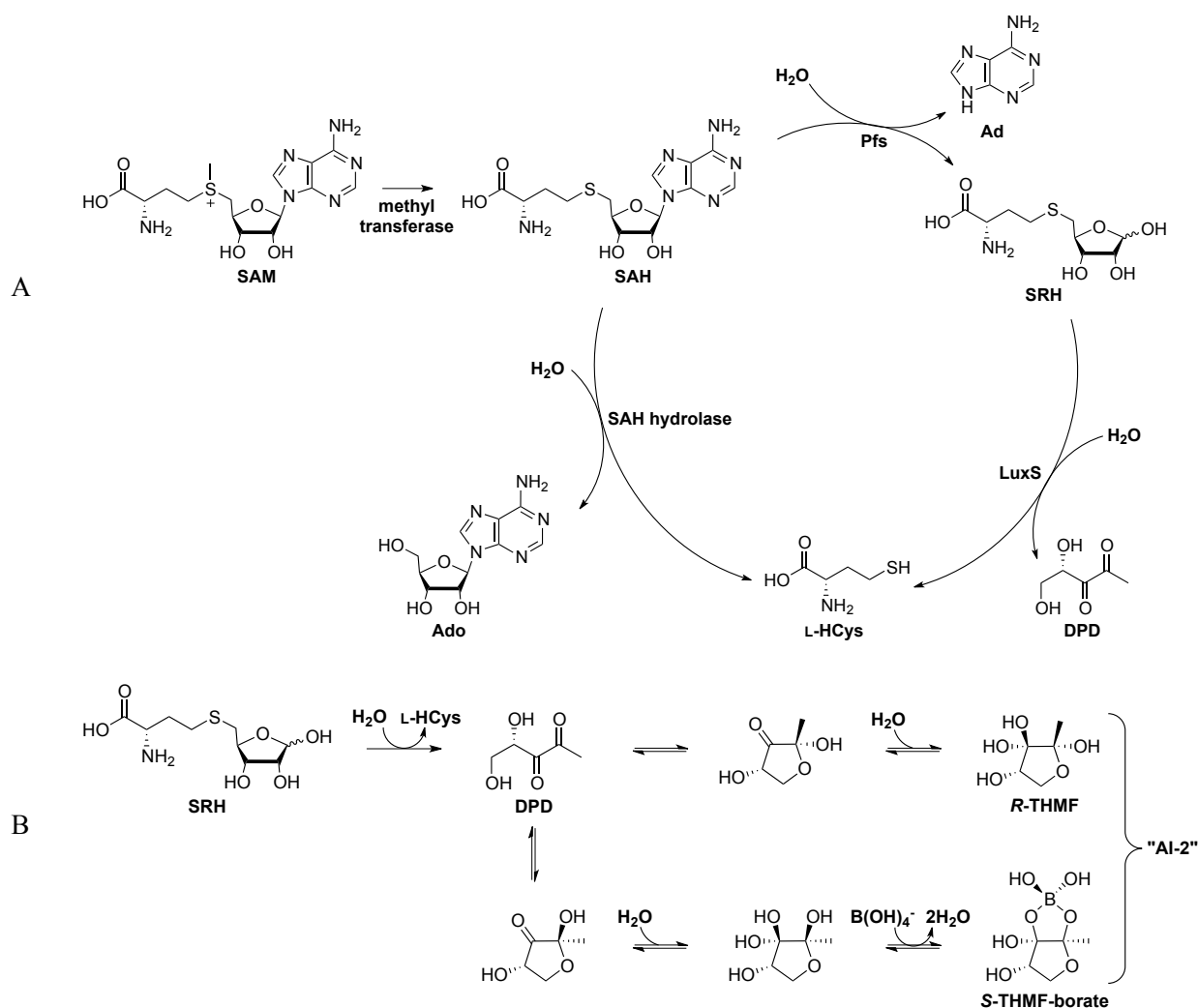


Figure 2. Biosynthetic production of AI-2 (A) Detoxification pathway of the AMC proceeds in one of two variations. The two step pathway using the enzymes Pfs and LuxS results in the formation of DPD. (B) An unstable molecule, DPD spontaneously cyclizes in aqueous solution. To date, two signaling molecules, *R*-THMF and *S*-THMF-borate, have been identified as AI-2 forms detectable by bacteria.^{32,33}

Other bacteria detoxify SAH in two steps: First, SAH is hydrolyzed by the Pfs enzyme, producing adenine (Ad) and *S*-D-ribosyl-L-homocysteine (SRH). In a second step, SRH is further catabolized by the enzyme *S*-ribosylhomocysteinase (LuxS) into L-HCys and 4(*S*),5-dihydroxy-2,3-pentanedione (DPD). DPD is an unstable compound that spontaneously cyclizes in aqueous environments, resulting in a set of equilibrating chemical species that exist collectively as “AI-2” (Figure 2B).^{5,20}

1.1.1.1 Discerning a Target Option in System Two QS

The *luxS* gene has been identified in over half of known genomes across the bacterial kingdom.³⁴ Within bacteria, the LuxS enzyme universally generates DPD from SRH (Figure 2B). The equilibrating nature of AI-2 allows various species of bacteria to sense the same chemical signal, despite the expression of different AI-2 receptor proteins.²⁰ To date, two conformations of AI-2 have been isolated which bind different AI-2 receptors. Chen et al. found that the species *Vibrio harveyi* binds a borate-containing form of AI-2 called *S*-THMF-borate (Figure 2B) using the receptor LuxP.³² Miller et al. later identified the receptor LsrB in *S. Typhimurium*, and characterized the bound conformation of AI-2 as *R*-THMF (Figure 2B).³³ Considering this example of two AI-2-detecting species with differences in both their receptors and the AI-2 conformation they are able to detect, the observation that the AI-2 biosynthesized by *S. Typhimurium* invoked QS-regulated behavior changes in *V. harveyi* is indicative of the conformational dynamism of DPD in biological systems. When a strain of *V. harveyi* deficient in the ability to produce endogenous AI-2 was treated with *in vitro* synthesized DPD, endogenously-produced LuxP ligand, or endogenously-produced LsrB ligand, each trial demonstrated a quantified bioluminescence response to all treatments (also dependent on the boron equilibrium). This dynamic equilibrium between DPD, *R*-THMF, and *S*-THMF-borate³³ indicates that targeting LuxS could lead to the development of a single inhibitor with the ability to slow or stop the production of AI-2 in many bacteria, broadly treating infections induced by a number of species without the need for multiple receptor-specific therapies.

1.1.1.2 Molecular Role of AI-2 *in vivo*

There has been some debate over whether AI-2 is an important QS signal or simply a byproduct of the essential SAH detoxification mechanism.²⁰ The ideas and evidence surrounding this debate are vast and complex. A selection of interesting arguments is summarized below:

- One hypothesis suggests that, in certain cases, a phenotype resembling a gene-activated behavior change could arise as the result of a defective metabolic route. This idea has been countered in a number of cases by restoring function in mutants lacking the ability to produce AI-2 by complementing the mutation with the introduction of chemically-prepared DPD.⁵
- The presence of AI-2 can be viewed as a marker for “fitness of population,” non-coincidentally produced when bacterial populations would most benefit from collective gene regulation. Increased methylation is correlated with cellular growth occurring in the log phase, and microbial populations are often successful when behavioral changes occur within a thriving population.^{5,20}
- Some bacteria (e.g., *P. aeruginosa*) degrade or uptake AI-2 as a possible carbon source, but this behavior has also been suggested as a means of depleting the communal AI-2 signal for the benefit of a particular species’ advantage in colonization.³⁵ Even as a metabolic byproduct, the presence of AI-2 could serve as a signal to other species benefiting somehow from the makeup of a complex bacterial community.⁵
- Another interesting question regarding the signaling nature of AI-2 is the rationale behind the evolution of the two-step detoxification mechanism. If SAH is easily detoxified in one step by SAH hydrolase, is there a significance to the evolution of a two-step sequence for another purpose (i.e., signaling), or is this process genetically conserved simply because of its involvement in the AMC?^{5,36}
- LuxS is not essential to survival, but there could be an unknown benefit for use of AI-2 as a metabolite, such as for the biosynthesis of sulfur-containing amino acids.³⁶

The fact that SAM is also a precursor to other types of species-specific AI's suggests there is some relationship between the AMC and QS.^{5,20} Nevertheless, while the function of AI-2 has not been universally made clear, evidence does suggest that in many circumstances AI-2 is an important factor in QS-regulated gene expression.

1.1.2 Targeting and Suppressing System Two QS

There are several intriguing facts about system two QS and its suitability as an anti-infective target. Namely, it is important for the coordination of certain virulent behaviors (Table 2). AI-2 is utilized by a significant number of bacterial species (including Gram-negative and Gram-positive pathogens), and the absence of LuxS in eukaryotes could enable it to be targeted without affecting regular cellular function in humans and other species.⁷ These features make system two QS a worthy subject for drug development research.

To this end, studies blocking AI-2 detection or using null mutant *luxS* strains have shown some interesting results regarding bacterial response to antibiotic treatments. For example, an increase in susceptibility to conventional antibiotics in *luxS* mutants was demonstrated by Nibras et al.³⁷ In these studies, *Streptococcus anginosus luxS* mutants showed increased susceptibility to two common antibiotics (erythromycin and ampicillin) when compared to a wild-type strain. Furthermore, when QS was complemented in the same *S. anginosus luxS* mutant by the addition of wild-type supernatant (presumably containing AI-2) or by the addition of DPD, susceptibility to both antibiotics decreased. This indicated that QS-based therapies may also be useful in weakening virulent populations to a level at which existing antibiotics may prove more effective.

This same trend of using a QS signaling prevention therapy in conjunction with a bactericidal treatment was demonstrated using DPD analogues to treat biofilms in combination with the antibiotic gentamicin. Here, although *E. coli* and *P. aeruginosa* biofilm formation were both diminished with treatment of an

inhibitory DPD analogue alone, preexisting biofilms exposed to a therapeutic combination of both the DPD analogue and gentamicin deteriorated more effectively than when treated with the antibiotic alone.³⁸ Additionally, these results were acquired using gentamicin in amounts similar to the minimal inhibitory concentration required for treatment of these species in the “planktonic” free swimming form rather than the increased dosage necessary when treating biofilms. This suggests an anti-QS treatment could improve susceptibility to antibiotics while also decreasing the concentration of antibiotic required to treat infection, addressing an issue around dosage which can be simultaneously detrimental to non-virulent microflora.³⁹

1.2 Competitive Inhibition of LuxS Using SRH Analogues

Past research targeting the LuxS enzyme has resulted in the development of a number of SRH analogues.⁴⁰⁻⁴⁴ In modifying the LuxS substrate, SRH, the objective is to create a competitive inhibitor with the ability to bind the LuxS active site and significantly slow AI-2 production from endogenous SRH.⁴⁰ Such SRH analogues can be strategically designed to impact a particular aspect of LuxS catabolic activity, since the mechanistic action of the enzyme has been well-studied.

1.2.1 The LuxS Mechanism

The crystal structure of the LuxS enzyme has been determined by a number of groups.⁴⁵ The enzyme exists as a homodimer, with its pair of active sites utilizing residues from both peptide subunits. Pei’s group has elucidated a mechanism for SRH metabolism (Figure 3) guided by these crystal structures and by the identification of catalytically-competent intermediates.^{46,47} Catalysis by LuxS utilizes an iron (II) ion cofactor along with key amino acid residues E57 (α -subunit) and C84 (β -subunit). These components assist in the migration of the carbonyl group from the C-1 aldehyde to the C-3 position on the ribose moiety of the SRH open chain. Ultimately β -elimination cleaves the thioether to yield L-HCys and a DPD tautomer.^{46,48}

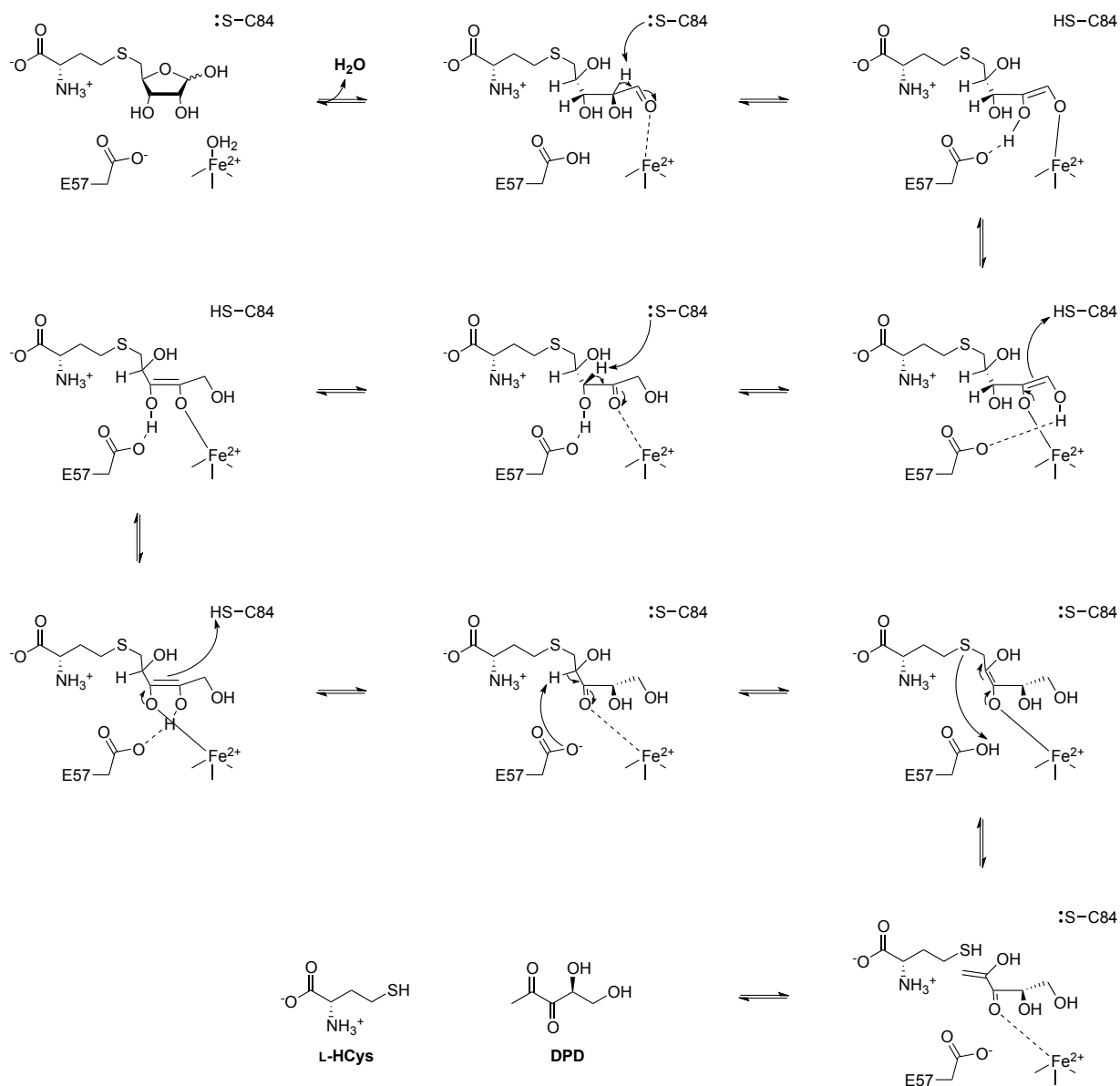


Figure 3. Catalytic mechanism of LuxS deduced by Pei and coworkers Within the active site of LuxS, an iron (II) ion (represented Fe²⁺) in conjunction with a glutamate residue at position 57 on the α -subunit (E57) and a cysteine at position 84 on the β -subunit (C84) assist in an eventual β -elimination whereby L-HCys and DPD are produced from SRH (adapted from Pei).⁴⁶

Because the ribose moiety of SRH undergoes many intramolecular conversions on the path to eventual β -elimination of L-HCys to produce DPD, many SRH analogues have been developed with modification about the carbohydrate moiety in efforts to prohibit this sequence of reactions.⁴⁰⁻⁴⁴ Presented in Figure 4 are some of the molecules developed with this objective. By removing or replacing key functional groups

on SRH, previously generated analogues were designed to directly affect the catalytic mechanism. These works have resulted in a number of SRH analogues possessing competitive inhibitory character, although in moderate concentrations.^{40-43,49}

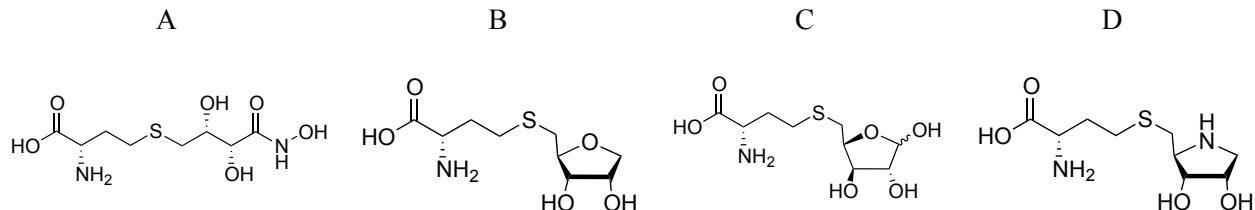


Figure 4. SRH analogues modified at the ribose moiety A selection of SRH analogues with alteration in the carbohydrate moiety. Each has demonstrated a degree of competitive inhibition of the LuxS active site.⁴⁰⁻⁴³

The most potent competitive inhibitor developed to date (Figure 4A) was reported by Shen, et al.⁴² When evaluated *in vitro* by an assay using *B. subtilis* LuxS, K_i values were reported in the submicromolar range when tested against SRH for both the Co(II) form of the enzyme ($K_i = 0.37 \pm 0.04 \mu\text{M}$) and with the native Fe(II) form ($K_i = 0.43 \pm 0.02 \mu\text{M}$).

1.2.2 Ellman's Bioassay for LuxS Activity

The Ellman's assay provides a method to quantify free thiols and has been applied to measure the activity of the LuxS enzyme *in vitro*. When LuxS cleaves the SRH thioether bond, DPD and L-HCys are released. The Ellman's assay uses 5,5'-dithiobis-(2-nitrobenzoic acid) (DTNB) to react with available thiols, in this case present on the liberated L-HCys. This reaction forms a stoichiometrically equivalent pigmented ion (NTB) quantifiable by colorimetric spectroscopy at 412 nm, which can be used to determine the equivalent concentration of AI-2 released by LuxS in the presence of SRH.⁵⁰

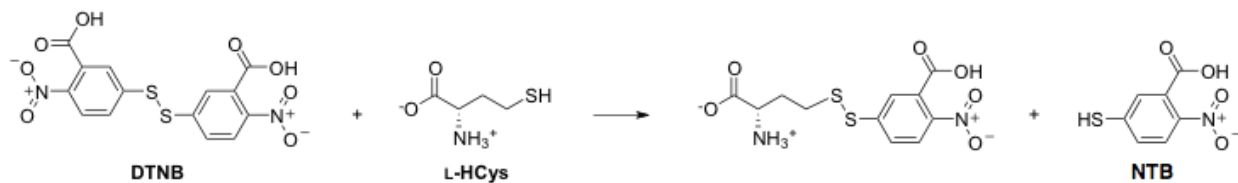


Figure 5. The Ellman's assay applied to LuxS Activity DTNB binds the thiol of L-HCys, releasing the measurable pigmented ion 2-nitro-5-thiobenzoate (NTB). This is stoichiometrically equivalent to the amount of DPD released from the activity of LuxS.⁵¹

This test may be also used to measure the ability of molecules to inhibit LuxS. An inhibitor may be introduced to the assay mixture, where it can compete with SRH for the enzyme and reduce the release of HCys and AI-2.⁴¹⁻⁴³ The result is a decreased absorbance at 412 nm.

1.3 Chemical Synthesis of SRH

The work performed for this thesis focuses on the need for a robust SRH synthesis. There are two desired outcomes within this goal. First, in order to screen LuxS activity and the inhibitory characteristics of SRH analogues *in vitro*, the Ellman's assay requires the use of significant quantities of SRH. Ideally, this SRH should be rigorously evaluated for purity and aliquotted exactly for reliable K_M (activity) and K_I (inhibition) determination. Thus, the desire to manufacture SRH in analytically pure, stable, and measureable form with the best possible yield and by a cost effective route was prioritized. Second, upon trials of various methods available for generating the SRH scaffold, in particular by creation of the central thioether bond, the complexity of the synthesis of SRH-like compounds might be better understood and applied to the thioether creation for future candidate LuxS analogues.

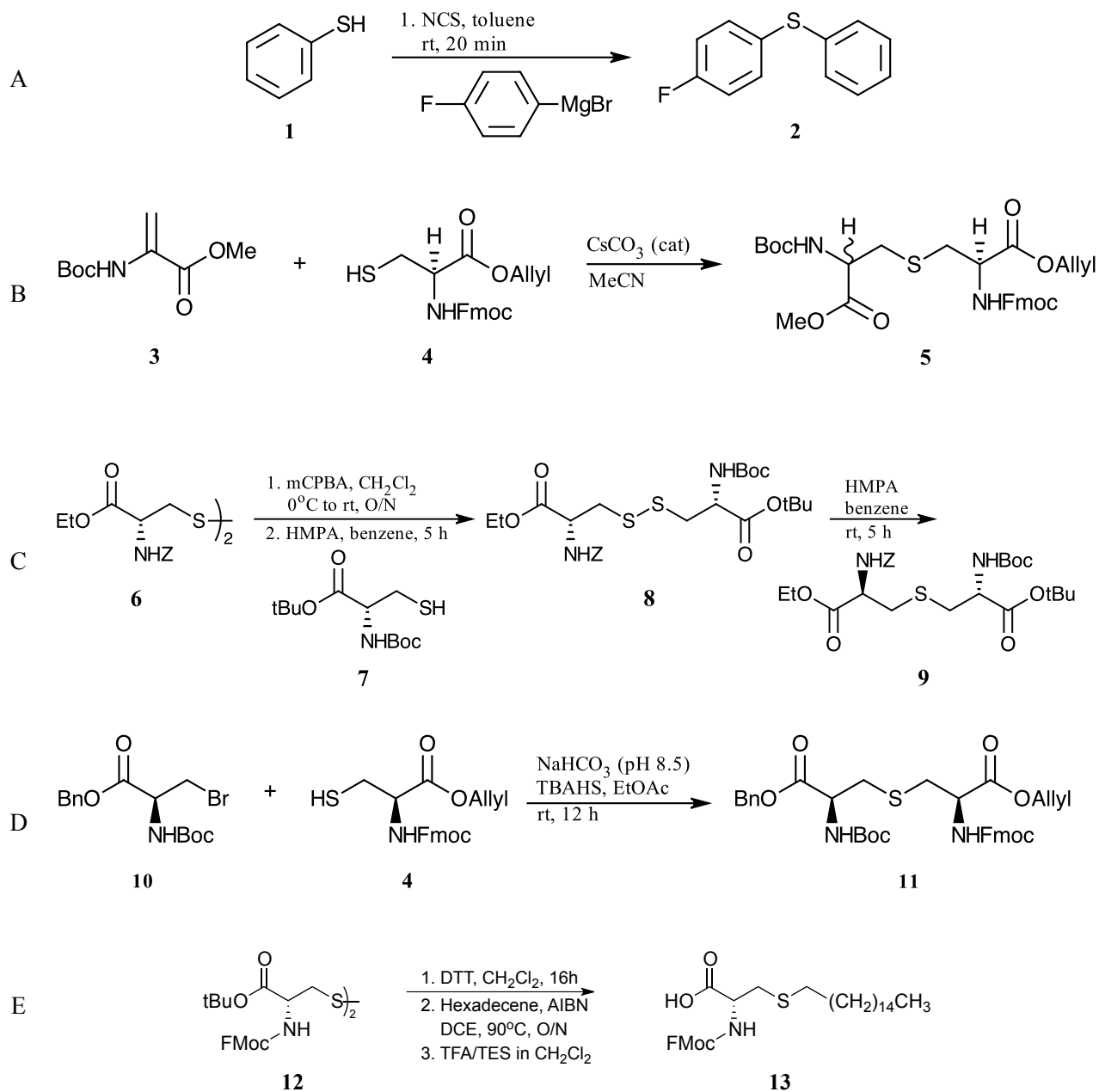
1.3.1 Routes to Thioether Generation

Past reports of the preparation of SRH and its analogues have employed a number of different strategies. At the core of each exists the challenge of producing the thioether carbon-sulfur bond with high efficiency. Consideration of C-S coupling from a biological perspective is possible, but is limited to a particular enzyme or specific amino acid residue to form thioether linkages in aqueous matrices. While SRH has been successfully produced enzymatically from SAH *in situ*, its final concentration can only be estimated by assuming quantitative conversion by the enzyme.^{43,50}

From a traditional synthetic perspective, a number of thioether-generating mechanisms are available; the challenge is identifying which can be applied successfully and with good yield for the preparation of SRH with limited competing reactions, byproducts, or undesired stereochemical outcomes. Additionally, some

mechanisms are demonstrated to be robust and yield good results, but they rely on functional groups that are impractical for our synthesis (i.e., thioether generation using aryl thiols). One such example, represented in Scheme 1A, is a one-pot reaction by Cheng et al. which is able to join thioether bonds using aryl thiols in a Grignard reaction in the presence of *N*-chlorosuccinimide (NCS).⁵²

Tabor reviewed multiple approaches used for generating thioethers between amino acids for lantibiotic development, and provided much insight around synthetic strategies for stereospecific targets requiring protection on amino and carboxylate groups.⁵³ In her review, examples of Michael addition approaches were demonstrated in good yield, but have resulted in non-stereospecific outcomes, such as the mixture of diastereomers, **5** (2:3 ratio), resulting from work by Bradley and coworkers⁵⁴ presented in Scheme 1B. Furthermore, methods using desulfurization of disulfides may yield target products, but result in poor yields due to reaction reversibility and would also narrow the options for the choice of protecting groups available. Olsen et al. used this method to create unsymmetrical lanthionines for lantibiotic research (Scheme 1C).⁵⁵ Tabor also reviewed S_N2 couplings, which have worked in applications to lantibiotic research, although many variables must be optimized for the specific reaction being performed. These include close monitoring of reaction sensitivity due to conditions, troubleshooting protecting group options, steric effects, and electrophile choice, all of which contribute to the level of success and potential for competing reactions.⁵³ Again citing lanthionine synthesis, Zhu and Schmidt used sodium bicarbonate as a base in a S_N2 reaction between starting components **10** and **4** to obtain a single stereoisomer of the desired product **11** (Scheme 1D).⁵⁶



Scheme 1. Sample applications of various mechanisms for thioether synthesis⁵²⁻⁵⁷ (A) An effective synthetic approach to thioether formation specific for use with aryl-thiols. Tabor reviewed the use of (B) Michael addition, (C) desulfurization of differential disulfides, and (D) nucleophilic substitution for thioether development applicable to lantibiotic research. (E) The thiol-ene coupling reaction may be applied to biological molecules demonstrated by Triola et al.

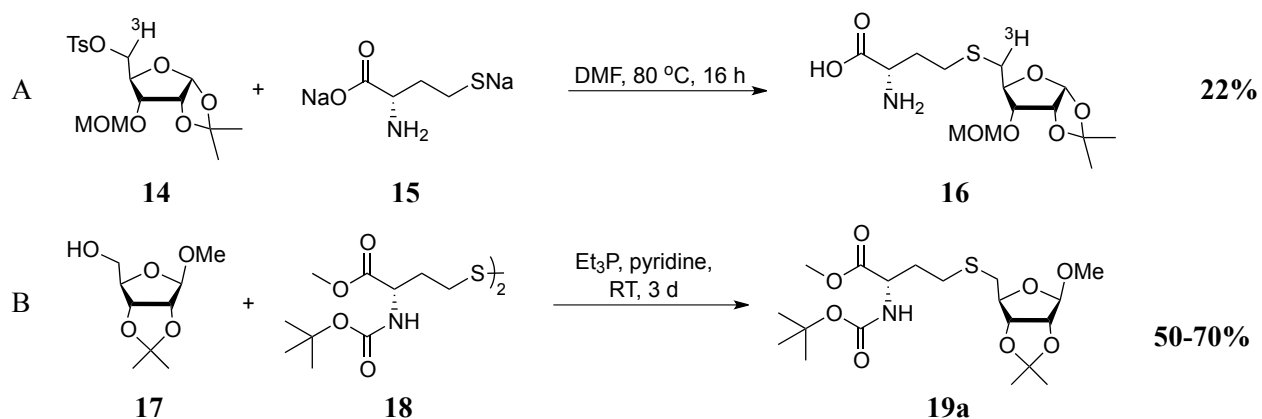
An adaptation of the previously mentioned Michael addition is the thiol-ene coupling reaction (TEC), which may be propagated by use of a radical mechanism. Like the Michael addition, these reactions may result in undesired stereochemistry, although they can be used under mild conditions with fast and good

yielding outcomes.⁵⁷ Among these examples is the report by Triola et al., who created cysteine derivatives (i.e., target molecule **13**) conjugated with *S*-linked alkyl groups utilizing 2,2'-azobis(2-methylpropionitrile) (AIBN) as the radical initiator (Scheme 1E).⁵⁷

While the previously listed mechanisms for thioether formation are not exhaustive (i.e., unmentioned organometallic reactions), two strategies were determined to be most suitable for SRH synthetic studies after consideration of reaction efficiency, necessary purification steps, cost, number of intermediates involved, and relationship to the existing groundwork research previously performed in our lab. This thesis follows the application of the bimolecular nucleophilic substitution (S_N2) and the thiol-ene coupling (TEC) reaction to SRH synthesis.

1.3.2 Groundwork SRH Thioether Generation by Bimolecular Nucleophilic Substitution

Acquisition of SRH by means of the S_N2 mechanism was first demonstrated in low yield by Guillerm and Allart (Scheme 2A).⁵⁸ A tritium-labeled SRH was created by heating tosyl-activated electrophile **14** in solution with thiolate nucleophile **15**, yielding protected derivative **16** in 22% yield. After acid deprotection of **16** (not shown) and subsequent lyophilization, the tritium-labeled SRH was isolated in 5% overall yield.



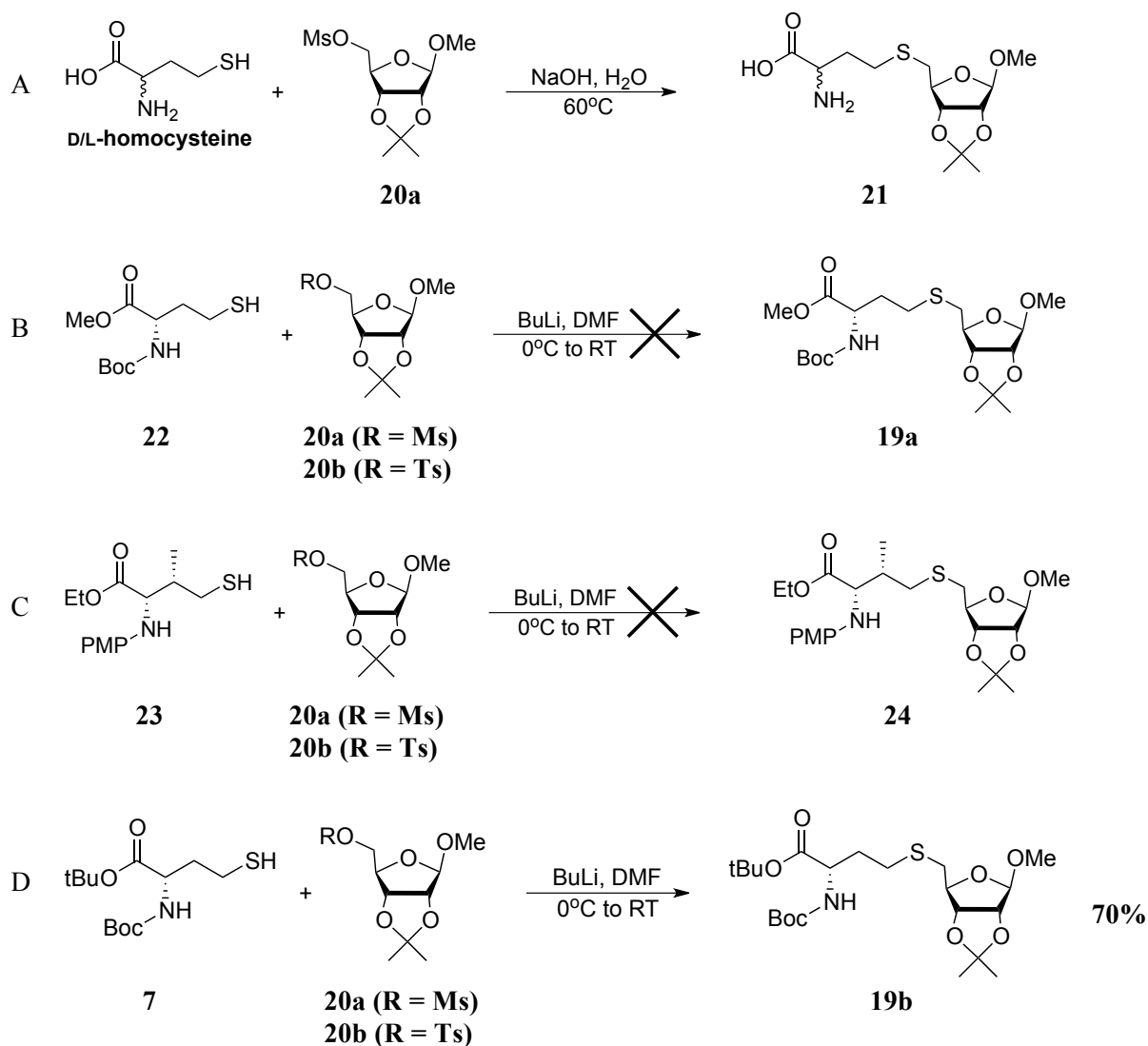
Scheme 2. Early SRH thioether generation^{58,59} (A) Tritium-labeled protected SRH **16** was synthesized by Guillerm and Allart (B) Mitsunobu-type synthesis of **19a** was demonstrated by Zhao et al.

Later Zhao et al. improved SRH synthesis by employing a Mitsunobu-type coupling reaction to create a protected SRH from starting components **17** and **18** (Scheme 2B).⁵⁹ The disulfide bond of the homocystine derivative **18** is reduced by triethylphosphine, generating a thiolate nucleophile *in situ* which reacts in the presence of pyridine in an S_N2-fashion with the protected ribose **17**. After flash column chromatography, the protected product **19a** was isolated with improved yield (50-70%) over Guillerm and Allart's coupling and later deprotected in two steps to a SRH·TFA salt (not shown).⁵⁹

Under trials performed in our lab, the Zhao strategy was both inconvenient in practice and inconsistent with the published results. Furthermore, it proceeds over many days, the progress of the reaction is not easily monitored due to apparent decomposition, and two steps are necessary to deprotect the SRH derivative **19a**. The reaction also uses an excess of **18** derived from the specialty chemical L,L-homocystine. For these reasons the motivation existed to develop a more straightforward synthesis of SRH that follows a more traditional S_N2 mechanism, uses more easily accessible starting materials, and has the ability to globally deprotect the new protected SRH molecule to high purity in a single step.

Initiating investigation into the desired improvement of SRH synthesis, former graduate student Ruoyi Liu performed work in our lab by adapting ideas from previously reported publications.⁶⁰ While attempting the Zhao method of C – S bond formation, decomposition was observed. After establishing that the disulfide was successfully cleaved by the phosphine reagent, it was suspected that the native unactivated 5'-hydroxyl group on the ribose derivative **17** might account for the poor nucleophilic coupling. Influenced by the work of Wnuk⁴¹ in the context of SRH analogue preparation, Liu proposed that introduction of a better leaving group would improve the coupling. After ascertaining that the introduction of the mesylate leaving group onto ribose component **20a** successfully promoted SRH synthesis using unprotected HCys under basic conditions (not quantified, Scheme 3A), attention was turned toward protecting groups for the amino acid. Although coupling proved successful without protecting groups present on the HCys moiety, the yield could not be quantified due to purification

problems resulting from the absence of HCys protection on product **21** and complications from byproduct contamination. Derivative **22** using methyl ester protection of the carboxyl group of HCys then failed to produce a coupled product under the alkaline reaction conditions used (Scheme 3B). This trend continued to be problematic when applied to SRH analogue production. Trials using the typical S_N2 strategy for the coupling of thiol **23** and sulfonates **20a** or **20b** (Scheme 3C) resulted in no reaction.⁶⁰ It was proposed that protecting group identities were significant contributors to the failure of these couplings.



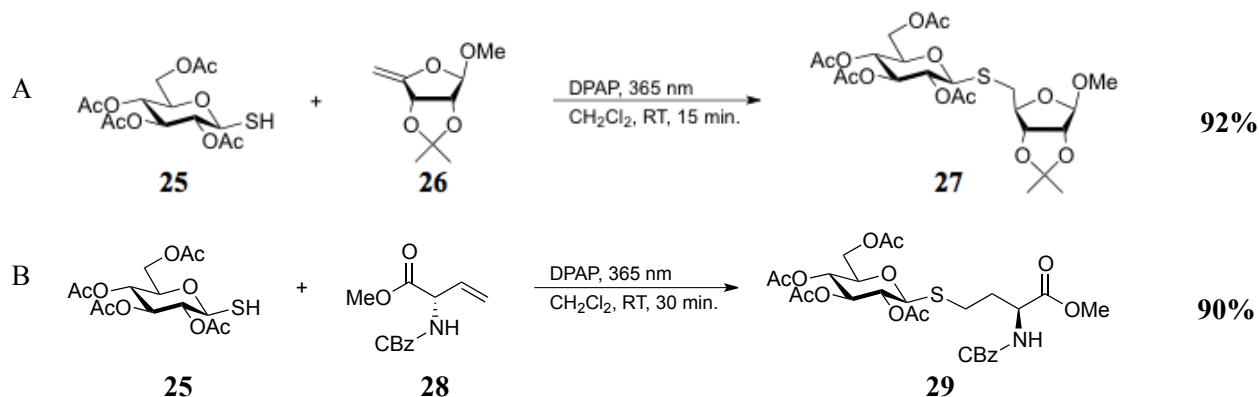
Scheme 3. Investigation into thioether coupling by S_N2 ⁶⁰ (A) Successful coupling was observed between unprotected HCys and an activated ribose derivative. Under alkaline conditions, amino acid protecting groups on the HCys moiety were suspected to impede the successful coupling in (B) protected SRH and (C) an SRH analogue. (D) Use of robust protecting groups under basic conditions resulted in successful production of protected SRH (up to 70%).

Utilizing the bulky *tert*-butyl carboxylate protecting group in conjunction with Boc carbamate protection on **7**, coupling with electrophiles **20a** or **20b**, Liu was able to successfully prepare the fully protected SRH **19b** by S_N2 in an alkaline environment in 70% yield (from **20b**) of the coupling reaction (Scheme 3D).⁶⁰

After these key observations were recorded, the focus of future research was directed to understanding the effect of each individual variable on this synthesis. Solvent and base identities, as well as equivalent reactant concentrations were strategically selected moving forward. Additionally, structural variables conducive to promoting successful coupling were also examined such as electrophile leaving group and amino acid protecting group identities.

1.3.3 Radical Generation of Thioethers

An alternate mechanism for formation of thioethers is the use of the intriguing radical-induced thiol-ene coupling (TEC) reaction. This “click” reaction couples thiol and olefin components together by a radical mechanism.⁶¹ Although they are more commonly used in polymer synthetic chemistry, examples of TEC-based couplings may also be used for application with biological molecules.⁶² Broadly setting the groundwork for our strategy, Dondoni’s group has used TEC to synthesize a number of compounds relevant to our research.⁶²⁻⁶⁴ In one of these reports by Fiore et al., erythrofuranoside derivative **26** was used in the joining of carbohydrates via *S*-glycoside bond formation with high efficiency using 2,2-dimethoxy-2-phenylacetophenone (DPAP) as the radical initiator (Scheme 4A).⁶³ In a later work, Fiore and coworkers also used DPAP to couple carbohydrates with amino acid residues, including examples resulting in the products containing HCys moieties (i.e., product **29**, Scheme 4B), mirroring SRH-type targets for development in our research.⁶⁴ These reports assisted in laying out a clear strategy for the development of an SRH synthesis that would be expedient and high-yielding, using the mild conditions of TEC.



Scheme 4. Applications of the TEC reaction to biological molecule synthesis^{63,64} Literature precedents have used radical-induced TEC reactions to create (A) *S*-linked alkyl cysteines (B) *S*-glycoside bonds, and (C) *S*-glycopeptides.

1.4 Project Summary

This project employs four routes to generation of the protected SRH thioether, visualized in the retrosynthetic breakdown to the necessary coupling components (Figure 6). Two possible approaches are outlined for each of the two mechanisms considered.

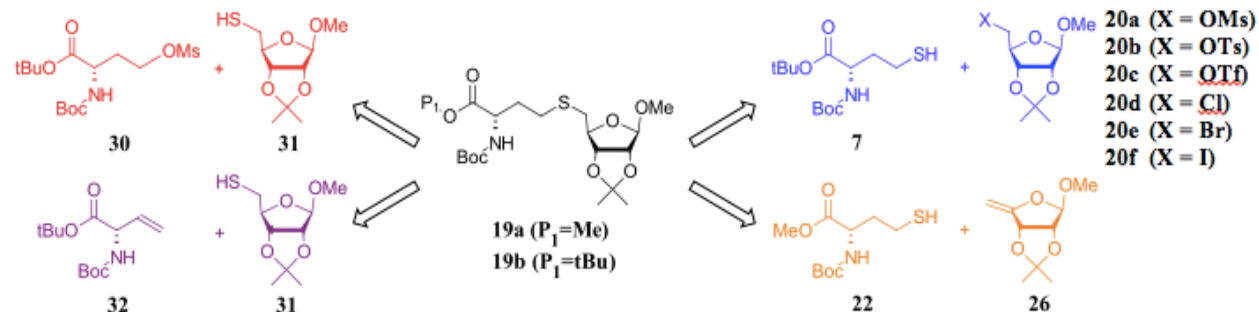


Figure 6. Retrosynthetic analysis of protected SRH Suggested disconnection of the thioether on either side of the sulfur atom leaves carbohydrate and amino acid components. Here two mechanisms are considered; S_N2 (red and blue) and TEC (purple and orange) mechanisms would generate the thioether in the forward direction.

Chapter 2 outlines the methods for the S_N2 reaction. After a set of conditions is optimized, the S_N2 is facilitated with the selection of an electrophile-bound leaving group used to react with a thiol-containing coupling partner. The thiol and leaving group functionalities are affixed to opposite partners to test the two S_N2 approaches (Figure 6, red and blue), and after reversing the nucleophile/electrophile roles, theoretic improvements to the S_N2 are assessed.

Navigation of the TEC mechanism for thioether generation is described in Chapter 3. Thiol- and alkene-equipped partners are joined after irradiation of a radical initiator. Again, functional group roles are reversed on the coupling components (Figure 6, purple and orange) and tested after investigation into the stereochemical outcomes of the TEC synthesis. Optimization considerations are then outlined for the TEC reaction and its application to SRH synthesis.

This thesis concludes with notes on efficient thioether generation for SRH synthesis and suggestions for further completion of this work. Based upon the information gleaned from the four approaches used in this research, future directions on preparation of some analogue options are also outlined, as well as suggestions for the possible methods that could be used to prepare those analogues.

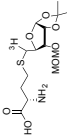
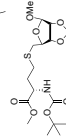
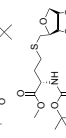
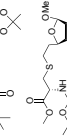
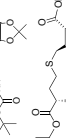
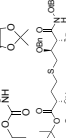
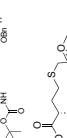
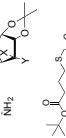
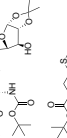
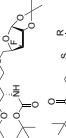
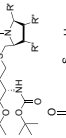
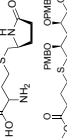
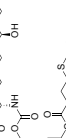
Chapter 2. Preparation of the SRH Thioether by Bimolecular Nucleophilic Substitution

The bimolecular nucleophilic substitution (S_N2) is a straightforward mechanism that can be adapted for many purposes. As outlined in Chapter 1, past use of the S_N2 has successfully generated the thioether bond in synthetically prepared SRH (and has similarly been utilized for thioether creation in several SRH analogues). As noted, however, many factors can influence the degree to which the S_N2 is successful. Previous reports in the literature that have employed S_N2 for SRH and analogue synthesis have used a number of different reaction conditions.⁴⁰⁻⁴⁴ In an effort to develop a focused route toward SRH synthesis by the S_N2 method, a selection of conditions based on theory was considered before optimization.

2.1 Previously Reported Generation of SRH-Related Thioethers by S_N2

SRH and many SRH-related thioethers have been synthesized by S_N2 with yields ranging from 22-92%.^{41-43,58,59} Reaction conditions have differed in choice of solvent (DMF,^{41-44,58} MeOH/water⁴¹), base identity (LDA,⁴¹⁻⁴³ BuLi,^{41,44} NaOH⁴¹), and reaction time (hours,^{41,43,44,58} days^{40-43,59}). Table 3 outlines past strategies for using S_N2 to prepare the thioether bond of SRH and analogues. Given the variations in approach, it was deemed prudent to consider from first principles the many factors involved for the application of this mechanism.

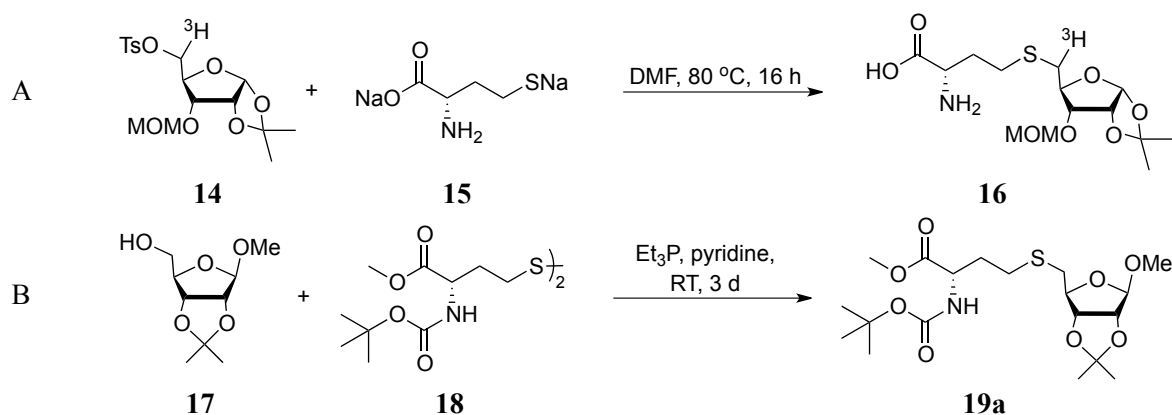
Table 3. Summary of reported preparations of the thioether bond in SRH and analogues^{40-44,58,59}

Entry	Authors	Compound/ Class	Amino Acid	Reaction Role	Carbohydrate	Reagent	Solvent	Time (h)	Temperature (°C)	Yield (%)
1	Guillerm & Allart		Nucleophile	Electrophile ^a	Electrophile ^a	N/A	DMF	16	80	22
2	Zhao et al.		Nucleophile	Electrophile ^a	Electrophile ^a	Et ₃ P	Pyridine	72	RT	50-70
3	Alfaro et al.		Nucleophile	Electrophile ^a	Electrophile ^a	Et ₃ P	Pyridine	72	RT	49
4	Alfaro et al.		Nucleophile	Electrophile ^a	Electrophile ^a	Et ₃ P	Pyridine	72	RT	34
5	Shen et al.		Nucleophile ^a	Electrophile	Electrophile	LDA	DMF	48	0 - RT	50
6	Shen et al.		Nucleophile ^a	Electrophile ^a	Electrophile	LDA	DMF	48	0 - RT	36
7	Wnuk et al.		Nucleophile	Electrophile ^a	Electrophile ^a	NaOH	H ₂ O MeOH	12	60	28-31
8	Wnuk et al.		Nucleophile	Electrophile ^a	Electrophile ^a	BuLi	DMF	4	0 - RT	67
9	Wnuk et al.		Nucleophile	Electrophile ^a	Electrophile ^a	LDA	DMF	28	0 - RT	92
10	Malladi et al.		Nucleophile	Electrophile ^a	Electrophile ^a	LDA	DMF	24 - 48	0 - RT	45 - 86
11	Malladi et al.		Nucleophile	Electrophile ^a	Electrophile ^a	NaH	DMF	12	0 - RT	75 ^c
12	Gopishetty et al.		Nucleophile	Electrophile ^a	Electrophile ^a	BuLi	DMF	4	0 - RT	80
13	Gopishetty et al.		Nucleophile	Electrophile ^a	Electrophile ^a	K ₂ CO ₃	Acetone	3 - 4	reflux	49 - 84

^a limiting reagent ^b three examples ^c racemic mixture ^d two examples

2.1.1 Previously Reported SRH Generation

As discussed in Chapter 1, two previous synthetic approaches have been reported for SRH. The Guillerm and Allart strategy (Scheme 5A) generated the partially protected tritium-labeled SRH **16** in low yield (22%) after heating the tritium-labeled tosylate **14** and unprotected cysteinyl starting components in DMF for 16 hours.⁵⁸ Later, Zhao used a Mitsunobu-inspired approach (Scheme 5B) to produce the protected SRH **19a** from the homocysteine thiolate generated *in situ* before reaction with the protected carbohydrate **17**.⁵⁹ While this method resulted in improved yields (50-70% reported), it did not provide a reliable synthesis in our hands.



Scheme 5. Previous synthesized protected SRH molecules^{58,59} (A) Guillerm and Allart generated a tritium-labeled SRH and (B) Zhao et al. used Mitsunobu-like coupling approach for SRH synthesis.

Additionally, the required excess of the nucleophile derived from specialty chemical L,L-homocysteine (HCySS), difficult reaction monitoring (in pyridine solvent), a long reaction time (3 d), required multistep deprotection, and the presence of the persistent, difficult to remove triethylphosphine oxide byproduct made this reaction undesirable for routine use.

2.1.2 Previously Reported SRH Analogues

Synthetic approaches towards SRH analogues have largely relied on either the aforementioned Mitsunobu-type coupling⁵⁹ or a traditional S_N2 reaction for thioether generation.⁴¹⁻⁴⁴ Nearly all of the approaches reported in the literature use excess nucleophile in combination with a base of varying strength.^{40,41,43,44,59} Among these syntheses, the variety of conditions indicate no particular pattern for the

most effective solvent, reaction time, base, or temperature. The moderate success of couplings by Wnuk, Malladi, and Gopishetty (all of the same research team; Table 3, Entries 8-12) suggest that some new combination using a non-nucleophilic base in a convenient solvent under controlled temperature might be explored for the development of a revised S_N2 approach.^{41,43,44} To facilitate a plan for investigation, some of the general features of the S_N2 were considered.

2.2 General Features of the Bimolecular Nucleophilic Substitution Mechanism

As a generic description of the mechanism (Figure 7), the S_N2 requires a lone pair of electrons on a nucleophilic species (Nu) to first attack the carbon adjacent (α) to a suitable leaving group. In a single step, the nucleophile attacks from the “back side,” opposite a leaving group, forming a new covalent bond as the existing bond between the carbon and the leaving group is simultaneously broken. This transition state is represented in central structure of Figure 7. As the leaving group is ejected, a new bond results between the original nucleophilic species and the carbon atom.⁶⁵

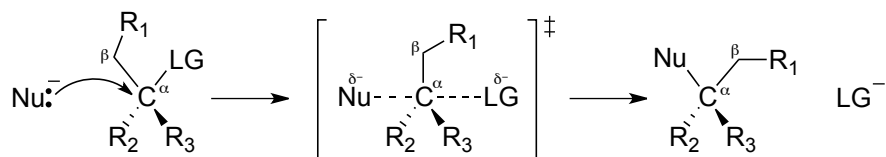


Figure 7. Generic S_N2 reaction between a negatively charged nucleophile and neutral electrophile⁶⁵
 The electrons on the nucleophile (Nu) attack the “back side” of the carbon α to the leaving group (LG). A new covalent bond is formed in the transition state as the existing bond to the leaving group is broken. In this example, the negative charge is dispersed through the transition state, and is better solvated than the nucleophile by aprotic, less polar solvents.

Several factors contribute to both the efficacy and the rate of this reaction. The size of the nucleophilic atom and, if present, the formal charge on that atom are important variables contributing to nucleophilic strength. For example, an anion will always have greater nucleophilic character than its conjugate acid. Also affected by the species involved is the ease of formation of the S_N2 transition state. This can be influenced by the sterics around the α and β positions (Figure 7) of the electrophile. If branching exists in either location, the transition state is established with greater difficulty, and thus negatively affects the

rate of reaction. Furthermore, the identity of the leaving group directly affects the rate because it is removed in the rate-determining step, and the ease of its departure corresponds to its stability after removal.⁶⁶ The stability of a free leaving group is typically inverse to that species' strength as a base. Some representative leaving groups are noted in Table 4, organized by their relative leaving ability.⁶⁶

Table 4. Select leaving groups ordered in decreasing leaving ability^a

Relative Leaving Ability	Leaving Group Name	Structural Composition
1	Triflate	ROSO ₂ CF ₃
2	Tosylate, Mesylate	ROSO ₂ C ₆ H ₄ CH ₃ , ROSO ₂ CH ₃
3	Iodide	RI
4	Bromide	RBr
5	Chloride	RCl

^aAdapted from *March's Advanced Organic Chemistry*⁶⁶

Additionally, choice of solvent can be very influential toward nucleophile strength. In the generation of SRH-related thioethers, the use of a thiolate anion nucleophile and a neutral electrophile is often employed. The negative charge of the nucleophile is “dispersed” through the transition state (Figure 7),⁶⁶ so use of a less polar solvent is more effective in stabilizing the transition state. In addition, aprotic solvents are more preferred than protic solvents in this scenario because the transition state is better solvated than the negatively charged nucleophile. This increased energy around the nucleophile reduces the needed activation energy and favors the reaction.⁶⁷

2.3 New S_N2 Conditions for Preparing the SRH Thioether

For the synthesis of the SRH thioether, a thiol-containing species is a logical option for use as the nucleophile. After the thiol is converted into a more nucleophilic thiolate anion under basic conditions, this thiolate could then attack a suitable electrophilic species, which upon release of the leaving group forms the desired thioether.⁶⁵ Using this approach for SRH synthesis, compatible coupling partners could be prepared from accessible starting materials for use in either of two methods. S_N2 method “A” (Figure 8A) would use an amino acid derivative in the role of the nucleophile while the carbohydrate species is fitted with a leaving group. Reversing the roles, Figure 8B depicts S_N2 method “B,” where the

carbohydrate derivative will act as the nucleophilic thiol in reaction with an electrophilic amino acid partner. Each of the methods should result in the formation of the desired protected SRH. Although to date method “A” has been the typical approach for this type of coupling, consideration of method “B” offers a potentially desirable advantage due to the steric accessibility around the carbon bearing the leaving group.

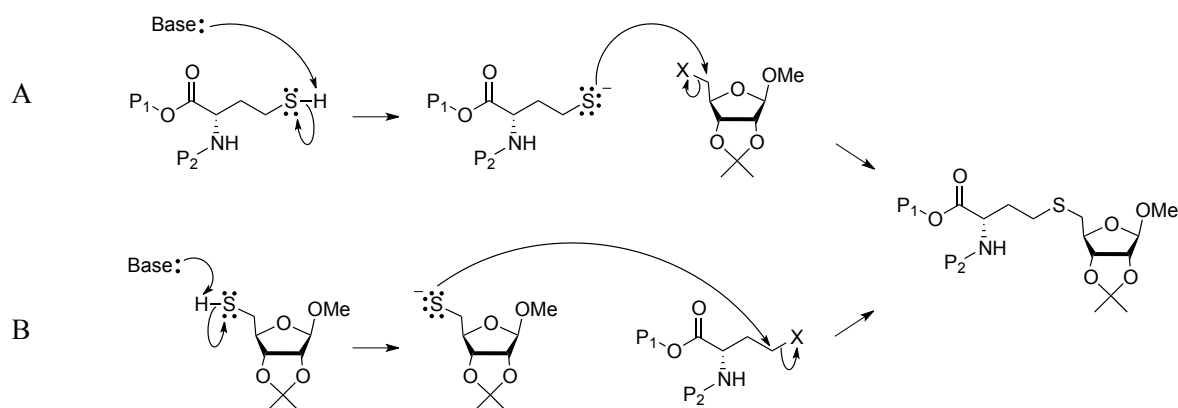


Figure 8. Postulated approaches for creation of the SRH thioether bond After deprotonation by a base, the nucleophilic thiolate resides on either (A) the amino acid component or (B) the carbohydrate derivative before a substitution reaction with the appropriate coupling partner forms the thioether.

In addition to nucleophilic and electrophilic roles, other variables will first be standardized for equivalent application to both S_N2 method “A” and method “B.” As was conveyed by some of the more positive outcomes for past SRH-related syntheses (Table 3), the desired strategy first necessitates the use of alkaline conditions to drive the initial deprotonation of the thiol used for each approach (Figure 8A or 8B). Therefore a non-nucleophilic base as well as a suitable solvent will be selected. Next, the identity of the leaving group that will be fixed onto either the electrophilic carbohydrate (method “A”) or amino acid (method “B”) will be determined. Finally, the limits of amino acid protecting groups will be tested to determine non-interfering protection options under these conditions.

2.3.1 S_N2 Retrosynthesis “A”: Nucleophilic Homocysteine

S_N2 retrosynthesis “A” employs the amino acid as the nucleophile (Figure 9). With guidance from previous syntheses, nucleophilic derivatives can easily be synthesized from L,L-homocysteine (HCySS), forming the desired thiol-containing HCys derivatives needed for nucleophilic coupling.

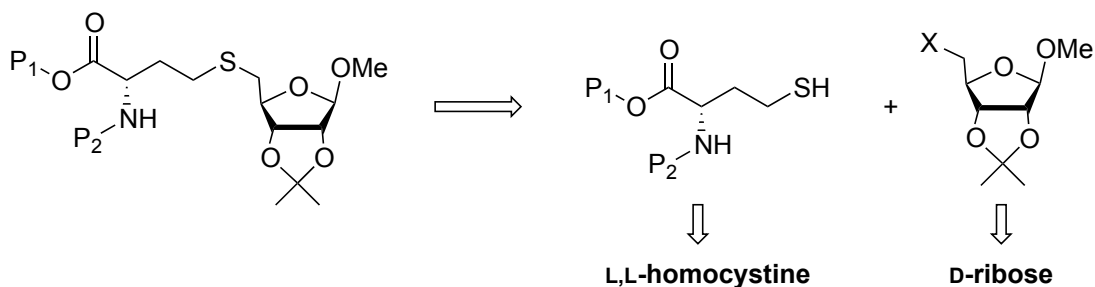


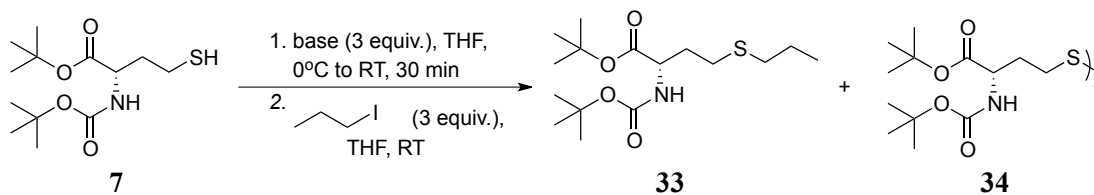
Figure 9. S_N2 retrosynthesis “A” Starting components are generated after standard transformations from HCySS and D-ribose.

Protection and electrophilic activation of D-ribose produces viable electrophilic coupling partners for this strategy. First, a set of trials were executed to determine S_N2 reaction conditions.

2.3.1.1 Reaction Condition Selection: Base and Solvent*

Initially, the reaction conditions for the S_N2 thioether generation required optimization. To test for appropriate conditions, standard starting components were first selected. A proven stable and successful nucleophile under basic conditions, and capable of one step deprotection from Liu’s previous work (outlined in Chapter 1),⁶⁰ the *tert*-butyl ester / Boc protected thiol **7** was prepared from HCySS. Standard amino acid protections were followed by tris(2-carboxyethyl)phosphine (TCEP)-mediated reduction of the disulfide into the respective thiol **7**.^{41,47,68} Propyl iodide served as a sterically available electrophile bearing a moderately reactive leaving group.

* Investigation of these reaction conditions was performed by M. Bolitho.

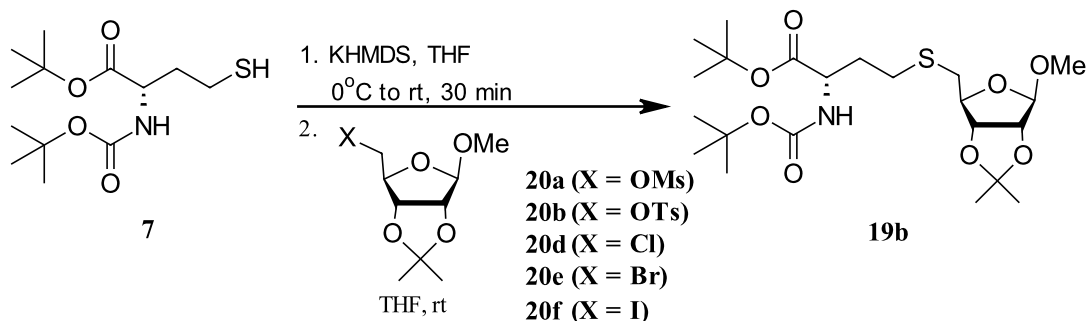


Scheme 6. Optimization of S_N2 thioether generation using a protected HCys and propyl iodide Non-nucleophilic base KHMDS produced relative product ratio of **33** to **34** (19:1 respectively) by ^1H NMR.

For use in the reaction depicted in Scheme 6, a pool of non-nucleophilic bases was tested for the ability to facilitate this reaction with minimal disulfide byproduct formation. Consistent with past analogue preparations, thiol **7** was treated for 30 minutes with a candidate base at 0 °C before the electrophile was introduced at room temperature; the conversion of starting materials was monitored by TLC.⁶⁹ THF served as a less polar, aprotic solvent alternative to DMF, the solvent used in a number of previously-reported analogue preparations (see Table 3). Additionally, using THF allowed for a more expedient workup free from lingering residual water. After assessment of factors including reaction time and the ratio of formation of the desired product **33** to an unexpected oxidation byproduct **34** (yield not quantified, 19:1 product ratio by ^1H NMR), potassium hexamethyldisilazane (KHMDS) was determined to be most effective base tested (data not shown) with minimal byproducts and no observed decomposition of starting components.⁶⁹ The competing disulfide product was observed despite precautions used to maintain an inert atmosphere and anhydrous solvents, and the reason behind its formation is unknown.

2.3.1.2 Electrophile Screen for Efficient Coupling

From the starting place of the ribose component used for Zhao's modified Mitsunobu coupling,⁵⁹ only minor transformations were necessary to develop protected ribose derivatives **20** needed to carry out an electrophile screen under the newly defined S_N2 reaction conditions (Scheme 7).

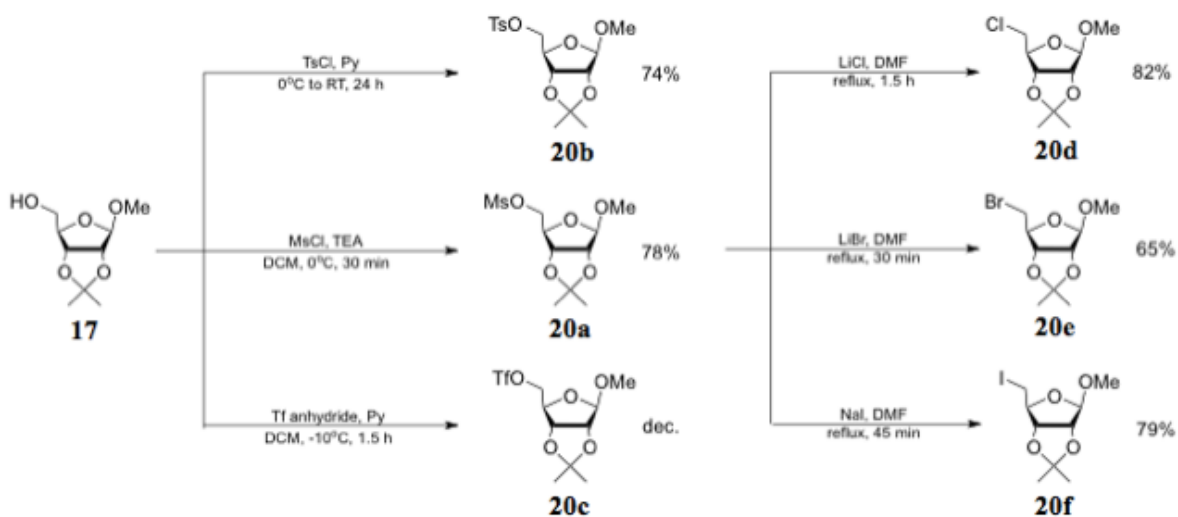


Scheme 7. Standard conditions for use in S_N2 coupling trials The tBu/Boc-protected homocysteine derivative **7** served as a standard nucleophile in the S_N2 reaction with KHMDS in THF. Candidate electrophiles **20a-20b** and **20d-20f** were screened for reaction efficiency.

Informed by species used in previously reported analogue syntheses (Table 3), the next variable scrutinized for this thioether generation strategy was the identification of an optimal leaving group on the carbohydrate moiety.⁴¹⁻⁴³ A series of candidate leaving groups were considered within the relative range of leaving ability for groups used in similar successful thioether syntheses. Trifluoromethanesulfonyl (Tf), toluenesulfonyl (Ts), and methanesulfonyl (Ms) sulfonates as well as iodide (I), bromide (Br), and chloride (Cl) halides were chosen as candidate leaving groups to affix to the C-5 position of the protected ribose (Scheme 7).^{41-43,66}

All derivatives were prepared from D-ribose after standard protection to **17** (Scheme 8).⁷⁰ Derivatives **20a** and **20b** were obtained as crystalline solids easily recovered in good yields (78% and 74%, respectively) after recrystallization from hot (~75° C) ethanol.^{41,71} Triflate **20c**, isolated as a yellow-brown oil,⁷² experienced rapid decay overnight under refrigeration.[†] Due to this instability, derivative **20c** was dismissed as an impractical option for this synthesis. The halogen-bearing electrophiles **20d**, **20e**, and **20f** were each prepared readily from mesylate derivative **20a** using the lithium or sodium salt of the desired halide.^{73,74} Each was recovered as an oil after flash column chromatography in good yield (65 - 82%).

[†] The mesylate **20a** decays in a similar way over an extended period of time (months) under refrigeration, while the tosylate **20b** is stable indefinitely).

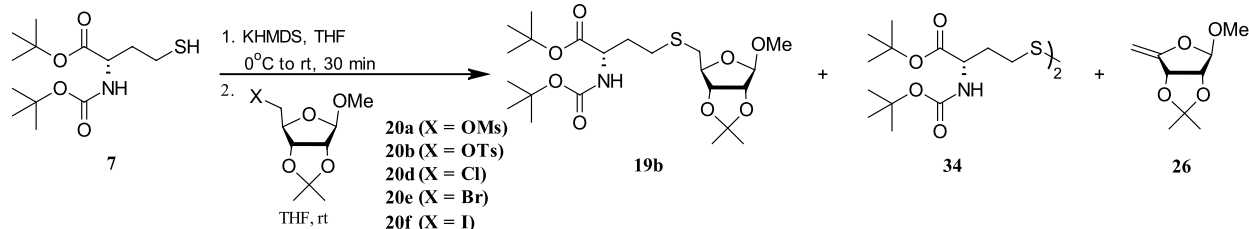


Scheme 8. Preparation of electrophilic ribose derivatives^{41,70-74} After standard protection to **17**, ribose derivatives bearing various sulfonate and halide leaving groups at the ribose C-5 position were generated.

Electrophiles **20a-20b** and **20d-20f** were each assessed for efficiency in both the formation of coupled product **19b** and the absence of oxidation and elimination byproducts (**34** and **26** respectively), using the predetermined conditions with the base KHMDS and THF as the solvent (Table 5). Examination of the success of each electrophile for SRH synthesis was performed by running three simultaneous trials on the same scale (~50 mg), using the different ribose derived electrophiles in reaction with the thiol **7**.[‡]

Coupling products were monitored for completion by TLC, and characterized by ¹H-NMR to determine the relative ratios of products.

[‡] Coupling trial reactions performed by M. Bolitho.

Table 5. Electrophile screen summary under standard conditions

Entry ^a	Electrophile	Electrophile Equivalents ^b	KHMDS Equivalents	Rxn Time ^c (h)	Product Ratio ^d (19b:34:26)
1	20d	3	3.6	>8	ND:ND:1
2	20e	3	3.6	>8	3:1:5
3	20f	3	3.6	3	5:1:5
4	20f	3	2.4	2.5	3:1:2
5	20b	3	2.4	6	6:1:ND
6	20a	3	2.4	6	7:ND:1
7	20a	2	2.4	7	1:ND:ND
8	20a	1	2.4	>8	11:ND:1
9	20a	3	1.2	2	3:1:ND

^aAll trials run on 100 mM scale of **7** in THF ^bAdded as 1 M concentration in THF ^cDetermined by TLC (1:3 EtOAc/hexanes) as consumption of starting materials ^dYields not calculated, product ratios determined by integration of peaks in ¹H NMR crude analysis ^eND = not detected

The rate of S_N2 coupling using the halogen derivatives varied significantly, with iodide **20f** capable of completion within 3 h (Table 5, Entry 3) while bromide **20e** progressed in >8 h (Table 5, Entry 2). Both the iodide and bromide trials resulted in oxidation and elimination byproduct formation (**34** and **26** respectively) in addition to the desired product **19b**. Somewhat unsurprisingly, derivative **20d** bearing the weaker chloride leaving group never reached completion after >8 h, with notable E2 elimination byproduct formation before the reaction was stopped (Table 5, Entry 1). Predictably, iodide **20f** initially resulted in the most promising outcome among the halogen derivatives and was selected to run in parallel trials with sulfonates **20a** and **20b** (Table 5, Entries 4-6).

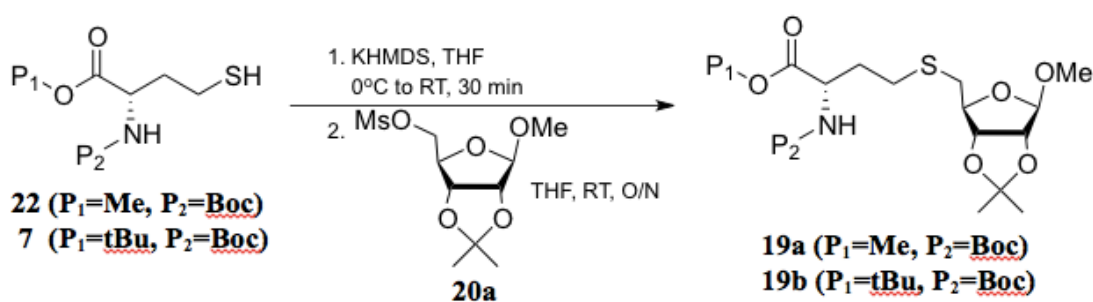
Although the iodide **20f** completed in a shorter reaction period (2.5 h) than the sulfonates, the ratios of byproducts complicated the coupling reaction and would most certainly decrease overall yield (Table 5, Entry 4). Mesylate derivative **20a** and tosylate **20b** afforded very similar coupling outcomes based on reaction time and product ratios, both completing within 6 h, with relatively minimal byproduct formation (Table 5, Entries 5 and 6). Mesylate **20a** was selected in preference to the tosylate as the electrophile of

choice for standardized SRH coupling due to its more expedient preparation. In further trials (Table 5, Entries 7-9) adjusting for electrophile and base equivalents, reaction conditions from Table 5, Entry 7 were chosen for preparative scale synthesis using the mesylate **20a** as the electrophile.

After scaling up to a 0.5 g preparative scale with **20a** as the electrophile, TLC monitoring and crude ^1H NMR analysis showed consistent consumption of thiol **7**. Isolation of the target product **19b** resulted in reproducible modest yields of up to 47%. These results are not unlike the yields isolated from some SRH analogue coupling reactions using similar conditions, reagents, and the nucleophile as the limiting reagent (Table 3). Further, the consistency of this reaction provides a means of reliable preparation of SRH with a faster coupling time and improved one-step deprotection compared to Zhao's preparation.⁵⁹

2.3.1.3 Protecting Group Strategy

As demonstrated by the work of Ruoyi Liu (summarized in Chapter 1), the identity of the protecting groups on some homocysteine-derived coupling molecules can contribute significantly to the success or failure of the $\text{S}_{\text{N}}2$ thioether generation.⁶⁰ Using mesylate derivative **20a** as the electrophile (Scheme 9), several variations in protection on the HCys backbone were prepared by graduate student colleague Emily Showell-Rouse⁷⁵ and used for testing under the conditions described above (Section 2.3.1.1). Protecting groups were selected with the ultimate objective of one-step deprotection capability. Only two thiol derivatives, **22** ($\text{P}_1=\text{Me}$, $\text{P}_2=\text{Boc}$) and **7** ($\text{P}_1=\text{tBu}$, $\text{P}_2=\text{Boc}$) successfully coupled under these conditions with 5% and 47% percent yields, respectively.



Scheme 9. Evaluation of protecting group options Several protection options were attempted to couple with mesylate derivative **20a** under standardized conditions.

Several other protection combinations were tried, but resulted in decomposition or no reaction.⁷⁵ The bulky *tert*-butyl ester protection (P₁) for the carboxylate moiety was viewed as necessary after other esters (i.e., Me, Et, Bz) proved very sensitive to KHMDS under these conditions.⁷⁶ Several additional carbamate protecting groups were also screened (i.e., Troc, Fmoc, Cbz), with only Boc-protection resulting in successful product formation.⁷⁵ While some rationale existed for why the ester protection failed (due to base sensitivity), with such poor yields resulting, the carbamate protecting group strategies did not work well enough to warrant troubleshooting or full investigation into their failure.

2.3.1.4 Summary of SRH Thioether Generation by S_N2 Approach “A”

In consideration of yield, this optimized synthesis is not an improvement over Zhao’s reported method.⁵⁹ These efforts, however, do offer a number of enhancements to SRH synthesis. First, the acid-labile protecting groups throughout both moieties allow for expedient global deprotection in a single step.⁶⁰ With an equal number of steps (5 conversions), as well as the coupling reaction executed in <8 h in comparison to three days, this coupling offers a much faster rate of preparation.⁶⁹ Cost considerations of this synthesis are also better, with the precursor HCySS derivative used as the limiting reagent rather than in 3-equivalent excess used by Zhao.⁵⁹ Table 6 summarizes the results of this strategy compared to those employed by Guillerm and Allart and those used by Zhao et al.^{58,59}

Table 6. Summary of synthetic routes to SRH

	Guillerm and Allart ⁵⁸	Zhao ⁵⁹	This work
Coupling Yield %	22	50-70	47
Overall Yield %	5	52	26
Reaction Time (h)	16	72	7
Leaving Group	OTs	OPEt ₃	OMs
Limiting Reagent	electrophile	electrophile	nucleophile
Deprotection steps	1	2	1
Number of Synthetic Steps to Unprotected SRH	8 ^a	5	5

^aTritium labeled SRH

Most importantly, this synthesis provides a reliable method for SRH synthesis to use in our lab, resulting in very pure chemically synthesized product easy for use in biochemical assays.⁶⁹

2.3.2 S_N2 Retrosynthesis “B”: Nucleophilic Thioribose

The alternate S_N2 strategy outlined in the following retrosynthesis (Figure 10) reverses the electrophilic and nucleophilic identity between the carbohydrate and amino acid components.

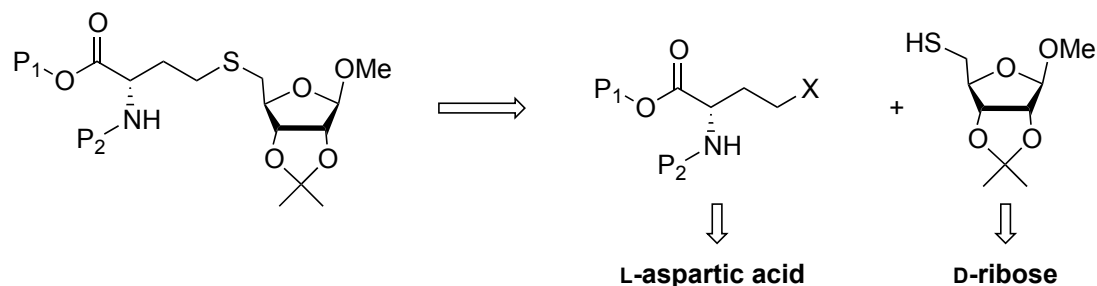


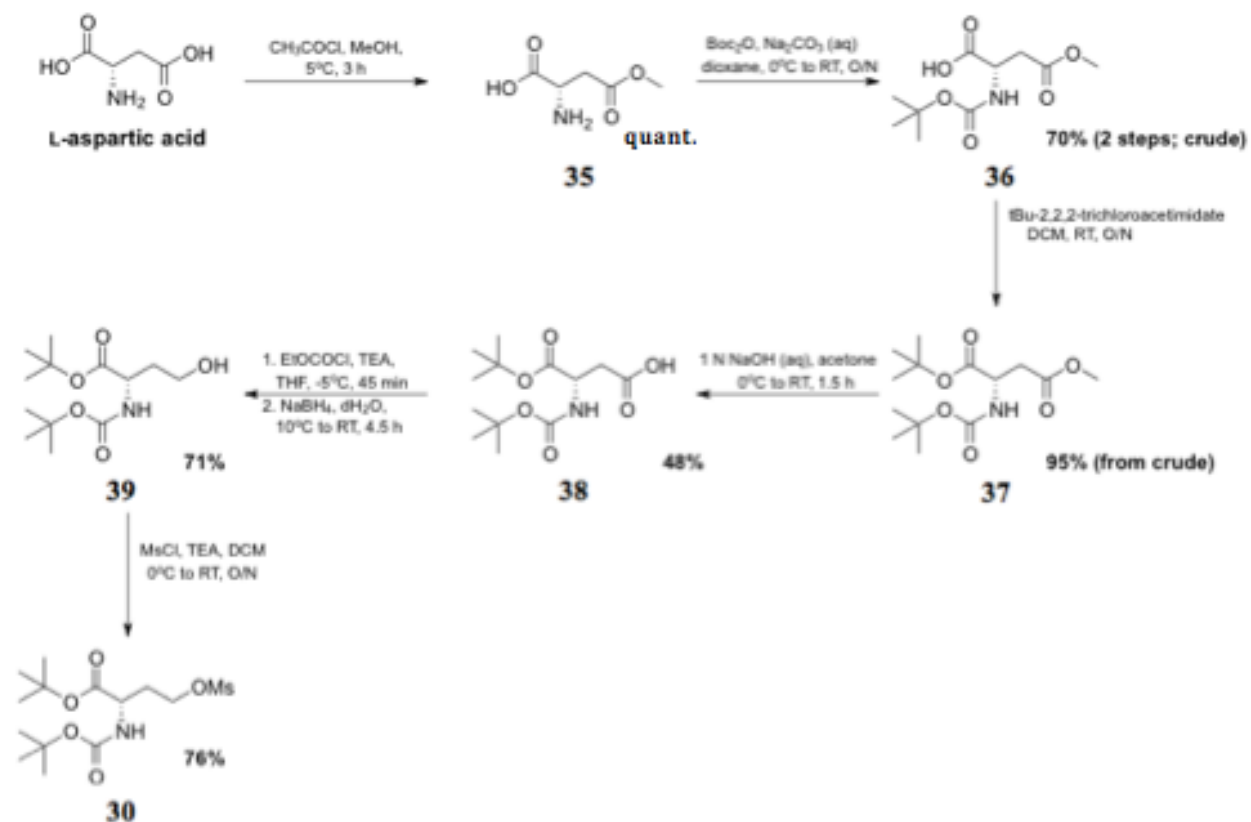
Figure 10. S_N2 retrosynthesis “B” Starting components are generated after standard transformations from L-aspartic acid and D-ribose.

This S_N2 strategy “B” theoretically has some advantages over approach “A.” First, the amino acid derivative bearing the leaving group “X” (Figure 10) offers less sterically hindered access for nucleophilic attack than the ribose derived electrophiles **20a-20f**. The reduced branching around the α and β carbons relative to the leaving group in an L-aspartic acid-derived electrophile is proposed to improve the S_N2 by potentially increasing the rate of reaction and/or improved yield over the S_N2 approach “A” which employs an electrophile bearing more branching proximal to the leaving group.⁶⁵ Second, the mechanistic competition of an E2 reaction, which was observed in approach “A,” is largely minimized due to the unlikely formation of a monosubstituted alkene from the activated L-homoserine electrophile.⁷⁷ Finally, both starting components can be prepared from easily obtained and inexpensive commodity chemicals: the thioribose is produced from D-ribose, and the homoserine derivative from L-aspartic acid.

2.3.2.1 Preparation of Amino Acid Derived Electrophile

In conjunction with efforts from undergraduate researchers Diana Cudia and Emily Murzinski, *tert*-butyl ester / Boc protected homoserine **30** was developed through synthetic Scheme 10 after appropriate troubleshooting.^{40,78-82} While it should be noted that aspartate **38** is commercially available (\$258.30/5g, Bachem), a thorough study of the synthetic pipeline leading up to **30** was deemed critical to understanding what possibilities exist for the future development of SRH analogues which would require manipulation in the midst of these earlier chemical transformations.

First, L-aspartic acid was selectively esterified with methyl protection before additional Boc carbamate and *tert*-butyl ester protection.^{40,78-82} No additional purification steps (apart from standard workup) were performed before crude aspartate derivative **37** was obtained after simple filtration.

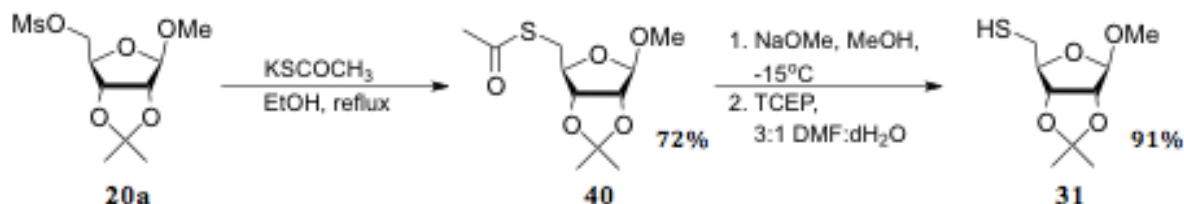


Scheme 10. Synthesis of the electrophilic homoserine^{40,78-82} Derivative **30** was obtained after six transformations from the amino acid L-aspartic acid.

Next, selective deprotection of the methyl ester resulted in **38**, which matched the commercially available product analytically.^{78,79} This was further reduced to **39** before activation to the electrophile **30** which was used in the S_N2 coupling reaction.^{81,82} Compound **30** was isolated as a white crystalline solid upon recrystallization from hexanes/ether and stable indefinitely under refrigeration (17% overall yield). Like S_N2 strategy “A,” the mesylate leaving group was initially chosen for S_N2 synthesis “B” for direct comparison on the preparative scale.⁸¹ Future introduction of other leaving groups onto homoserine derivative **39** remains a possibility for this synthesis.

2.3.2.2 Nucleophilic Thioribose Preparation

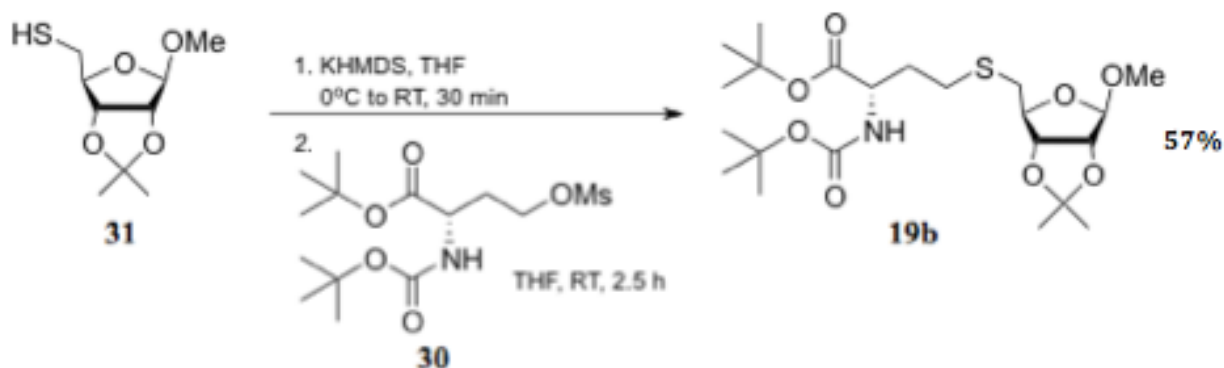
Thiol **31** was prepared in three chemical transformations from mesylate **20a** in 66% overall yield (Scheme 11).^{41,83,84} After conversion to the thioacetate intermediate **40** (72%), acetate deprotection was undergone to attain a mixture of the thiol derivative **31** and its oxidized disulfide (not pictured). The thiol **31** was purified by flash column chromatography, and the recovered disulfide was fully converted to thiol **31** after TCEP·HCl reduction resulting in additional thiol ready for use without any further purification (91%). An unexpected benefit of S_N2 synthetic strategy “B” was the stability of the thiol **31** under ambient conditions, which are not tolerated by thiols with the homocysteine backbone[§]. Thiol **31** remained pure by ¹H NMR, without any oxidation under typical refrigeration conditions, for greater than two months, while it was routinely necessary to use homocysteine derived thiols for strategy “A” within hours of reduction.⁶⁰



Scheme 11. Synthesis of the thioribose nucleophile Thiol **31** was prepared in two steps from the previously generated mesylate **20a** in the chemical pipeline.

[§] After reduction, protected homocysteine derivatives began oxidative reversion into disulfide form under argon storage within hours or days.

After both nucleophilic thioribose **31** and electrophilic component **30** were obtained, an initial coupling trial was conducted (Scheme 12) under identical conditions established in the previous S_N2 strategy “A.” Improved yield over the S_N2 strategy “A” and faster reaction time for SRH thioether generation than that previously reported by both us⁶⁹ and Zhao⁵⁹ were observed from this initial trial approach, as had been



Scheme 12. Trial reaction of S_N2 coupling strategy “B” Protected SRH **19b** was successfully prepared in a trial reaction with modest yield and improved reaction time.

hypothesized. The true efficiency of this coupling reaction remains under consideration, though to date, 57% yield in only 2.5 h has been acquired before optimization. This synthesis represents a potentially significant improvement over any of the aforementioned methods of SRH thioether synthesis.

Furthermore, it enables SRH acquisition from easily obtained starting components and opens possible routes to analogue creation with modifications at the amino acid moiety.

2.4 Summary, Conclusions, and Future Directions of S_N2 Thioether Generation

The investigation of the S_N2 mechanism as a straightforward means to access the SRH thioether has enabled us to obtain SRH more consistently and conveniently (at least in our hands) than previously reported methods.^{58,59} Furthermore, the S_N2 coupling strategies have supplied a solid, measureable, and very pure SRH salt for confident use in biochemical assays, all while returning modest yields with the nucleophile acting as the limiting reagent. S_N2 synthetic strategy “A” provided much improved insight into the limitations and consistency of the S_N2 method using the amino acid thiolate nucleophile. Initial results are encouraging for S_N2 synthetic strategy “B,” although it remains an unrefined and not yet

replicated approach using the carbohydrate component as the nucleophile for the first time. The opportunity for optimization of strategy “B” is an option for further research, while the benefits of improved reaction time and modest gains in yield are already apparent.

The background research for strategy “B,” particularly in cultivation of the electrophilic homoserine derivative, allowed for greater understanding for possible syntheses involving the introduction of modifications onto an electrophilic amino acid analogue. One generic design (Figure 11), which will be discussed further in the following chapter, would introduce one or more substituents onto the C-3 position of the amino acid (β).

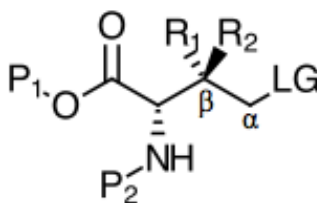


Figure 11. Postulated amino acid electrophile for analogue synthesis Introduction of a substituent onto the C-3 position of the amino acid component before S_N2 coupling could lead to a series of analogues modified on the HCys moiety.

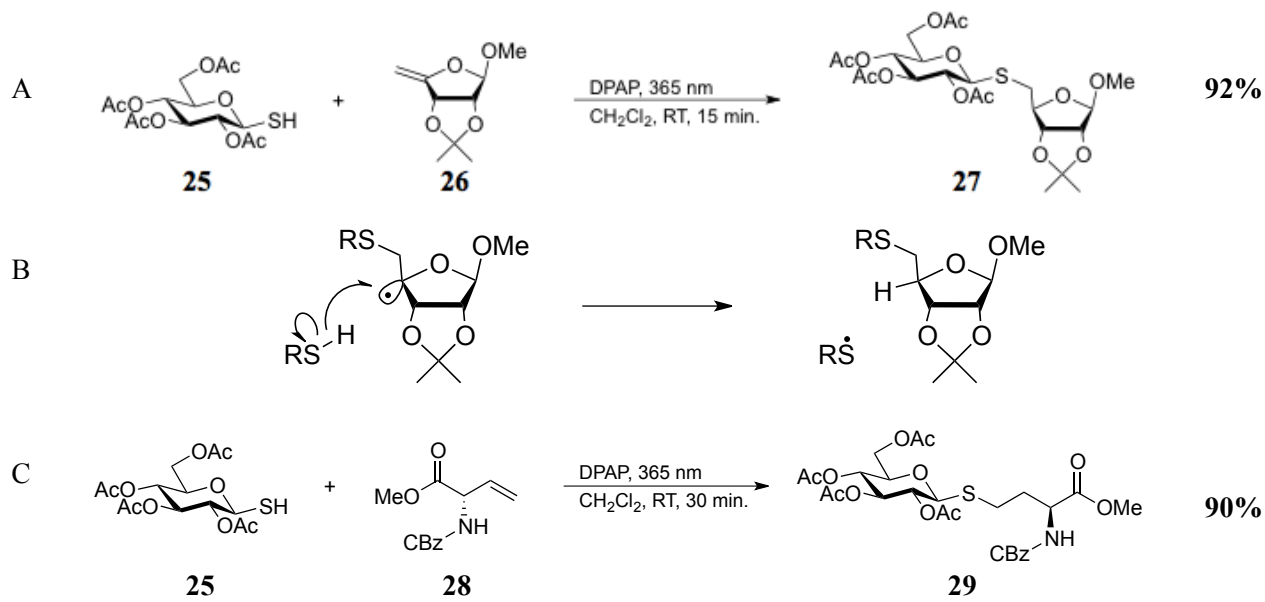
Limits on the structure of this derivative would undoubtedly be imposed by the conditions of involved in the synthetic plan and the conditions required for coupling (namely the alkaline environment). Steric considerations at the position β to the leaving group may also be of concern if the substituent introduced is too bulky for efficient S_N2 coupling.

Chapter 3: Preparation of the SRH Thioether Bond by Thiol-Ene Coupling

While the S_N2 strategies for SRH preparation have resulted in consistent output of the target molecule, they have not yet fulfilled the concurrent goal of improving yield. As noted, there is still potential for optimizing the S_N2 , and further trials remain enticing particularly for approach “B”. We must also acknowledge that S_N2 conditions may not always be a viable option for thioether generation in the context of SRH analogue creation. The goals of improving yield and eventually generating a large number of SRH analogues for inhibition studies motivate the consideration of as many coupling options as feasible. Benefits of the thiol-ene coupling include its track record as an inexpensive, quick, and robust reaction, often high-yielding, and resilient to ambient conditions.^{61,62} This chapter will detail the investigation into TEC as a mechanism for thioether creation in SRH.

3.1 Previously-Reported TEC Preparations of Thioether Bonds in Small Biomolecules

The radical-induced TEC reaction was considered for synthesis of SRH due to its record as a versatile and expedient method. In addition to countless applications within synthetic polymer chemistry and other fields, the TEC reaction has been adapted to the synthesis of several biologically-related molecules.⁸⁵ Research performed by Fiore and coworkers has successfully demonstrated well-optimized use of the TEC reaction for consistent formation of thioether bonds between various carbohydrate and amino acid derivatives (Scheme 13).^{63,64}



Scheme 13. Groundwork TEC reactions by Fiore and coworkers^{63,64} (A) Protected carbohydrates bond by TEC mechanism to form an *S*-glycoside. (B) Fiore cites steric reasons for the formation of a single stereoisomer. (C) Carbohydrate and amino acid partners are coupled by TEC.

Interested in forming *S*-glycoside bonds between sugars, work reported by Fiore et al. first created a number of thioethers between various protected sugars using a catalytic amount of the radical initiator 2,2-dimethoxy-2-phenylacetophenone (DPAP) in a solution of methylene chloride at room temperature and exposure to UV radiation at 365 nm.⁶³ These derivatives included the use of alkene-containing erythrofuranside **26** (Scheme 13A), which was coupled with glucose derivative **25** to form thioether linkages in high yield (92%), and resulted in the reported formation of product **27** containing the same ribofuranside moiety sought for SRH synthesis. Reillustrated in Scheme 13B is the description by Fiore and coworkers for the stereochemical preference at the newly formed chiral center in derivative **27** which results after the propagation step of the reaction.⁶³ The authors note that “these intermediates expose the less hindered face to a molecule of thiol from which they abstract a H• radical in the final and irreversible locking step.”

Similarly, the same mild reaction conditions were later applied by Fiore and coworkers for *S*-glycopeptide bond formation between carbohydrate and amino acid moieties.⁶⁴ Scheme 13C illustrates this method

whereby a protected vinyl glycine derivative **28** was used, which after coupling with glucose derivative **25**, results in the formation of product **29** bearing the homocysteine moiety desired in SRH synthesis. This reaction also proceeded with good yield (90%) and a brief reaction time (30 min). These synthetic outcomes largely outlined the groundwork for adaptation of TEC for SRH synthesis. Before trials of this method were performed, however, a better understanding of the TEC mechanism was garnered for shrewd application.

3.2 General Features of the TEC Mechanism

The TEC mechanism results in anti-Markovnikov addition between thiol and alkene substituents by hydrothiolation of the double bond.⁶¹ Employing this reaction by radical mechanism (Figure 12), an initiating radical abstracts the hydrogen from a thiol, producing a thiyl radical about the sulfur atom. The thiyl radical then steals an electron from the double bond of the alkene, binding the two components by anti-Markovnikov addition onto the double bond as the radical stabilizes on the adjacent secondary or tertiary carbon atom.

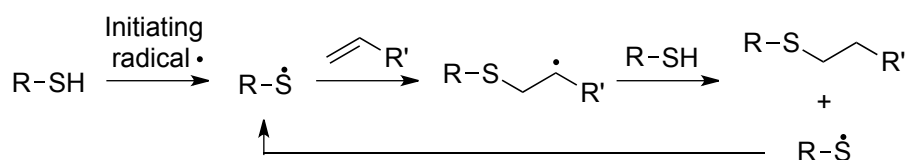


Figure 12. Generic TEC reaction by radical mechanism An initiating radical activates a thiol molecule. This bonds with available alkenes in an anti-Markovnikov addition. The reaction propagates when a hydrogen is abstracted from a new thiol molecule and the thioether is created.

The new thioether is finalized when the carbon-centered radical abstracts a hydrogen atom from a new thiol molecule, simultaneously activating a new thiyl radical and propagating the chain reaction. The reaction eventually terminates with any of the typical termination combinations for radical reactions.⁸⁶

3.2.1 Conditions Used in TEC Reactions

Radical reactions are by their nature reactive with a need for only low catalytic initiator concentration for the chain reaction to progress.⁸⁷ Just as specifics surrounding the S_N2 coupling were involved in the success or failure of those reactions, several factors can affect a TEC reaction. While the particular conditions used for TEC reactions are important, they do not theoretically play as significant a role as the identity of the reactants themselves. TEC is generally tolerant to water and air exposure so long as their concentration(s) are much less than the thiol used (disulfide byproducts from the homocoupling of the thiol may be observed in these reactions).⁶¹ Solvent effects are also limited; while polar solvents can affect the reaction due to hydrogen bonding, thiols are generally poor hydrogen bonders, and these effects are more often observed in situations using particular classes of reactants.⁸⁶

While TEC methods using either no catalyst or a base/nucleophile mechanism exist, problems surrounding the use of protecting groups under alkaline conditions that we had previously observed (see section 1.3.2) combined with the demonstrated ease of the radical mechanism prompted no apparent benefit in exploring these as options for this synthesis.⁶¹

3.2.1.1 Reaction Effects from the Alkene Substituent

Many types of alkenes can successfully undergo TEC, even substituted olefins which could be useful in future SRH analogue development.⁶¹ There can be substantial differences, however, in the coupling results. Much variation in reactivity and rate is due to the olefin, which is subject to steric effects as well as the nature of the double bond itself.^{61,86} Terminal alkenes are generally more reactive than internal substituted olefins for steric reasons. Reactivity generally decreases directly with reduced electron density of the double bond; this is correlated to the structural positioning of other functional groups around the alkene. Bond angle stability and intermediate radical stability also play a significant role in whether the reaction will progress.⁶¹

TEC reactions are also reversible, as often observed with the use of alkenes having internal *cis*-double bonds, which may isomerize into the *trans*- isomer.^{61,86} While target *cis*-products can still be made, the yields are affected by the competing *trans-cis* equilibrium.⁶¹ Another structural effect of the alkene on the reaction can come from heteroatom placement when situated at vinylic or allylic positions, leading to fragmentation or altered regioselectivity.⁸⁶

3.2.1.2 Reactivity of the Thiol Substituent

The structure of the thiol can also influence the reaction, though the reasons are not as well studied as their alkene partners. Thiyl radicals can form from an initiator radical, light or heat, or one-electron oxidants. The formation of the radical is dependent on the bond dissociation energy of that particular thiol, and whether or not the reaction proceeds is based upon its thermodynamic feasibility.⁸⁶ It is also believed that polar effects and hydrogen bonding may influence the reactivity of the thiol in certain scenarios.⁶¹

3.3 Identification of TEC Strategies for Preparation of the SRH Thioether

Like the S_N2 strategy, two obvious possibilities are available for the application of this mechanism for SRH synthesis. In either scenario, the carbohydrate or amino acid component contains the alkene functional group complemented by the thiol on the opposite coupling partner. “TEC method A” (Figure 13A) starts with the same type of protected HCys thiol used in the “ S_N2 method A.” In this mechanism, however, an initiating radical abstracts the hydrogen from the thiol to form a thiyl radical on the HCys component. This progresses with the thiyl coupling onto an olefin-containing erythrofuranside

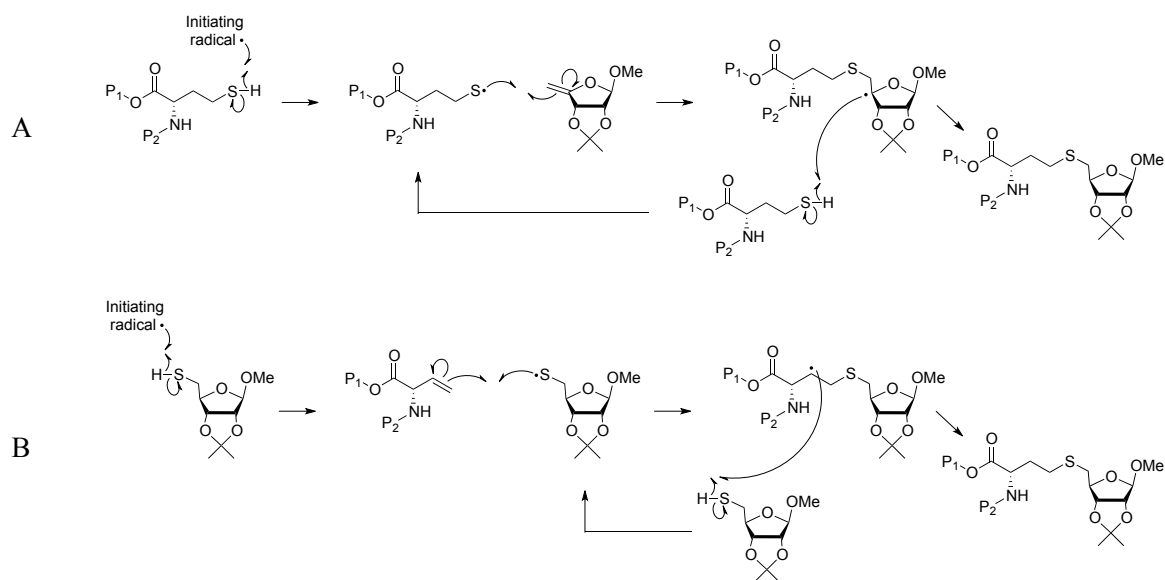


Figure 13. TEC strategies for SRH synthesis The desired thioether could be generated in a protected SRH molecule using the TEC mechanism by either of two accessible strategies. (A) A HCys derivative couples with a carbohydrate bearing an alkene group. (B) Protected vinylglycine bonds an available thioribose.

derivative. The reaction is propagated when the radical, now on the tertiary center of the carbohydrate moiety, abstracts a hydrogen from another protected HCys and secures the formation of the new stereocenter (as modeled by Fiore et al. (Scheme 13B)) on the protected SRH molecule.⁶³

The TEC strategy also has the option of method “B” (Figure 13B), beginning with the same resilient thioribose used in “S_N2 method B.” After hydrogen abstraction, the radical bonds with a protected vinyl glycine similar to the derivative used by Fiore et al. (Scheme 13C). The reaction propagates onto another thioribose, but in this scenario, there is no formation of a new stereocenter as the desired chiral structure is already in place in the existing thioribose.

Success of either of these strategies with application to SRH synthesis could also provide mild conditions suitable for analogue preparation, particularly in situations when a S_N2 mechanism may not be effective in joining the requisite sugar and amino acid moieties.

3.4 TEC Retrosynthesis “A”: Carbohydrate as the Alkene Substituent

As previously outlined, the proposed retrosynthesis for the preparation of the SRH thioether using the TEC approach “A” is shown in Figure 14. Fiore et al. used the molecule **26** and suggested exclusive formation of coupling products with desired stereochemistry about the newly formed stereocenter. Based on Fiore’s reported outcome, derivative **26** could be used in conjunction with a protected HCys to generate a fully protected SRH by TEC.⁶³

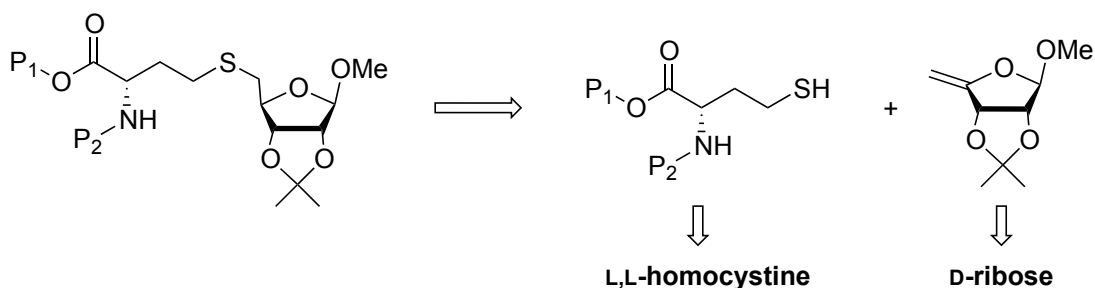
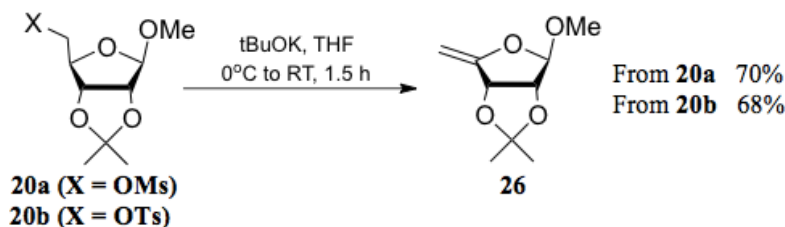


Figure 14. Retrosynthetic construction of the SRH thioether using TEC method “A” Components may be synthesized after standard conversions of commercially available molecules D-ribose and HCySS.

The alkene **26** may be produced from products **20a** or **20b** derived from D-ribose. Like the S_N2 strategy “A”, the HCys derivative **22** was prepared after reduction from the corresponding protected HCySS.

3.4.1 Generation of the Erythrofuranoside Olefin

After consideration of the synthesis pipeline for previously generated ribose derivatives (Scheme 8, Chapter 2), the alkene **26** was prepared with only one additional conversion via an elimination reaction (Scheme 14).

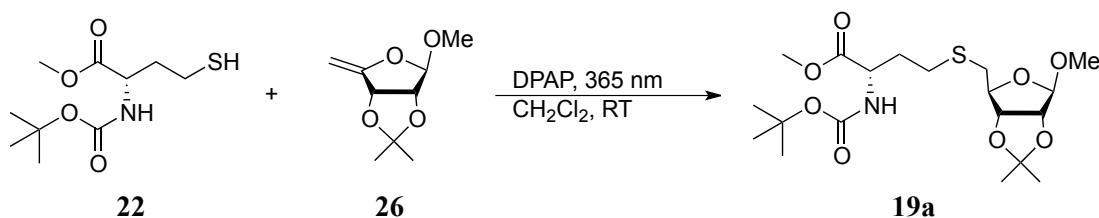


Scheme 14. Synthesis of the alkene-containing erythrofuranoside derivative Using an elimination reaction on existing ribose derivatives generates the desired alkene.

Using either ribose derivative **20a** or **20b**, the target molecule was obtained by reaction with potassium *tert*-butoxide (tBuOK) in THF.⁸⁸ Similar yields resulted from use of either starting material after the product was purified by silica gel flash column chromatography and isolated as an oil.

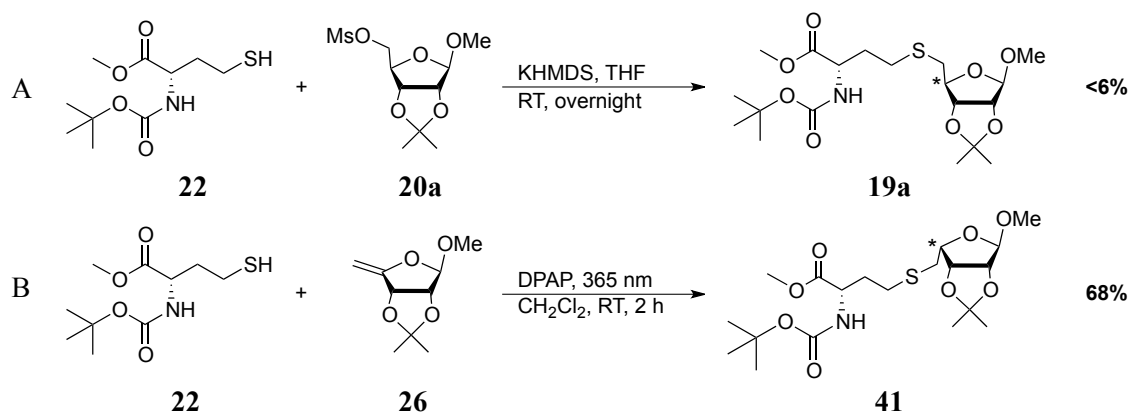
3.4.2 TEC Strategy “A” for the Synthesis of SRH

Similar to the protected homocysteine derivative **7** used in Chapter 2, the methyl ester / Boc protected thiol **22** was synthesized from HCySS using standard protection and TCEP-mediated reduction of the preceding disulfide.^{40,41} Together with compound **26**, thiol **22** was coupled by the TEC radical mechanism under conditions adapted from Fiore et al.⁶³ Using a substoichiometric amount of DPAP (10 mol% of thiol concentration) to generate an initiating methyl radical,⁸⁹ the starting components were mixed in a solution of anhydrous methylene chloride and irradiated at 365 nm (Scheme 15).



Scheme 15. Anticipated protected SRH synthesis by TEC Based on theoretical representations by Fiore and coworkers, desired compound **19a** was sought by reaction components **22** and **26**.

As anticipated, the coupling product in this reaction existed with formation of a single stereoisomer isolated after flash column chromatography. Based on outcomes of TEC coupling reactions reported by Fiore et al., HCys component **22** and ribose derivative **26** were predicted to generate the thioether bond in protected SRH **19a** with the appropriate stereochemistry at the neighboring asymmetric carbon (Scheme 15). Surprisingly, ¹H NMR indicated a product that differed from previously-synthesized protected SRH derivative **19a** (Scheme 16A) generated by S_N2 coupling.



Scheme 16. Synthesis of protected SRH and diastereomer (A) The protected SRH derivative was produced by S_N2 coupling outlined in Chapter Two. (B) Postulated formation of the SRH-like diastereomer by TEC coupling.

These differences were apparent in significant shift and splitting patterns of the peaks representing hydrogen atoms adjacent to and directly at the newly formed chiral center on the ribose moiety. With two possible stereochemical outcomes in the product, it was postulated that initial trials of this reaction resulted in the exclusive creation of the L-lyxofuranoside-containing diastereomer **41** exhibiting a difference about that newly formed stereocenter (Scheme 16B). This reaction nonetheless progressed with moderately good yield, >68%, proceeding with notable improvement over S_N2 couplings.

3.4.2.1 Definitive Identification of Major Product as the SRH-like Diastereomer

Careful analysis of 1D and 2D ^1H NMR spectra was conducted in order to definitively characterize the isolated product from this synthesis as diastereomer **41**. The primary difference between the two possible coupling products can be observed in changes to those ^1H NMR peaks representing hydrogen atoms around the newly formed stereocenter (Figure 15).

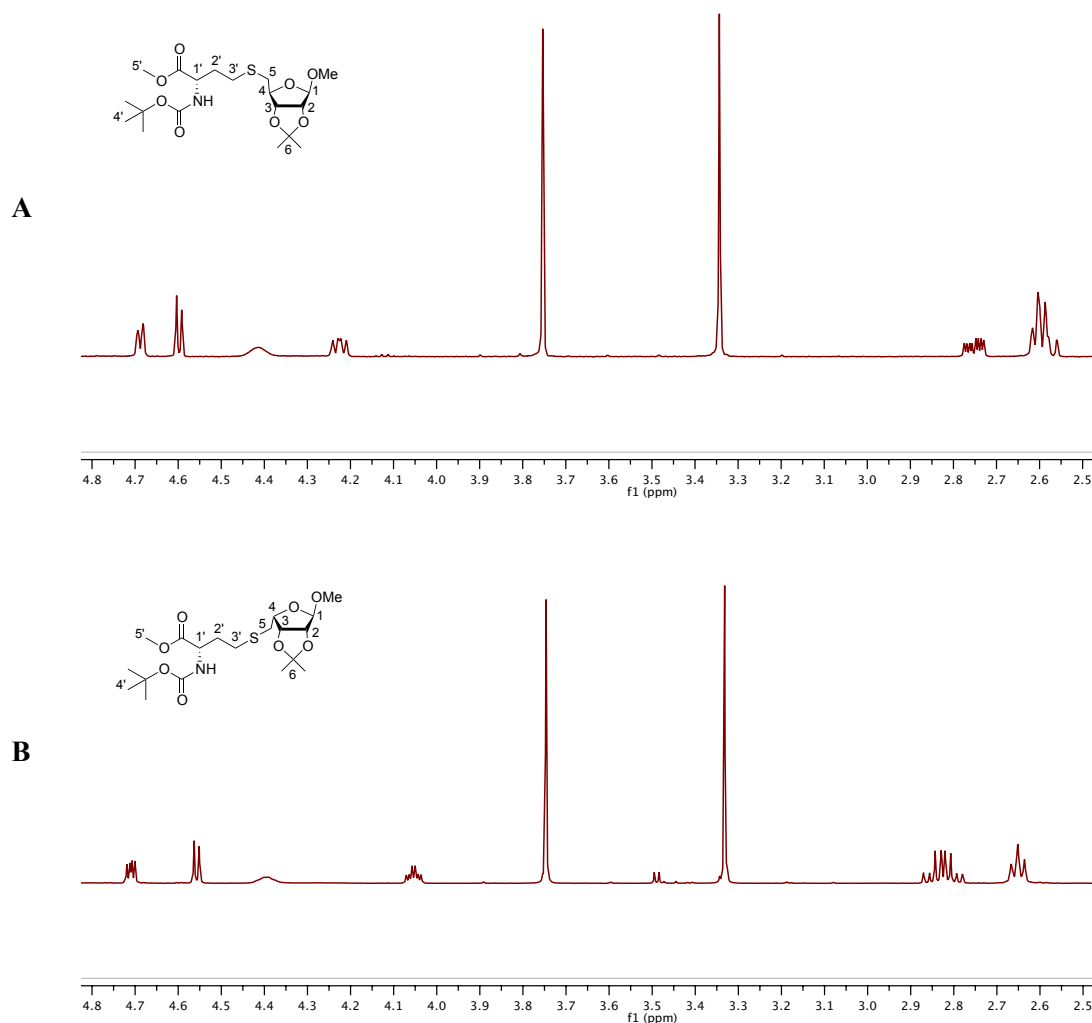


Figure 15. ¹H NMR spectra of key hydrogen peaks in SRH and diastereomer Spectra in the range of 2.5 – 4.8 ppm inclusive of key shifts and splitting patterns in SRH and diastereomer derivatives.

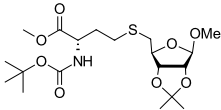
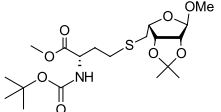
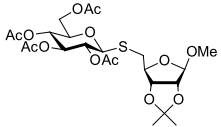
Peaks in the range between 2.5 and 4.8 ppm from ¹H NMR analysis of compound **19a** previously synthesized by S_N2 (Figure 15A) and the postulated diastereomer (Figure 15B) were considered. Verified by the reported NMR analysis of the same compound by Albiniak, protected SRH derivative **19a** produces doublets at δ 4.69 ppm and 4.60 ppm (Figure 15A) representing hydrogen atoms at positions 3 and 2 respectively.⁷⁰ These neighboring protons split each other with a *J*-value of 6.0 Hz. Indeed this coupling constant relationship is maintained throughout many ribose-derived molecules; compounds **20a-20f**, **26**, **31**, and **40** all produce ¹H NMR peaks for hydrogen atoms 3 and 2 as doublets, with coupling

constants in the range of $J = 5.8 - 6.0$ Hz. Furthermore hydrogen 4 on derivative **19a** produces a doublet-doublet at δ 4.23 ppm (Figure 15A), which 2D analysis (see supporting information) by COSy NMR indicates is a result of splitting between H-4 and hydrogen atoms 5a and 5b (δ 2.75 ppm and δ 2.59 ppm), with coupling constants of $J = 9.5$, $J = 6.2$ Hz.

Analysis for the newly formed isomer **41** indicates notable deviations from these patterns (Figure 15B). While the coupling relationship between hydrogen atoms 2 and 3 on the diastereomer are maintained ($J = 5.9$ Hz), the hydrogen at position 3 (δ 4.71 ppm) now splits as a doublet-doublet, with the additional coupling constant $J = 3.6$ Hz. COSy analysis indicates that hydrogen 3 is now interacting with hydrogen 4 in addition to hydrogen 2. The splitting pattern of hydrogen atom 4 (δ 4.05 ppm) also reflects this relationship, now producing a triplet-doublet with additional interactions between both hydrogen atoms at position 5 (δ 2.78 – 2.87 ppm) and now hydrogen atom 3.

Interestingly, the same pattern for those proton peaks in diastereomer **41** can be observed in the reported ^1H NMR spectrum (not shown) of Fiore's compound **27**.⁶³ Namely, hydrogen atoms at positions 2 and 3 split each other with a coupling constant $J = 5.9$ Hz, and also like diastereomer **41**, hydrogen 3 also splits hydrogen atom 4 ($J = 3.6$ Hz). Summarized in Table 7 is the coupling relationship between these key peaks.

Table 7. Representative ¹H NMR peak splitting of SRH and related compounds^{63,70}

Compound	$J_{2,3}$	$J_{3,4}$
 19a	6.0 Hz	No interaction
 41	5.9 Hz	3.6 Hz
 27	5.9 Hz	3.6 Hz

While additional coupling constant evidence was at times unclear due to peak overlap or indistinct peak splitting, evidence of these spatial relationships was noted in observation of COSy ¹H NMR spectra (see supporting information).

3.4.2.2 Three Dimensional Modeling of SRH Diastereomers

With this information, it is proposed that the model described by Fiore et al.,⁶³ involving the final irreversible step of hydrogen abstraction by the carbon-centered radical, indicated the opposite stereochemistry around the newly formed chiral center than what was actually produced. Modeling the SRH and diastereomer structures on Spartan, using the PM3 method, the calculated dihedral angle between hydrogen atoms 3 and 4 was found to be -114.78° for the SRH derivative **19a** and 24.84° for the diastereomer **41**. A traditional Karplus-type calculation is not available for five-membered rings, having coupling constants that are difficult to diagnose.⁹⁰ Though generic calculators exist for calculating coupling constants in furanose sugars,⁹¹ their characterization is complicated by pseudorotational variation,⁹² and no supporting data was found in the literature enabling us to infer J -values for structures having the skeleton of the two diastereomers presented.

As Fiore correctly argues, however, the hydrogen should be abstracted and form the new chiral center from the less sterically hindered side.⁶³ Figure 16 depicts the skeletal structure of the intermediate molecule; after the joining of the C-S bond, the radical would be centered on the indicated carbon. While

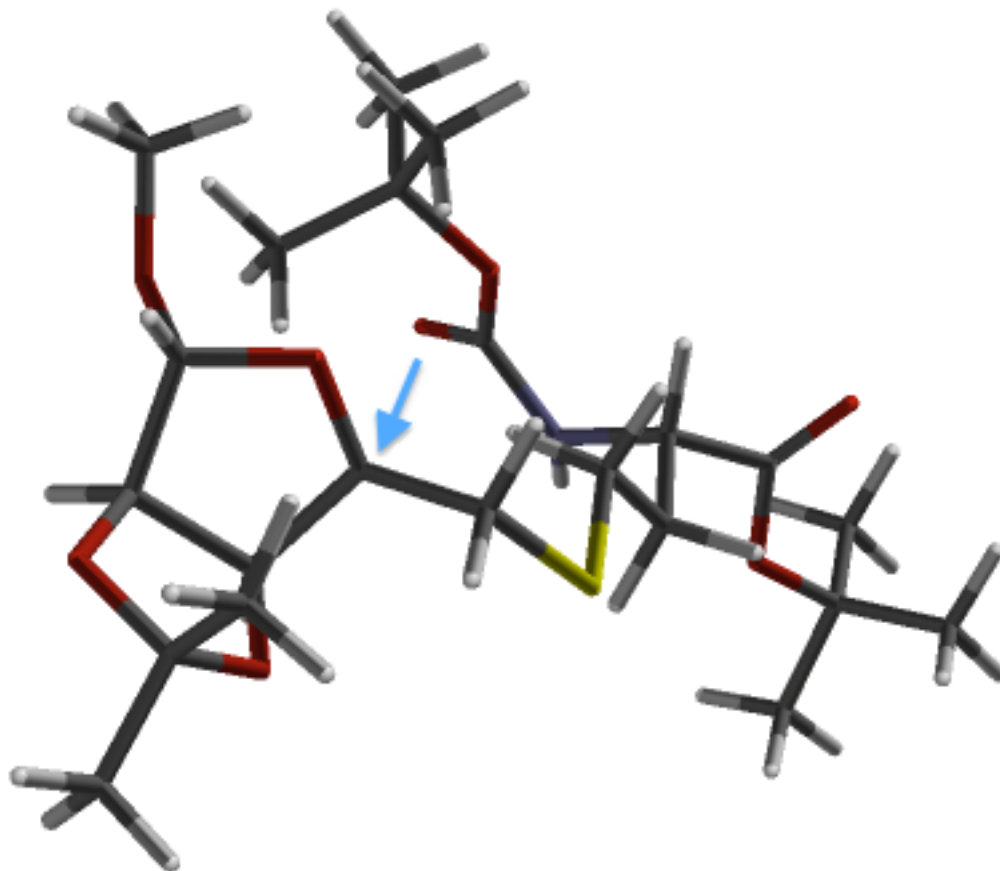


Figure 16. Three-dimensional model of radical intermediate With the radical stabilized on the tertiary carbon (blue arrow), abstraction of a hydrogen to complete the thioether could occur from either the front or reverse side. The acetonide (bottom left) could hinder abstraction on that side, leading to the preferred outcome of diastereomer **41**.

the three-dimensional model does not provide a calculated coupling constant, it does model a concave shape due to the bulky acetonide protection. This could hinder the propagating hydrogen abstraction from that side and favor formation of the L-lyxofuranoside moiety instead of the D-ribofuranoside found in SRH.

3.4.3 Summary of TEC Coupling Strategy “A”

Compared to both S_N2 strategies previously attempted, the coupling components using TEC method “A” bonded by the TEC mechanism with improved reaction time (2 h) and overall yield (>68%), although the resulting product was exclusive formation of diastereomer **41**. The reason for this deviation from the expected outcome is uncertain. Knowledge of steric influences on radical reactions and the 3D spatial relationship around the new stereocenter of the molecule from the acetonide protection strongly support the claim that the final hydrogen abstraction step would favor the L-lyxofuranoside-containing structure. Other possible steric influences might prevent the final step from occurring for the same reason, such as hindrance from the thiol coupling partner, though similarities from the coupling of Fiore’s compound **27** provide at least one example that the trend does not change with a varied thiol.⁶³

Confident in the analysis of coupling product **41** and pleased with the good initial yield and purity after employment of the TEC mechanism in this context, the preparation of the SRH thioether with correct stereochemistry was pursued by TEC strategy “B.”

3.5 TEC Retrosynthesis “B”: Vinylglycine as the Alkene Substituent

The final SRH synthetic strategy considered was use of the TEC method “B” using a vinyl glycine derivative and the thiol again positioned on the ribose moiety. The possibility of the undesired stereoselective outcome should be resolved with this strategy, as the alkene terminates at a secondary carbon on the vinyl group of amino acid component, and the appropriate SRH stereocenter is predetermined in thioribose (Figure 17).

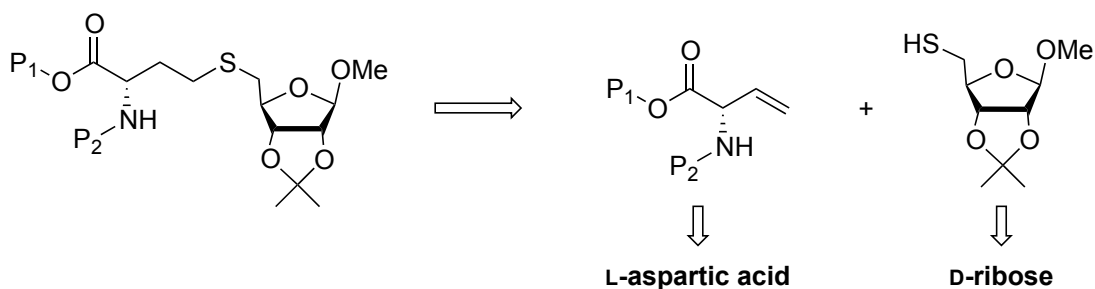


Figure 17. Retrosynthetic construction of the SRH thioether using the TEC method “B”

Components may be synthesized after standard conversions of commercially available molecules D-ribose and L-aspartic acid.

As previously generated for use in S_N2 strategy “B,” the thioribose derivative was obtained from D-ribose.

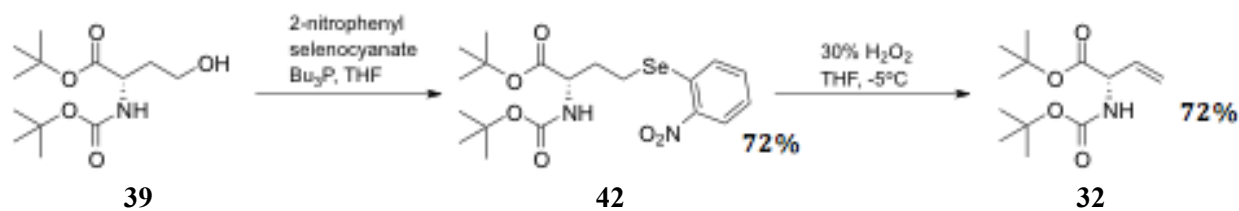
The vinyl glycine was procured from the pipeline of molecules previously acquired for the S_N2 mechanism starting from L-aspartic acid.

3.5.1 Preparation of Vinyl Glycine by Grieco Elimination

Aiming to generate the vinyl glycine derivative **32** from an amino acid derivative in the existing chemical pipeline, synthetic routes were examined from starting compound **38** or **39**. Building off of one of these derivatives would allow for limited additional synthetic steps, leave open the possibility for adding substituents for future analogue development at earlier precursor stages, and again start from the inexpensive amino acid L-aspartic acid.

Though Fiore et al. utilized alternate amino acid protection in their trials,⁶⁴ the mild conditions of the TEC mechanism indicated no foreseeable complication with *tert*-butyl ester and Boc protection. Additionally, maintaining these same protecting groups allowed for direct comparison of synthetic outcomes obtained from the S_N2 coupling trials. Siebum et al. has conveniently developed a method for vinyl glycine synthesis compatible with *tert*-butyl and Boc protection.⁹³ Using the “Grieco elimination” shown in Scheme 17, the target molecule **32** was prepared from protected homoserine **39** in two transformations (52% overall). First, activation to the selenide **42** was accomplished using 2-nitrophenyl selenocyanate

and tributylphosphine (72%). After purification, **42** underwent elimination upon treatment with 30% hydrogen peroxide to generate the target molecule **32** (72%).



Scheme 17. Synthesis of a protected vinyl glycine derivative⁹³ From homoserine derivative **39**, Grieco elimination was employed to form the desired vinyl glycine **32**.

A trial of the first reaction in this sequence was executed, but ^1H NMR analysis and purification by flash column chromatography were greatly complicated by the overwhelming presence of excess selenium and phosphine reactants and byproducts. After having been placed aside for extended time (greater than three months under refrigeration), the crude residue was later purified successfully by flash column chromatography using a different mobile phase. Subsequent extensive ^1H NMR analysis of the isolated material indicated that the reaction intended to produce intermediate **42** had spontaneously continued, completing the second step of Scheme 17 and resulting in production of the target molecule **32**, with 27% yield.

Whether extended time in refrigeration or some unknown reaction influenced the formation of the final product, this inspired the possibility of a one pot sequence of the reactions outlined in Scheme 17, which has been successfully accomplished in similar Grieco elimination models in published literature.⁹⁴ After resulting in a poor yield (<29%) after a single trial using the one pot synthesis, the selenide intermediate **42** was again synthesized with better knowledge of the complexity of the purification. The selenide was isolated after flash column chromatography and was subjected to treatment with hydrogen peroxide in THF. This trial resulted in an improved yield (52% over two steps), with product identity and purity of **32** confirmed by ^1H NMR analysis.

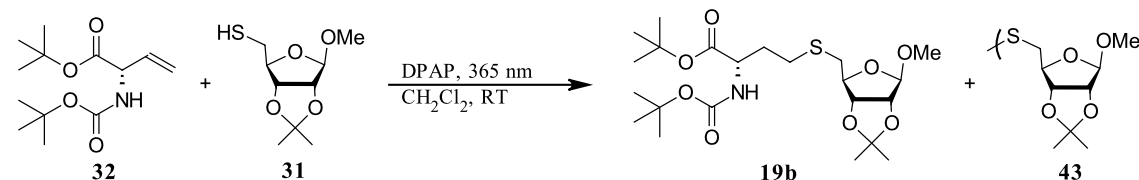
3.5.2 Preparation of D-Thioribose Derivative

Having utilized the thioribose **31** in the S_N2 strategy “B,” further preparations of this molecule were obtained with ease. Again, this synthesis proved convenient with the extended stability observed with the thioribose when compared to other more oxidation susceptible thiols presented earlier.

3.5.3 Formal Synthesis of SRH by TEC

With verified vinyl glycine **32** and D-thioribose **31** components, the alternate radical coupling strategy was assessed for potential use for SRH synthesis using conditions similar to those set by Fiore and coworkers.^{63,64} The results of several coupling trials are summarized in Table 8. The initial trial of this reaction (Table 8, Entry 1) used 1.2 equivalents of the thiol and an initial addition of approximately 9 mol% DPAP initiator. After isolation of the product by flash column chromatography, Trial 1 resulted in disappointing yield (29.8%), although the correct diastereomer **19b** was successfully produced by this TEC strategy. A significant amount of the disulfide **43** resulting from homocoupling of **31** was also isolated from the column purification in addition to unreacted **32**.

Table 8. Optimization of SRH thioether generation by TEC



Entry	Equivalents of Thiol	Concentration Thiol (M)	Mol% of thiol	Rxn Time (h)	Yield (%)
1	1.2	0.07	34.1 ^a	23.75 ^b	29.8
2	3.0	0.5	22.5 ^a	4.33	88.2
3	2.9	0.5	25	1.50	93.2
4	2.0	0.5	25	1.50	89.5
5	2.0	0.5	15	1.50	87.5

^aAdded intermittently in doses ^bUV radiation turned off for O/N stir

Additionally, similar to what was observed in some early trials of TEC strategy “A,” monitoring of the reaction indicated very quick formation of product (within ~30 min), suggesting a good initial reaction rate. The reaction progression seemed to plateau, however, after hours of TLC monitoring. The radical mechanism being catalytic, it was unknown why this appeared to be occurring, and additional aliquots of DPAP were added intermittently to the reaction (Table 8, Entries 1 and 2) until consumption of the limiting reactant **32** was observed by TLC.

Due to the poor yield of the first trial, improvements were considered from an earlier publication by Dondoni.⁶² His work presented results indicating potential contributors to poor yields, specifically, initial thiol concentration, thiol equivalents, and the amount of DPAP used. Each of these variables was adjusted to be consistent with the optimized conditions Dondoni used in this synthesis (Table 8, Entry 2). Using three equivalents of the thiol **31** in a significantly higher concentration (0.5 M) resulted in much improved results (88.2 % yield) over the first trial, though the initial addition of 13.7 mol% DPAP still prompted the necessity for additional aliquots to be added throughout the reaction.

Trial 3 adjusted this initial DPAP concentration to a one time initial addition of 25 mol%. This resulted in extremely encouraging results of 93% isolated product yield after flash column chromatography.

Additionally, the reaction was complete in just 1.5 h, providing much improvement over past syntheses. Despite the literature indicating the success of TEC reactions under exposure to ambient conditions, flame dried equipment and anhydrous solvent was used under an argon atmosphere. Even so, formation of disulfide **43** was still observed in all trials. While excess thiol is deemed necessary to accommodate for disulfide conversion, the isolation of less than one equivalent of disulfide byproduct from trial 3 prompted the testing of this reaction using two equivalents of the thiol (Table 8, Entry 4). The use of two equivalents resulted in comparable yield (89.5%) in the same reaction time as the previous trial. Lastly, entry 5 reduced the amount of photoinitiator to 15 mol% and two equivalents of thiol. The resulting yield was reduced (87.5%), although isolation of the product was still favorable.

The optimization of this strategy represents a clear enhancement over any of the previously attempted SRH coupling reactions. The improved reaction time, mild conditions, coupling yield, preparation of components from accessible commodity chemicals, stability of the necessary thiol, and the possibility of use in analogue development are all extremely notable attributes to this synthesis.

3.6 Summary and Future Directions

SRH synthesis was reexamined by testing four strategies for thioether generation using two different mechanisms. Both the S_N2 and TEC methods can be further optimized for better results and insight into the possibilities and limitations of the chemical synthesis of SRH. In further refining the methods studied in this thesis, some important additional steps could be completed. With the relative success of the TEC strategy “B,” this reaction has not yet been performed at a preparative scale. To best complete the goal of obtaining larger amounts of SRH used for testing in the Ellman’s Assay, this should be a priority moving forward. Additionally, the components needed for TEC strategy “B,” the thioribose **31** and vinylglycine **32**, have been isolated with moderate yields and could be improved on. Other more fundamental variables have also not yet been tested, such as solvent identity in the TEC coupling, use of a different radical initiator, or protecting group selection. The S_N2 coupling should also be further studied. Full consumption of the starting materials is consistently observed, and yet after purification, only moderate yields are isolated. S_N2 strategy “B” has not yet been replicated, and improved results over S_N2 strategy “A” suggest it could be a valuable synthesis moving forward after optimization, particularly for use in analogue development. Although optimization of either the S_N2 or TEC mechanism for SRH synthesis may be still be refined, the described trials have established a good framework and understanding for generating the thioether bond of SRH with acceptable yields of a pure, solid, and stable target molecule.

Moving forward, attention should also turn to the synthesis of SRH analogues. A number of design possibilities exist for analogue structures that could be developed and tested for inhibitory activity against

LuxS. Identification of target molecules have included the design of an analogue with the addition of any number of changes at the homocysteine C-3 position (Figure 18).

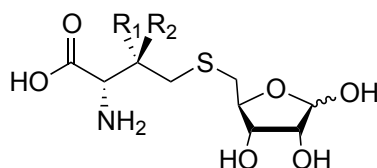


Figure 18. Target SRH analogue with modification at the HCys C-3 position A novel approach to SRH analogue preparation, modification on the HCys moiety could allow for competitive active site binding while disrupting enzyme activity.

This strategy has not been considered in the literature for SRH analogues, as Zhao⁵⁹ verified the importance of the amino acid moiety for enzyme activity, and Pei modeled the action of DPD production facilitated on the ribose moiety. Introducing a small structural change in the homocysteine moiety at the C-3 position, however, could result in an inhibitory mechanism whereby the inhibitor could tightly bond with key residues in the LuxS active site while disrupting the three-dimensional positioning of catalytic factors needed to catabolize the ribose moiety into DPD. Although not directly interfering with the identity of the carbohydrate moiety acted upon by Pei's mechanism,⁴⁶ disrupting the positioning of the enzyme's spatial relationship to these functional groups on SRH could compete for the enzyme's active site while inhibiting its activity.⁶⁰

3.6.1 Proposed Synthesis for an Alkylated Vinyl Glycine Suitable for TEC Coupling

Considering either of the mechanisms for thioether generation in SRH, there are available strategies for creating a methylated analogue that could be employed for each synthetic route. Application of a Julia-

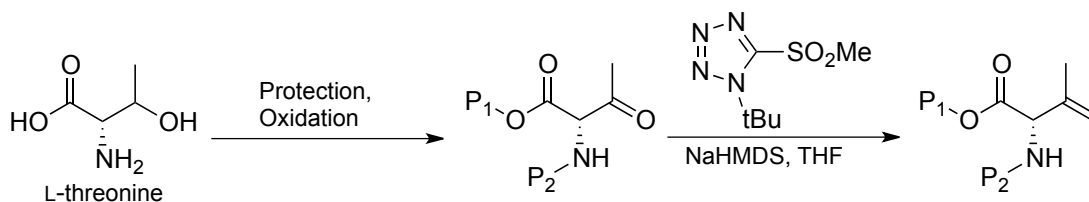
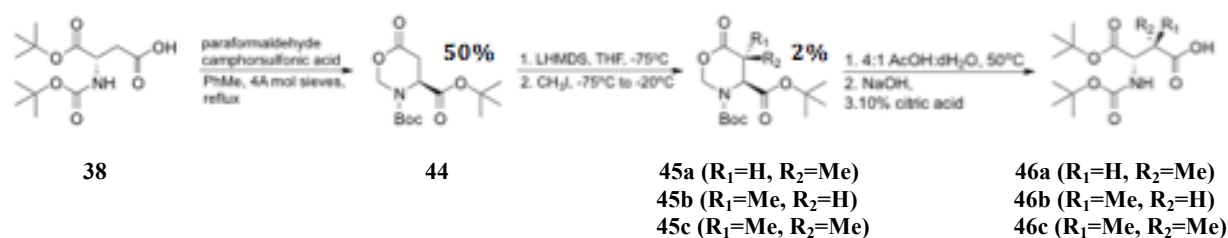


Figure 19. Postulated generation of an alkylated olefin⁹⁵ Applying the method by Aïssa to L-threonine could be a convenient synthesis for an alkylated olefin for use in TEC.

Kocienski conversion onto a different commodity amino acid, L-threonine, after standard protection, could result in generation of a desired alkylated olefin (Figure 19). Aissa has evaluated this mechanism for robust application,⁹⁵ creating many alkene-containing products by conversion of the carbonyl with the use of the reagent 1-*tert*-butyl-1H-tetrazol-5-ylmethyl sulfone, which can be easily generated from *tert*-butyl isothiocyanate. This procedure has been demonstrated as compatible with ester and carbamate protecting groups, and results in good reported yields of various products.

3.6.2 Proposed Synthesis for an Alkylated Homoserine Derivative for S_N2 Coupling

For use in a S_N2 approach, alkyl-substituted aspartates have been successfully prepared by Burtin et al. (Scheme 18).⁹⁶ After conversion of protected aspartate **38** into the lactone **44**, alkyl substitution can occur at the original C-3 position, resulting in mono-substituted diastereomers or the di-substituted product.



Scheme 18. Projected synthesis of alkylated aspartate for conversion to S_N2 electrophile Alkylation demonstrated by Burtin et al. could lead to up to three protected aspartate derivatives. Cudia has successfully reproduced **44** and **45** in 50% and 2% yield respectively.

Undergraduate researcher Diana Cudia has replicated one method used by Burtin et al. through the step introducing the alkyl substituent(s), although recovered yield was extremely low (2%) and resulted as a mixture of the possible products **45a-45c**.^{78,96} Isolation by chromatography is also a challenging factor until this reaction step can be optimized for improved conversion to the target molecule(s). Ideally the cyclization could then be reversed followed by a reduction reaction and the introduction of a leaving group (i.e., mesylate). This method could result in the formation of any of the three possible analogues.

3.6.3. Additional LuxS Inhibition Targets

An interesting analogue examination could be to deprotect the erroneously generated SRH diastereomer to derivative **41** into **47** (Figure 20A), and test it against SRH for inhibitory action on LuxS. Wnuk created a xylofuranose analogue (Figure 20B), differing from SRH only in stereochemistry of the carbohydrate.⁴¹ When tested, this analogue resulted in moderate inhibition of LuxS ($K_i = 4.2 \pm 1.2 \mu\text{M}$).

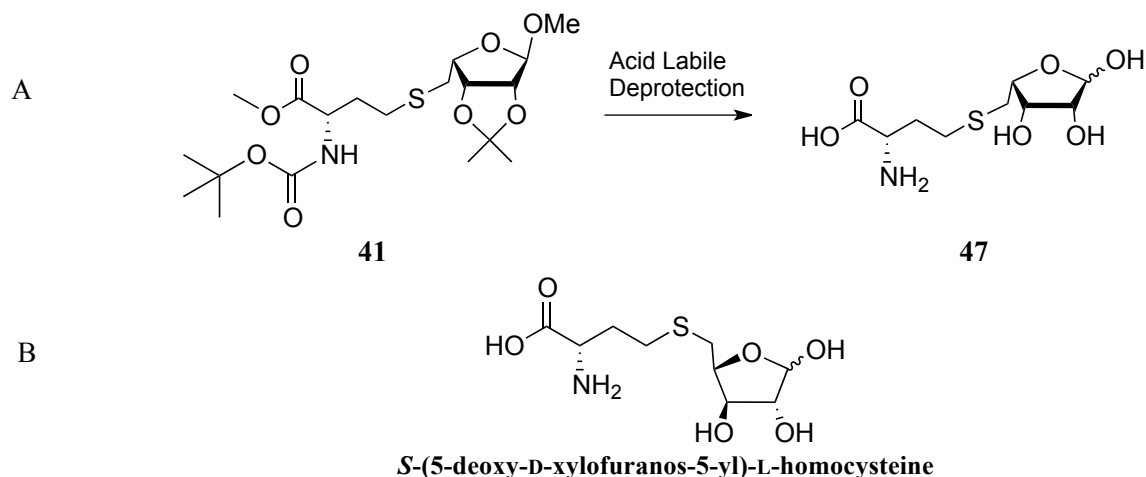


Figure 20. Analogues containing alternate furanose sugars (A) Deprotection of the SRH diastereomer and (B) xylosyl analogue prepared by Wnuk et al. offer isomeric options for competitive inhibition of LuxS.⁴¹

This also prompted the idea of synthesizing some additional analogues varying in the carbohydrate moiety. Generation of a thiol derivative after standard protection of commodity sugars may be an easy-to-access route for a set of analogues in addition to Wnuk's xylosyl derivative and the L-lyxose diastereomer prepared in this thesis.⁴¹ The possibility may also exist to recreate the xylosyl derivative with the ease of the TEC reaction through a possibly less tedious method.

Experimental

Methods

All glassware was flame- or oven-dried, and reactions were performed under an argon atmosphere unless noted otherwise. Reagents were purchased from vendors at reagent grade or higher purity. Ethyl acetate (EtOAc), hexanes, dioxane, dimethylformamide (DMF), ethanol (EtOH), triethylamine (TEA), toluene (PhMe), methanol (MeOH), and acetone solvents were purchased dry from commercial vendors. Anhydrous dichloromethane (CH₂Cl₂), tetrahydrofuran (THF), and diethyl ether (ether) were dispensed from a Glass Contour Solvent Purification System (SG Waters). Notable reagents used were L,L-homocystine (Bachem), tris(2-carboxyethyl)phosphine hydrochloride (TCEP·HCl, Amresco), potassium hexamethyldisilazane (KHMDs, 15% w/w in toluene, Alfa Aesar), and 2,2-dimethoxy-2-phenylacetophenone (DPAP). Thin layer chromatography (TLC) monitoring was performed using Silica G plates (SORBENT Technologies) with UV254, and unless otherwise stated, used with a potassium permanganate (KMnO₄) stain. Target molecules were purified using flash column chromatography with 60Å, 230-400 mesh silica gel (SORBENT Technologies). Solvents were removed by rotary evaporation (Buchi R-114, Welch DirecTorr pump) and high vacuum oil pump. NMR analysis was performed on a VNMRS spectrometer (Agilent) with an oneNMR probe (500MHz for ¹H, 125 MHz ¹³C) and spectra were processed on Mnova software (Mestrelab) with residual solvent references of CDCl₃ at 7.26 ppm (¹H) and 77.16 ppm (¹³C). FTIR spectra were acquired on a Spectrum 100 FTIR spectrometer (Perkin Elmer). Melting points were found using a Stuart SMP10. High-resolution mass spectrometry (ESI-HRMS) analysis was performed by the Scripps Research Institute Center for Mass Spectrometry in La Jolla, CA.

Chemical Synthesis Procedures

General procedure for TCEP-mediated reductions

Modification of published procedure.⁴¹ To an approximately 100 mM solution of disulfide in DMF was added an approximately 700 mM solution of tris(2-carboxyethyl)phosphine hydrochloride (TCEP·HCl) in ddH₂O in one portion at room temperature. The reaction was monitored for consumption of starting material by TLC (1:3 EtOAc/hexanes) after stirring overnight at room temperature. The reaction mixture was poured onto brine (100 mL), and the product was extracted with one portion of diethyl ether (100 mL) then with three portions of diethyl ether (50 mL). Each organic layer was washed individually with four portions of water (75 mL). The organic layers were then combined and washed with a single portion of brine (100 mL) and dried over magnesium sulfate. After filtration, bulk solvent was removed via rotary evaporation and trace solvent was removed by high vacuum to constant mass. The desired thiol was stored with refrigeration under argon and typically used within 24 h.

General Procedures for generation of the thioether linkage in protected SRH target compounds by two methods.

Method A: General procedure for S_N2 reactions between thiols and mesylate electrophiles, preparative scale (0.70 – 1.5 mmol)⁶⁹

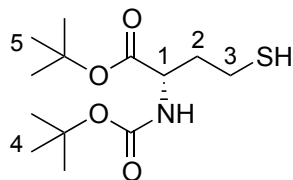
To an approximately 100 mM solution of thiol in THF at 0 °C was added KHMDS (15% w/w in PhMe, 2.4 equiv) dropwise by addition funnel over ten min. The reaction mixture was then moved to ambient temperature and stirred for 30 min. The reaction mixture was returned to 0 °C, and an approximately 1 M solution of mesylate electrophile **20a** or **30** (2 equiv) in THF was added in one portion via cannula. The reaction mixture was moved to ambient temperature and stirred. After monitoring by TLC (1:3 EtOAc/hexanes) indicated consumption of the thiol, the reaction mixture was quenched with saturated aq. NH₄Cl (20 mL) and stirred for 30 min. The reaction was then poured onto dH₂O (40 mL) and extracted with four portions of CH₂Cl₂ (75 mL). The combined organic layers were washed with five portions of water (75 mL), then 75 mL brine. The organic layer was dried over anhydrous MgSO₄, and filtered. Concentration via rotary evaporation was facilitated by the addition of ethanol (30 mL).

Method B: General procedure for TEC reactions of vinyl glycine derivative with thiol, (0.15 mmol scale)

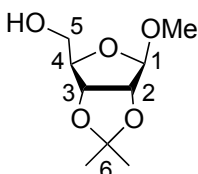
Adapted from published procedure.^{62,64} Vinyl glycine derivative **32** (1 equiv) and thiol **31** (2-3 equiv) were dissolved in anhydrous CH₂Cl₂ (1.0 M thiol) and transferred to a flat-bottomed test tube (10.5 mm diameter, 0.7 mm wall thickness) sealed with a rubber septum with an argon balloon. A solution of DPAP (15-25 mol% of thiol) in an equal volume of anhydrous CH₂Cl₂ was added, and the reaction stirred under UV radiation at 365 nm. After monitoring by TLC for the disappearance of the limiting reagent, the reaction was stopped by solvent removal *in vacuo*.

General procedure for preparation of ribose halides

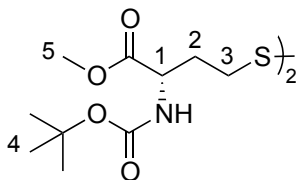
Halides **20d**, **20e**, and **20f** were prepared from the mesylate **20a** with modifications to literature procedures.^{73,74} In general: To an approximately 100 mM solution of **20a** in DMF was added 10 equivalents of the relevant halide salt in one portion. The reaction was refluxed and monitored to completion by TLC (1:1 EtOAc/hexanes). After the reaction mixture cooled to room temperature, it was partitioned between diethyl ether (50 mL) and dH₂O (25 mL). The organic layer was washed with four portions of dH₂O (25 mL) and one portion of brine (25 mL). The organic layer was dried over MgSO₄ and filtered, and the solvent was removed via rotary evaporation.



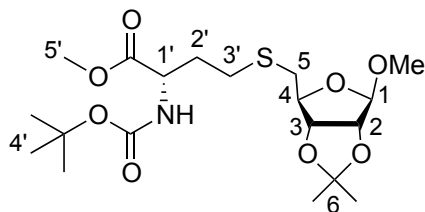
***N*-tert-butoxycarbonyl-L-homocysteine, *tert*-butyl ester (7)** From **General procedure for TCEP-mediated reductions**, isolated as a clear oil from disulfide **34** (0.280 g, 0.961 mmol, 92.9%). TLC (1:3 EtOAc/hexanes): R_f 0.53; ^1H NMR (500 MHz, CDCl_3): δ 5.05 (br d, $J = 7.1$ Hz, 1H, -NH), 4.31 (m, 1H, H-1); 2.58 (m, 2H, H-3), 2.08 (m, 1H, H-2_a), 1.90 (m, 1H, H-2_b), 1.59 (m, 1H, -SH), 1.47 (s, 9H, H-4 or H-5), 1.45 (s, 9H, H-4 or H-5); ^{13}C NMR (125 MHz, CDCl_3): δ 171.6, 155.6, 82.4, 80.0, 53.1, 37.8, 28.5, 28.1, 20.9; IR (ATR): 3351, 2978, 2935, 1698, 1502, 1366 cm^{-1} . NMR spectra are consistent with published report.⁴⁷



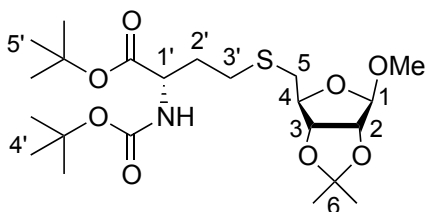
1-*O*-methyl-2,3-*O*-isopropylidene-D-ribofuranoside (17) Prepared from D-ribose according to literature procedures.⁷⁰ D-ribose (6.987 g, 46.54 mmol) was dissolved in a 60 mL solution of 1:1 methanol/acetone. Approximately 1 mL of concentrated HCl was added dropwise before reaction was heated to reflux for 90 min. The reaction was monitored by TLC (2:1 EtOAc/hexanes) and allowed to cool to room temperature upon consumption of starting material. The reaction mixture was brought to pH 6 with pyridine and concentrated by rotary evaporation. The crude material was partitioned between ethyl acetate (40 mL) and dH_2O (100 mL). The aqueous layer was extracted with three portions of ethyl acetate (40 mL), and the organic layers were combined and washed with saturated aq. CuSO_4 (75 mL), two portions of dH_2O (75 mL), and brine (75 mL), and dried over MgSO_4 . After filtration, the product was concentrated by rotary evaporation and isolated as a light yellow oil after short-path distillation (4.299 g, 21.05 mmol, 45.2%) but crude material (5.738 g, 28.10 mmol, 60.4%) was typically used to prepare sulfonates **20a** and **20b**. TLC (2:1 EtOAc/hexanes): R_f 0.44; ^1H NMR (500 MHz, CDCl_3): δ 4.97 (s, 1H, H-1), 4.84 (d, $J = 6.0$ Hz, 1H, H-2), 4.59 (d, $J = 6.0$ Hz, 1H, H-3), 4.44 (~t, 1H, H-4), 3.70 (m, 1H, H-5_a), 3.62 (m, 1H, H-5_b), 3.44 (s, 3H, -OMe), 3.22 (dd, $J = 10.8$, $J = 2.5$ Hz, 1H, -OH), 1.49 (s, 3H, H-6_a), 1.32 (s, 3H, H-6_b); ^{13}C NMR (125 MHz, CDCl_3): δ 112.2, 110.1, 88.5, 85.9, 81.6, 64.1, 55.6, 26.5, 24.8; IR (NaCl): 3460, 2989, 2941, 2837, 1456, 1374 cm^{-1} . All analytical data are consistent with published report.⁹⁷



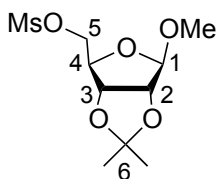
***N,N'*-Di(*tert*-butoxycarbonyl)-L,L-homocystine, bis(methyl) ester (18)** Work performed by Megan Bolitho. Prepared with modification of published procedures.⁴⁰ Thionyl chloride (10 mL, 137.8 mmol) was added dropwise to dry methanol (100 mL, distilled from Mg) over a period of 15 min at 0 °C. The reaction mixture was moved to room temperature for 15 min. After returning the reaction mixture to 0 °C, L,L-homocystine (3.00 g, 11.2 mmol) was added in one portion. The reaction mixture was allowed to warm to room temperature and stirred overnight. The reaction was monitored by TLC (1:1 MeOH/CH₂Cl₂) for consumption of starting material, and concentration under reduced pressure yielded a thick foamy solid. Deionized water (10 mL) and dioxane (10 mL) were added to the crude material under ambient conditions and the mixture stirred until homogeneous. A 1 M aq. solution of Na₂CO₃ was added in 1 mL aliquots at 0 °C until the pH of the reaction increased to pH 9. A solution of di-*tert*-butyl dicarbonate (5.95 g, 27.3 mmol) in dioxane (10 mL) was added dropwise to the reaction mixture over 15 min, at which time the pH of the reaction mixture had dropped to pH 7.5. Additional 1 mL aliquots of 1 M Na₂CO₃ were added to return the solution to pH 9, and the reaction mixture was allowed to warm to room temperature. Monitoring by TLC (1:4 MeOH/CH₂Cl₂) indicated consumption of starting material after stirring overnight. The reaction was extracted with three portions of CH₂Cl₂ (100 mL). The combined organic layers were dried over MgSO₄, filtered, and concentrated under reduced pressure to a yellow liquid. The crude material was taken up in EtOAc (150 mL), washed with three portions of saturated aq. NaHCO₃ (75 mL) and brine (75 mL) and dried over MgSO₄. After filtration, concentration under reduced pressure resulted in a white solid which was recrystallized from EtOAc/hexanes (3.79 g, 7.63 mmol, 68.1%). The solid powder is stable indefinitely at room temperature. TLC (1:1 EtOAc/hexanes): R_f 0.44; mp 96-98 °C; ¹H NMR (500 MHz, CDCl₃): δ 5.12 (br d, *J* = 5.6 Hz, 2H, -NH), 4.40 (br s, 2H, H-1), 3.76 (s, 6H, H-5), 2.71 (m, 4H, H-3), 2.24 (m, 2H, H-2_a), 1.99 (m, 2H, H-2_b), 1.44 (s, 18H, H-4); ¹³C NMR (125 MHz, CDCl₃): δ 172.8, 155.5, 80.3, 77.4, 52.6, 34.7, 32.7, 28.4; IR (ATR): 3364, 2984, 1752, 1683, 1516, 1436, 1366 cm⁻¹. Analytical data are largely consistent with published reports.⁹⁸



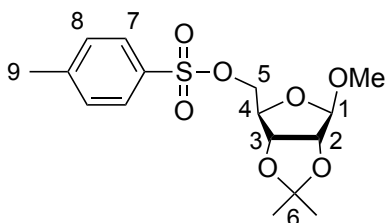
***N*-tert-butoxycarbonyl-*S*-(5-deoxy-1-*O*-methyl-2,3-*O*-isopropylidene-*D*-ribofuranos-5-yl)-*L*-homocysteine, methyl ester (**19a**)** From **General Procedures for generation of the thioether linkage in protected SRH target compounds by two methods. Method A:** From thiol **22** (0.250 g, 1.003 mmol) and mesylate **20a** after overnight stir: Silica gel flash column chromatography in 1:3 EtOAc : hexanes provided protected SRH derivative **19a** as a colorless oil (0.024 g, 0.055 mmol, 5.5%). TLC (1:3 EtOAc : hexanes): R_f 0.18; $^1\text{H NMR}$ (500 MHz, CDCl_3): δ 5.11 (br d, $J = 8.9$ Hz, 1H, -NH), 4.97 (s, 1H, H-1), 4.69 (d, $J = 6.0$ Hz, 1H, H-3), 4.60 (d, $J = 6.0$ Hz, 1H, H-2), 4.42 (br s, 1H, H-1'), 4.23 (dd, $J = 9.5$ Hz, $J = 6.2$ Hz, 1H, H-4), 3.75 (s, 3H, H-5'), 3.34 (s, 3H, -OMe), 2.75 (ddd, $J = 13.5$ Hz, $J = 6.2$ Hz, $J = 2.9$ Hz, 1H, H-5_a), 2.59 (m, 3H, H-3' and H-5_b), 2.12 (m, 1H, H-2'_a), 1.92 (m, 1H, H-2'_b), 1.48 (s, 3H, H-6_a), 1.45 (s, 9H, H-4'), 1.32 (s, 3H, H-6_b); $^{13}\text{C NMR APT}$ (125 MHz, CDCl_3): δ 112.6, 109.8, 85.9, 85.4, 83.5, 55.1, 52.9, 52.6, 35.9, 35.8, 33.0, 32.9, 28.5, 28.0, 27.9, 26.6, 25.1; IR (ATR) 3348, 2978, 2935, 1743, 1713, 1512, 1367 cm^{-1} ; Previously reported without analytical data.⁵⁹ $^1\text{H NMR}$ peak assignments were made after analysis by COSY $^1\text{H NMR}$.



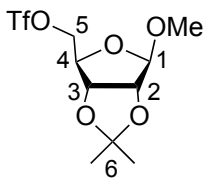
***N*-tert-butoxycarbonyl-*S*-(5-deoxy-1-*O*-methyl-2,3-*O*-isopropylidene-*D*-ribofuranos-5-yl)-*L*-homocysteine, *tert*-butyl ester (**19b**)** From **General Procedures for generation of the thioether linkage in protected SRH target compounds by two methods. Method A:** Reported values from work performed by Megan Bolitho. Using thiol **7** (0.438 g, 1.50 mmol) and mesylate **20a** after overnight stir: Silica gel flash column chromatography (1:5 EtOAc: hexanes) provided protected SRH derivative **19b** as a white oil (0.330 g, 0.691 mmol, 46.1%). Using thiol **31** (0.335 g, 1.52 mmol), and mesylate **30** after 2 h stir: Silica gel flash column chromatography (1:3 EtOAc/hexanes) afforded a yellow oil (0.411 g, 0.861 mmol, 56.6%). **Method B:** Using vinylglycine **32** (0.040 g, 0.155 mmol) and thiol **31** (0.099 g, 0.449 mmol) with 25 mol% DPAP after irradiation at 365 nm for 1.5 h: Reaction was purified by flash column chromatography (1:10 EtOAc : hexanes) to obtain **19b** as a viscous, colorless oil (0.069 g, 0.144 mmol, 93.2%). TLC (1:3 EtOAc: hexanes): R_f 0.39; $^1\text{H NMR}$ (500 MHz, CDCl_3 , δ): 5.09 (br d, 1H, -NH), 4.96 (s, 1H, H-1), 4.69 (d, $J = 5.9$ Hz, 1H, H-3), 4.59 (d, $J = 5.9$ Hz, 1H, H-2), 4.23 (m, 2H, H-1' and H-4), 3.33 (s, 3H, -OMe), 2.75 (dd, $J = 13.4$ Hz, $J = 6.2$ Hz, 1H, H-5_a), 2.58 (m, 3H, H-3' and H-5_b), 2.08 (m, 1H, H-2'_a), 1.87 (m, 1H, H-2'_b), 1.46 (s, 12H, H-6_a and H-4' or H-5'), 1.44 (9H, H-4' or H-5'), 1.31 (s, 3H, H-6_b); $^{13}\text{C NMR}$ (125 MHz, CDCl_3): δ 171.4, 155.5, 112.6, 109.7, 85.9, 85.4, 83.4, 82.4, 80.0, 55.1, 53.5, 35.8, 28.5, 28.2, 28.1, 27.9, 26.6, 25.2; IR (NaCl): 3362, 2979, 2934, 1716 (br.) 1505, 1368 cm^{-1} ; ESI-HRMS (m/z): $[\text{M}+\text{H}]^+$ calcd for $\text{C}_{22}\text{H}_{39}\text{NO}_8\text{S}$, 478.2469, found 478.2470. $^1\text{H NMR}$ peak assignments were made after analysis by COSY $^1\text{H NMR}$.



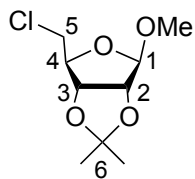
1-*O*-methyl-2,3-*O*-isopropylidene-5-*O*-(methanesulfonyl)-β-*D*-ribofuranoside (20a) Prepared from protected ribose derivative **17** according to modified literature procedures.⁷¹ Protected ribose **17** (1.733 g, 8.487 mmol) was dissolved in CH₂Cl₂ (250 mL) and cooled to 0 °C. Triethylamine (3.6 mL, 25.8 mmol) was added in one portion, and the solution was allowed to stir for 10 min before the dropwise addition of methanesulfonyl chloride (1.0 mL, 12.9 mmol). Monitoring by TLC (1:1 EtOAc/hexanes) indicated full conversion of starting material after the reaction had stirred at 0 °C for 35 min. The reaction mixture was poured onto saturated aq. NaHCO₃ (100 mL), and the aqueous layer was extracted with three portions of CH₂Cl₂ (50 mL). Organic fractions were pooled, washed with one portion of brine (100 mL), dried over MgSO₄, filtered, and the solvent was removed by rotary evaporation to give the crude product as an orange solid. Recrystallization from hot ethanol gave fluffy white crystals (1.868 g, 6.617 mmol, 78%). The solid product is stable for ~6 weeks under refrigeration with decomposition evident after several months. TLC (1:1 EtOAc/hexanes): R_f 0.42; mp 78-80 °C, lit.⁷⁴ 78-79 °C; ¹H NMR (500 MHz, CDCl₃): δ 4.99 (s, 1H, H-1), 4.70 (d, *J* = 5.8 Hz, 1H, H-2), 4.61 (d, *J* = 5.9 Hz, 1H, H-3), 4.41 (~t, 1H, H-4), 4.21 (d, *J* = 7.7 Hz, 2H, H-5), 3.35 (s, 3H, -OMe), 3.07 (s, 3H, -OMs), 1.49 (s, 3H, H-6_a), 1.32 (s, 3H, H-6_b); ¹³C NMR APT (125 MHz, CDCl₃): δ 113.0, 109.8, 85.1, 84.0, 81.5, 68.6, 55.4, 38.0, 26.6, 25.1; IR (ATR): 3032, 2991, 2944, 2923, 1379, 1349 cm⁻¹. All spectral data are consistent with published reports.⁹⁹



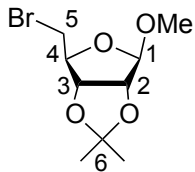
1-*O*-methyl-2,3-*O*-isopropylidene-5-*O*-(*p*-toluenesulfonyl)-β-*D*-ribofuranoside (20b) Compound **20b** was prepared from protected ribose derivative **17** according to modified literature procedures.⁴¹ *p*-toluenesulfonyl chloride (1.413 g, 7.412 mmol) was added to a stirred solution of the protected ribose derivative **17** (0.757 g, 3.707 mmol) in pyridine (8 mL) at 0 °C. The reaction gradually moved to room temperature while stirring for 26 h. Monitoring by TLC (1:1 EtOAc/hexanes) revealed no visible starting material remaining, and the pyridine was coevaporated with three portions of toluene (8 mL) by rotary evaporation. The crude product was taken up in EtOAc (60 mL), washed with two portions of saturated aq. NaHCO₃ (25 mL) and one portion of brine (25 mL). The organic layer was dried over MgSO₄, filtered, and solvent was removed by rotary evaporation. Product **20b** was isolated as fibrous white crystals after recrystallization from hot ethanol (0.984 g, 2.746 mmol, 74.1%). The solid product is stable indefinitely with refrigeration. TLC (1:3 EtOAc/hexanes): R_f 0.28; mp 82-83 °C, lit.⁸⁸ 80-81 °C; ¹H NMR (500 MHz, CDCl₃): δ 7.81 (d, *J* = 7.9 Hz, 2H, H-7), 7.36 (d, *J* = 7.9 Hz, 2H, H-8), 4.93 (s, 1H, H-1), 4.60 (d, *J* = 5.6 Hz, 1H, H-2), 4.53 (d, *J* = 5.8 Hz, 1H, H-3), 4.31 (~t, 1H, H-4), 4.02 (m, 2H, H-5), 3.24 (s, 3H, -OMe), 2.46 (s, 3H, H-9), 1.45 (s, 3H, H-6_a), 1.29 (s, 3H, H-6_b); ¹³C NMR APT (125 MHz, CDCl₃): δ 145.2, 132.9, 130.1, 128.1, 112.9, 109.6, 85.0, 83.7, 81.5, 69.3, 55.2, 26.5, 25.0, 21.8; IR (ATR): 2991, 2947, 1597, 1385, 1357 cm⁻¹. Analytical data are largely consistent with published reports.⁸⁸



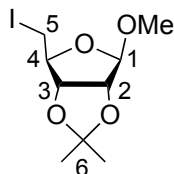
1-O-methyl-2,3-O-isopropylidene-5-O-(trifluoromethanesulfonyl)-β-D-ribofuranoside (20c) Modified from published procedure.⁷² To a solution of pyridine (0.20 mL, 2.48 mmol) and CH₂Cl₂ (8.0 mL) at -10 °C was added dropwise trifluoromethanesulfonyl anhydride (0.37 mL, 2.20 mmol). A solution of protected ribose **17** (0.225g, 1.10 mmol) in anhydrous CH₂Cl₂ (2.0 mL) was added dropwise and stirred at -10 °C. After 1.5 h, monitoring by TLC (1:1 EtOAc/hexanes) indicated consumption of starting material **17**. To the reaction was added cold dH₂O (10 mL). The aqueous layer was extracted with three portions of CH₂Cl₂ (10 mL). Organic layers were pooled and washed with dH₂O (15 mL) and brine (20 mL), dried over MgSO₄, filtered, and concentrated *in vacuo* to a yellow-brown oil as crude product (0.383 g, 1.14 mmol, quantitative). Product decomposed rapidly overnight under refrigeration. TLC (1:1 EtOAc/hexanes): R_f 0.68; ¹H NMR (500 MHz, CDCl₃): δ 5.02 (s, 1H, H-1), 4.68 (d, *J* = 5.9 Hz, 1H, H-2), 4.62 (d, *J* = 5.9 Hz, 1H, H-3), 4.47 (m, 3H, H-4 and H-5), 3.36 (s, 3H, -OMe), 1.49 (s, 3H, H-6_a), 1.33 (s, 3H, H-6_b). ¹H NMR data are consistent with published reports.⁷²



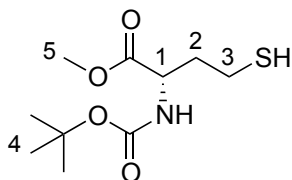
1-O-methyl-2,3-O-isopropylidene-5-chloro-5-deoxy-D-ribofuranoside (20d) From **General procedure for preparation of ribose halides** using LiCl, 90 min. reflux. Product was isolated as a yellow oil after silica gel flash column chromatography with 1:3 EtOAc/hexanes (0.514 g, 2.308 mmol, 82.2%). TLC (1:3 EtOAc/hexanes): R_f 0.63; ¹H NMR (500 MHz, CDCl₃): δ 4.98 (s, 1H, H-1), 4.74 (d, *J* = 5.9 Hz, 1H, H-2), 4.60 (d, *J* = 6.0 Hz, 1H, H-3), 4.31 (dd, *J* = 9.7, *J* = 6.0 Hz, 1H, H-4), 3.55 (m, 1H, H-5_a), 3.46 (m, 1H, H-5_b), 3.33 (s, 3H, -OMe), 1.48 (s, 3H, H-6_a), 1.32 (s, 3H, H-6_b); ¹³C NMR APT (125 MHz, CDCl₃): δ 112.8, 109.6, 86.8, 85.2, 82.3, 55.2, 44.3, 26.5, 25.1; IR (NaCl): 2990, 2939, 2836, 1728, 1450, 1382, 1375 cm⁻¹. ESI-HRMS (*m/z*): [M+H]⁺ calcd for C₉H₁₅ClO₄, 223.0732, found 223.0734.



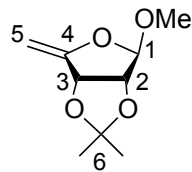
1-*O*-methyl-2,3-*O*-isopropylidene-5-bromo-5-deoxy-D-ribofuranoside (20e) From **General procedure for preparation of ribose halides** using LiBr, 30 min. reflux.⁷³ Product was isolated as a yellow oil after silica gel flash column chromatography with 1:1 EtOAc/hexanes (0.172 g, 0.644 mmol, 64.7%). TLC (1:1 EtOAc/hexanes): R_f 0.63; $^1\text{H NMR}$ (500 MHz, CDCl_3): δ 5.01 (s, 1H, H-1), 4.77 (d, $J = 5.8$ Hz, 1H, H-2), 4.62 (d, $J = 5.9$ Hz, 1H, H-3), 4.39 (dd, $J = 10.0$, $J = 5.9$ Hz, 1H, H-4), 3.43 (m, 1H, H-5_a), 3.35 (s, 3H, -OMe), 3.32 (m, 1H, H-5_b), 1.49 (s, 3H, H-6_a), 1.33 (s, 3H, H-6_b); $^{13}\text{C NMR APT}$ (125 MHz, CDCl_3): δ 112.8, 109.7, 86.8, 85.3, 82.7, 55.2, 32.6, 26.5, 25.1; IR (NaCl): 2990, 2938, 2835, 1731, 1382, 1374 cm^{-1} . NMR data are largely consistent with published reports.⁸⁸



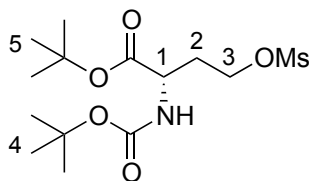
1-*O*-methyl-2,3-*O*-isopropylidene-5-iodo-5-deoxy-D-ribofuranoside (20f) From **General procedure for preparation of ribose halides** using NaI (dried), 45 min. reflux.⁷⁴ Product isolated as a yellow oil after silica gel flash column chromatography with 1:1 EtOAc/hexanes (0.460 g, 1.465 mmol, 79.1%). TLC (1:1 EtOAc/hexanes): R_f 0.64; $^1\text{H NMR}$ (500 MHz, CDCl_3): δ 5.05 (s, 1H, H-1), 4.77 (d, $J = 5.9$ Hz, 1H, H-2), 4.63 (d, $J = 5.9$ Hz, 1H, H-3), 4.44 (dd, $J = 10.0$, $J = 6.1$ Hz, 1H, H-4), 3.37 (s, 3H, -OMe), 3.29 (m, 1H, H-5_a), 3.16 (m, 1H, H-5_b), 1.48 (s, 3H, H-6_a), 1.33 (s, 3H, H-6_b); $^{13}\text{C NMR APT}$ (125 MHz, CDCl_3): δ 112.8, 109.8, 87.6, 85.5, 83.2, 55.4, 26.6, 25.1, 6.8; IR (NaCl): 2989, 2937, 2833, 1382, 1374 cm^{-1} . All analytical data are consistent with published report.¹⁰⁰



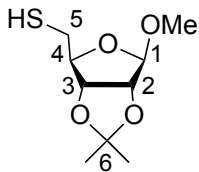
***N*-tert-butoxycarbonyl-L-homocysteine, methyl ester (22)** From **General procedure for TCEP-mediated reductions**, isolated as a clear yellow oil from disulfide **18** (0.495 g, 1.985 mmol, 96.7%). TLC (1:2 EtOAc/hexanes): R_f 0.29; $^1\text{H NMR}$ (500 MHz, CDCl_3): δ 5.06 (br d, $J = 7.1$ Hz, 1H, -NH), 4.47 (m, 1H, H-1), 3.76 (s, 3H, H-5), 2.59 (m, 2H, H-3), 2.11 (m, 1H, H-2_a), 1.93 (m, 1H, H-2_b), 1.57 (m, 1H, -SH), 1.45 (s, 9H, H-4); $^{13}\text{C NMR APT}$ (125 MHz, CDCl_3): δ 173.0, 155.5, 80.3, 52.6, 52.4, 37.4, 28.5, 20.9; IR (ATR): 3357, 2977, 2571, 1740, 1698, 1513, 1165 cm^{-1} . All analytical data are consistent with published reports.⁹⁸



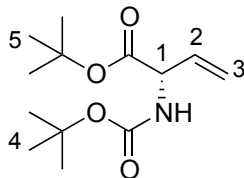
1-*O*-methyl-2,3-*O*-isopropylidene-4-methylene- β -D-erythrofuranoside (26) Independently synthesized with modifications to published procedures.⁸⁸ Mesylated ribose derivative **20a** (0.342 g, 1.21 mmol) was dissolved in THF (12 mL) and cooled to 0 °C. A solution of potassium *tert*-butoxide (2.0 mL, 1 M in THF, 2.0 mmol) was added in one portion. The reaction stirred at room temperature for 1.5 h before vacuum filtration. After the filtrate was evaporated under reduced pressure, the crude product remained a colorless oil. Product **26** was purified to afford a colorless oil after silica gel flash column chromatography in 1:9 EtOAc/hexanes (0.159 g, 0.854 mmol, 70.6%) TLC (1:9 EtOAc/hexanes): R_f 0.38; ^1H NMR (500 MHz, CDCl_3): δ 5.11 (s, 1H, H-1), 5.02 (d, $J = 5.9$ Hz, 1H, H-2), 4.60 (s, 1H, H-5_a), 4.50 (d, $J = 5.9$ Hz, 1H, H-3), 4.39 (s, 1H, H-5_b), 3.41 (s, 3H, -OMe), 1.47 (s, 3H, H-6_a), 1.35 (s, 3H, H-6_b); ^{13}C NMR APT (125 MHz, CDCl_3): δ 161.3, 113.3, 108.4, 88.8, 82.8, 78.8, 55.8, 26.8, 25.8; IR (NaCl): 2990, 2939, 2840, 1672, 1457, 1383, 1374 cm^{-1} . NMR data are largely consistent with published report.⁸⁸



***N*-(*tert*-butoxycarbonyl)-*O*-(methanesulfonyl)-L-homoserine, 1-*tert*-butyl ester (30)** Work performed by Diana Cudia. Modified from published procedure.⁸¹ Homoserine derivative **39** (1.351 g, 4.91 mmol) was dissolved in dry CH_2Cl_2 (45 mL) and cooled to 0 °C. TEA (1.4 mL, 10.04 mmol) and mesyl chloride (0.8 mL, 10.34 mmol) were added successively to the cooled solution. The reaction was warmed to room temperature and stirred overnight (21 h). After monitoring by TLC (1:1 EtOAc/hexanes) indicated completion of the reaction, the solution was concentrated *in vacuo* and the resulting yellow oil was dissolved in CH_2Cl_2 (30 mL). The solution was washed with three portions of dH_2O (40 mL) and the combined aqueous layers were extracted with three portions of CH_2Cl_2 (40 mL). The organic layers were pooled and dried over anhydrous MgSO_4 and filtered. Crude product **30** was isolated after rotary evaporation as a yellow solid. After recrystallization from hexanes/ CH_2Cl_2 (160 mL/25 mL), the product was isolated as white needle-like crystals (1.327 g, 3.75 mmol, 76.5%). TLC (1:1 EtOAc/hexanes): R_f 0.50; mp 91-93 °C, lit.¹⁰¹ 85-87 °C; ^1H NMR (500 MHz, CDCl_3): δ 5.16 (br d, $J = 6.7$ Hz, 1H, -NH), 4.30 (m, 3H, H-1 and H-3), 3.03 (s, 3H, -OMs), 2.31 (m, 1H, H-2_a), 2.06 (m, 1H, H-2_b), 1.48 (s, 9H, H-4 or H-5), 1.45 (s, 9H, H-4 or H-5); ^{13}C NMR (125 MHz, CDCl_3): δ 110.2, 83.0, 66.3, 51.1, 37.5, 32.4, 28.5, 28.1; IR (ATR): 3384, 3008, 2992, 2977, 2944, 1736, 1715, 1515, 1342 cm^{-1} . NMR spectra are consistent with published reports.¹⁰¹



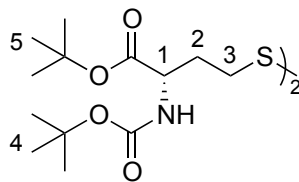
1-*O*-methyl-2,3-*O*-isopropylidene-5-thio- β -D-ribofuranoside (31**)** Thioacetate **40** was deprotected into thiol **31** with modifications to a published procedure.⁸⁴ Thioacetate **40** (0.260 g, 0.991 mmol) was dissolved in MeOH (10 mL) and cooled to -15 °C. A commercial solution of 5.4 M sodium methoxide in methanol (0.51 mL, 2.754 mmol) was added dropwise to the solution. The reaction was allowed to stir for 15 minutes and monitored by TLC (1:3 EtOAc/hexanes) to indicate consumption of starting material. Reaction was moved to room temperature and Amberlite resin IR-120 was quickly added until pH was neutral by pH paper. The resin was filtered off by vacuum filtration, and the solvent was removed under reduced pressure. The resulting crude product was a mixture of thiol **31** and the corresponding oxidized product **43**. Purification by silica gel flash column chromatography (1:10 \rightarrow 1:5 EtOAc/hexanes) afforded thiol **31** as a clear oil (0.112 g, 0.508 mmol). The recovered disulfide product **43** (0.090 g, 0.205 mmol, see below) was subjected to TCEP-mediated reduction: To a ~68 mM solution of **43** in DMF (3 mL) was added a solution of TCEP·HCl in ddH₂O (1 mL). The reaction stirred overnight, and was monitored by TLC (1:3 EtOAc/hexanes) after 19 h to indicate full conversion of the disulfide. The solution was poured onto brine (10 mL) and the aqueous solution was extracted with diethyl ether in series (20 mL, then 3 x 10 mL). Each individual ether layer was washed with four portions of dH₂O (10 mL). The combined washed organic fractions were pooled, washed with brine (25 mL), dried over MgSO₄, filtered, and concentrated by rotary evaporation. The resulting product matched the thiol **31** by ¹H NMR and required no further purification. It was pooled with the thiol isolated after the column to afford **31** with an overall yield of 0.199 g (0.903 mmol, 91.2%). TLC (1:3 EtOAc/hexanes): R_f 0.49; ¹H NMR (500 MHz, CDCl₃): δ 4.97 (s, 1H, H-1), 4.70 (d, J = 5.9 Hz, 1H, H-3), 4.60 (d, J = 5.9, 1H, H-2), 4.18 (t, J = 7.7 Hz, 1H, H-4), 3.36 (s, 3H, -OMe), 2.79 (m, 1H, H-5_a), 2.56 (m, 1H, H-5_b), 1.49 (s, 3H, H-6_a), 1.33 (s, 3H, H-6_b); ¹³C NMR APT (125 MHz, CDCl₃): δ 112.7, 109.7, 89.0, 85.4, 83.1, 55.3, 28.4, 26.6, 25.2; IR (ATR): 2989, 2937, 2834, 2565, 1442, 1373 cm⁻¹. ¹H NMR data are consistent with published report.¹⁰²



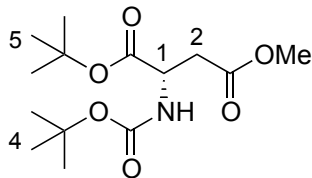
***N*-(*tert*-butoxycarbonyl)-*L*-vinylglycine, *tert*-butyl ester (**32**)** Modified from published procedures.⁹³

Selenide **42** (0.526 g, 1.15 mmol) was dissolved in THF (38 mL) and cooled to -5 °C on a NH₄Cl ice bath for 10 min. A solution of 30% H₂O₂ (11.6 mL) was added dropwise to the solution and allowed to stir at -5 °C. When TLC monitoring (1:3 EtOAc/hexanes) indicated incomplete consumption of starting material after 1 h at -5 °C, the reaction was moved to room temperature and stirred for 2.5 h. Again, the reaction was cooled to, and an additional portion of 30% H₂O₂ (10.0 mL) was added dropwise. After 30 min, TLC indicated consumption of starting material. The reaction was extracted with three portions of ether (50 mL). Organic layers were pooled and washed with one portion each of dH₂O (50 mL) and brine (50 mL), dried over MgSO₄, filtered and concentrated *in vacuo* to a yellow solid coexisting with a clear oil.

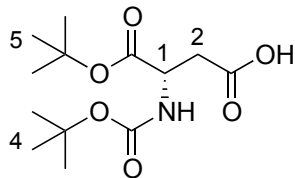
Residue was purified by flash column chromatography (93:7 hexanes/ether) to isolate the product **32** as a clear oil (0.211 g, 0.82 mmol, 71.6%). TLC (1:3 EtOAc/hexanes): R_f 0.47; ¹H NMR (500 MHz, CDCl₃): δ 5.89 (m, 1H, H-2), 5.33 (d, *J* = 17.0 Hz, 1H, H-3_{cis}), 5.22 (d, *J* = 10.4 Hz, 1H, H-3_{trans}), 5.18 (br s, 1H, -NH), 4.73 (br s, 1H, H-1), 1.47 (s, 9H, H-4 or H-5), 1.45 (s, 9H, H-4 or H-5); ¹³C NMR (125 MHz, CDCl₃): δ 169.9, 155.2, 133.5, 116.8, 82.5, 80.0, 56.4, 28.5, 28.1; IR (ATR): 3368, 2979, 2934, 1712, 1494, 1367 cm⁻¹. ¹H NMR data are consistent with published report.⁹³



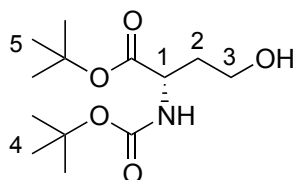
***N,N'*-Di(*tert*-butoxycarbonyl)-L,L-homocystine, bis(*tert*-butyl) ester (**34**)** Work performed by Emily Showell-Rouse with modification of published procedure.^{47,68} To a solution of L,L-homocystine (1.00 g, 3.73 mmol) in 1 M aqueous sodium carbonate (33.5 mL) was added dioxane (30 mL) under ambient conditions. Di-*tert*-butyl dicarbonate (1.72 g, 7.88 mmol) was added in one portion. The cloudy reaction mixture was stirred overnight at room temperature. A 10% w/v solution of aqueous citric acid was added to the milky reaction mixture dropwise at 0 °C. During acidification, the reaction mixture first clarifies while visibly evolving gas (to pH ~ 5.5) and then becomes gelatinous (at pH ~ 4.5). The gelled product was extracted with four portions of EtOAc (40 mL). The organic layers were combined and washed with five portions of dH₂O and one portion of brine (40 mL) and dried over MgSO₄. After filtration, solvent was removed via rotary evaporation to afford a dry, crusty white solid as the intermediate *N,N'*-di(*tert*-butoxycarbonyl)-L,L-homocystine) in good yield (1.52 g, 3.24 mmol, 86.9%). The crude intermediate (1.43 g, 3.05 mmol) was then suspended in 35 mL CH₂Cl₂ and placed at 0 °C. Reagent *tert*-butyl-2,2,2-trichloroacetimidate (2.8 mL, 15.6 mmol) was added in one portion and the reaction allowed to warm to room temperature. After stirring overnight, the reaction mixture was cooled to low temperature (i.e. -80 °C), and the bulk of byproduct 2,2,2-*tert*-butyltrichloroacetimide was removed by filtration. The crude material was concentrated to a thick yellow oil by rotary evaporation. Residual byproduct was removed by filtration from warm hexanes (40 – 50 °C); the product **34** was then isolated after trituration from cold hexanes (1.51 g, 2.60 mmol, 70% over two steps) as a white powder. The solid powder is stable indefinitely at room temperature. TLC (2:1 EtOAc/hexanes): R_f 0.76; mp 65 – 68 °C, lit.⁶⁸ 66-68 °C; ¹H NMR (500 MHz, CDCl₃): δ 5.10 (br d, *J* = 5.4 Hz, 2H, -NH), 4.26 (m, 2H, H-1), 2.69 (m, 4H, H-3), 2.20 (m, 2H, H-2_a), 1.98 (m, 2H, H-2_b), 1.48 (s, 18H, H-4 or H-5), 1.45 (s, 18H, H-4 or H-5); ¹³C NMR (125 MHz, CDCl₃): δ 171.4, 155.5, 82.4, 80.0, 53.4, 34.7, 33.1, 28.5, 28.2; IR (ATR): 3389, 2981, 2937, 1742, 1690, 1506, 1366 cm⁻¹. NMR data are consistent with published reports.⁴⁷



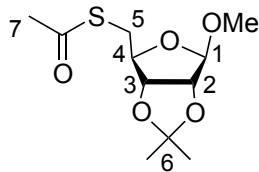
***N*-(*tert*-butoxycarbonyl)-L-aspartic acid, 4-methyl ester, 1-*tert*-butyl ester (**37**)** Work performed in collaboration with Diana Cudia and Emily Murzinski from modified literature procedures.^{40,79,80} Thionyl chloride (0.33 mL, 4.52 mmol) was added dropwise to anhydrous MeOH (33 mL) over 10 min at 0 °C. L-aspartic acid (0.550 g, 4.132 mmol) was added, and the reaction was warmed to room temperature. The reaction stirred for 3.5 h and was monitored by TLC (MeOH). The crude material was concentrated *in vacuo* to afford initial intermediate product **35** (L-aspartic acid, 4-methyl ester) in quantitative yield (0.855 g, 5.81 mmol) as a white solid. Intermediate **35** was then added to a solution of Na₂CO₃ (0.629 g, 5.94 mmol) in dioxane (12 mL) and H₂O (6 mL) at 0 °C. An additional portion of Na₂CO₃ (0.628 g, 5.93 mmol) and (Boc)₂O (1.802 g, 8.26 mmol) were added once CO₂ evolution ceased. The reaction was stirred at 0 °C for 1 h before being warmed to room temperature and continued to stir overnight (16 h). Residual dioxane was removed via rotary evaporation, and the residue was poured onto ice-water (100 mL) and extracted with ether (3 x 50 mL). Saturated aq. NaHSO₄ was added to the water layer dropwise to acidify to pH ~ 2.5. The aqueous layer was extracted with three portions of ether (50 mL) and organic layers were pooled and washed with dH₂O (100 mL). The second intermediate **36** (*N*-(*tert*-butoxycarbonyl)-L-aspartic acid, 4-methyl ester) was recovered as a yellow oil after rotary evaporation (0.711 g, 2.88 mmol, 69.7% (crude) over 2 steps). Lastly, to a solution of crude **36** (0.200 g, 0.809 mmol) in CH₂Cl₂ (1.7 mL) was added *tert*-butyl-2,2,2-trichloroacetimidate (0.589 g, 2.696 mmol) at room temperature. The reaction was stirred overnight (18.5 h) and monitored to completion by TLC (1:1 EtOAc/hexanes). The reaction mixture was cooled to 0 °C. The solid white byproduct was removed by vacuum filtration and the fully-protected aspartic acid derivative **37** was isolated as yellow crystals after filtration from hot hexanes (0.232 g, 0.765 mmol, 65.9% (from crude) over three steps. TLC (1:1 EtOAc/hexanes; ninhydrin stain): R_f 0.57; mp 49-51 °C, lit.⁸⁰ 52-54 °C; ¹H NMR (500 MHz, CDCl₃): δ 5.43 (br d, *J* = 7.1 Hz, 1H, -NH), 4.44 (m, 1H, H-1), 3.68 (s, 3H, -OMe), 2.94 (dd, *J* = 16.6, 3.6 Hz, 1H, H-2_a), 2.76 (dd, *J* = 16.6, 4.9 Hz, 1H, H-2_b), 1.44 (~d, 18H, H-4 and H-5); ¹³C NMR APT (125 MHz, CDCl₃): δ 171.5, 170.1, 155.5, 82.5, 80.0, 52.0, 50.7, 37.1, 28.5, 28.0; IR (ATR): 3409, 2983, 2932, 1736, 1702, 1502 cm⁻¹. NMR spectra are consistent with published reports.⁸⁰



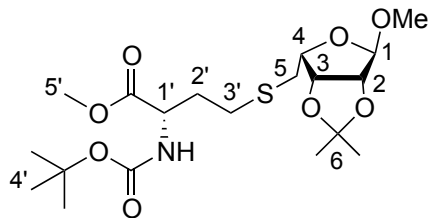
***N*-(*tert*-butoxycarbonyl)-*L*-aspartic acid, 1-*tert*-butyl ester (**38**)** Modified from published procedure.⁷⁹ The fully protected aspartate derivative **37** (0.700 g, 2.308 mmol) was dissolved in a solution of 6:1 acetone/dH₂O (12.25 mL) at 0 °C. A 1 M aq. solution of NaOH (0.960 mL) was added in 10 μL aliquots to maintain a pH ~8.5 – 9. The reaction mixture then stirred at room temperature overnight. The reaction was returned to 0 °C, and additional aliquots of 1 M NaOH (0.620 mL) were added before again stirring overnight at room temperature. The reaction was returned to 0 °C and a final 0.070 mL 1 M NaOH was added in 10 μL aliquots to the solution. The reaction was concentrated by rotary evaporation to ~ 2 mL, and the residue was taken up in 4 mL of dH₂O and washed with one portion of diethyl ether (10 mL). The aqueous layer was brought to 0 °C and acidified to pH 4.5 with dropwise addition of 0.5 M HCl (3.530 mL). The white precipitate that formed was extracted with four portions of diethyl ether (10 mL) and the combined organic layers were washed with dH₂O (10 mL) and brine (10 mL). The organic layer was dried over MgSO₄, filtered, and the solvent was removed by rotary evaporation. Product **38** was isolated as a white solid after recrystallization from hexanes/ether (15 mL/2 mL), (0.319 g, 1.103 mmol, 47.8%). TLC (1:1 EtOAc/hexanes; ninhydrin stain): R_f 0.45; mp 104-105 °C, lit.⁷⁹ 105-106 °C; ¹H NMR (500 MHz, CDCl₃): δ 5.45 (br d, *J* = 7.6 Hz, 1H, -NH), 4.46 (m, 1H, H-1), 3.00 (dd, *J* = 16.9, 3.2 Hz, 1H, H-2_a), 2.83 (dd, *J* = 17.1, 3.9 Hz, 1H, H-2_b), 1.45 (s, 18H, H-4 and H-5); ¹³C NMR (125 MHz, CDCl₃): δ 176.1, 169.9, 155.6, 82.7, 80.3, 50.5, 37.0, 28.5, 28.0; IR (ATR): 3423, 2982, 2934, 2702, 2644, 2568, 1746, 1738, 1694, 1501 cm⁻¹. NMR spectra are consistent with published reports,⁸² all spectra match those of commercial sample.



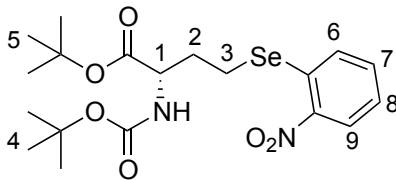
***N*-(*tert*-butoxycarbonyl)-*L*-homoserine, 1-*tert*-butyl ester (**39**)** Work performed in collaboration with Diana Cudia and Emily Murzinski. Modified from published procedures.^{81,82} To a stirring solution of *N*-(*tert*-butoxycarbonyl)-*L*-aspartic acid, 1-*tert*-butyl ester **38** (0.306 g, 1.11 mmol) in dry THF (3.25 mL) at -5 °C was added triethylamine (0.15 mL, 1.08 mmol). Ethyl chloroformate (0.10 mL, 1.05 mmol) was added dropwise, and the reaction was allowed to stir at -5 °C. After 45 min, a precipitate had formed and was removed via vacuum filtration and washed with 5 mL of anhydrous THF. The resulting filtrate was added dropwise over ~20 min to a stirred solution of sodium borohydride (0.096 g, 2.56 mmol) in 0.80 mL of dH₂O at 10-12 °C. The reaction was allowed to warm to room temperature and stirred for an additional 4 h. The solution was brought to 0 °C and acidified to pH 2 with 1 M HCl. The solution was extracted with diethyl ether (3 x 10 mL). The combined organic layers were dried with anhydrous MgSO₄ and filtered before concentration by rotary evaporation to give a colorless oil. After purification by silica gel flash column chromatography (1:4 EtOAc/hexanes), the protected-homoserine product **39** was isolated as a colorless oil (0.218 g, 0.792 mmol, 71.4%) TLC (1:1 EtOAc/hexanes; ninhydrin stain): R_f 0.65; ¹H NMR (500 MHz, CDCl₃): δ 5.33 (br d, *J* = 7.4 Hz, 1H, -NH), 4.36 (m, 1H, H-1), 3.71-3.60 (m, 2H, H-3), 3.40 (br d, *J* = 3.9 Hz, 1H, -OH), 2.14 (m, 2H, H-2), 1.47 (s, 9H, H-4 or H-5), 1.45 (s, 9H, H-4 or H-5); ¹³C NMR (125 MHz, CDCl₃): δ 172.2, 156.8, 82.5, 80.5, 58.4, 51.0, 36.8, 28.4, 28.1; IR (ATR): 3378, 2978, 2934, 1692, 1501, 1366 cm⁻¹. NMR data are consistent with published report.⁸²



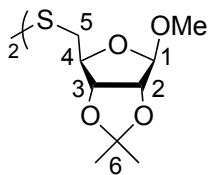
S-acetyl-1-O-methyl-2,3-O-isopropylidene-5-thio- β -D-ribofuranoside (40) Adapted with modifications to published procedure.⁸³ A mixture of mesylate **20a** (0.398 g, 1.41 mmol) and potassium thioacetate (0.318 g, 2.78 mmol) in absolute ethanol (14 mL) was heated to reflux for 2.5 days. The reaction refluxed for 6 hours per day with 0.5 equivalent of potassium thioacetate added at three hour intervals during the reflux period (reaction stirred at room temperature overnight). After consumption of the starting material was determined by TLC (1:3 EtOAc/hexanes), heat was removed and the mixture was brought to room temperature. The reaction mixture was poured onto CH₂Cl₂ (20 mL) and washed with dH₂O (20 mL). The aqueous layer was extracted with three portions of CH₂Cl₂ (15 mL). The organic layers were pooled, washed with 20 mL portions each of dH₂O and brine, dried over MgSO₄ and filtered. After concentration by rotary evaporation, product was recovered as a yellow-white oily solid. Purification by silica gel flash column chromatography (1:9 \rightarrow 1:4 EtOAc/hexanes) afforded thioacetate **40** as a yellow oil (0.267 g, 1.02 mmol, 72.3%). TLC (1:3 EtOAc : hexanes): R_f 0.43; ¹H NMR (500 MHz, CDCl₃): δ 4.96 (s, 1H, H-1), 4.62 (d, J = 5.9 Hz, 1H, H-3), 4.58 (d, J = 5.9 Hz, 1H, H-2), 4.19 (t, J = 7.8 Hz, 1H, H-4), 3.35 (s, 3H, -OMe), 3.02-3.12 (m, 2H, H-5), 2.35 (s, 3H, H-7), 1.45 (s, 3H, H-6_a), 1.30 (s, 3H, H-6_b); ¹³C NMR APT (125 MHz, CDCl₃): δ 194.8, 112.7, 109.9, 85.9, 85.5, 83.4, 55.1, 32.8, 30.7, 26.6, 25.2; IR (ATR): 2989, 2937, 2834, 1693, 1373 cm⁻¹.



N-tert-butoxycarbonyl-S-(5-deoxy-1-O-methyl-2,3-O-isopropylidene-L-lyxofuranos-5-yl)-L-homocysteine, methyl ester (41) Adapted with modifications to published procedure.⁶³ In a flat-bottom test tube (10.5 mm diameter, 0.7 mm wall thickness) with rubber septum, the alkene **26** (0.037 g, 0.199 mmol) was dissolved in a solution of thiol **22** (0.5 mL, 0.050 g/mL, 0.100 mmol) in anhydrous CH₂Cl₂ under an atmosphere of argon. A solution of DPAP (0.5 mL, 0.003 g/mL, 0.012 mmol) in anhydrous CH₂Cl₂ was then added to the reaction. The reaction was again placed under an argon atmosphere, sealed with the rubber septum and set to rotate in a carousel irradiated under UV at 365 nm. The tube was manually shaken every 5 min for first half hour to ensure adequate mixing. After 2 h, TLC (1:3 EtOAc/hexanes) indicated apparent consumption of the thiol. The reaction was stopped by solvent removal *in vacuo*. After purification by silica gel flash column chromatography (1:4 EtOAc/hexanes) the product **41** was isolated as a colorless oil (0.030 g, 0.069 mmol, 68.9%). TLC (1:3 EtOAc/hexanes): R_f 0.31; ¹H NMR (500 MHz, CDCl₃): δ 5.14 (br d, J = 8.1 Hz, 1H, -NH), 4.88 (s, 1H, H-1), 4.71 (dd, J = 5.9, J = 3.6 Hz, 1H, H-3), 4.56 (d, J = 5.9 Hz, 1H, H-2), 4.40 (m, 1H, H-1'), 4.05 (m, 1H, H-4), 3.75 (s, 3H, H-5'), 3.33 (s, 3H, -OMe), 2.78-2.87 (m, 2H, H-5), 2.65 (t, J = 7.8 Hz, 2H, H-3'), 2.14 (m, 1H, H-2'_a), 1.96 (m, 1H, H-2'_b), 1.46 (s, 3H, H-6_a), 1.44 (s, 9H, H-4'), 1.33 (s, 3H, H-6_b); ¹³C NMR APT (125 MHz, CDCl₃): δ 112.8, 107.2, 85.2, 80.2, 80.1, 54.8, 53.0, 52.5, 32.8, 30.0, 28.7, 28.5, 26.3, 25.2; IR (ATR): 3359, 2979, 2935, 1744, 1716, 1512, 1367 cm⁻¹.



tert-butyl, 2-tert-butoxycarbonylamino-4-(2-nitrophenylselenyl)butanoate (42) Modified from published procedure.⁹³ To 2-nitrophenyl selenocyanate (0.796 g, 3.51 mmol) was added a solution of protected homoserine intermediate **39** (0.438 g, 1.59 mmol) in dry THF (20 mL). To this mixture was added dropwise a solution of tri-*n*-butyl phosphine (0.54 mL, 2.19 mmol) in dry THF (5 mL) over a period of ~5 min. The reaction stirred at room temperature for 105 minutes before monitoring by TLC (1:3 EtOAc/hexanes) indicated consumption of starting material **39**. The reaction was concentrated by rotary evaporation and the remaining residue was purified by silica gel flash column chromatography (9:1 3:1 hexanes/ether) after which product was recovered as a yellow solid (0.528g, 1.15 mmol, 72.2%). TLC (1:3 EtOAc/hexanes; ninhydrin stain): R_f 0.29; $^1\text{H NMR}$ (500 MHz, CDCl_3): δ 8.30 (d, $J = 8.2$ Hz, 1H, H-9), 7.52 (m, 2H, H-6 and H-7), 7.33 (m, 1H, H-8), 5.20 (br d, $J = 7.6$ Hz, 1H, -NH), 4.32 (m, 1H, H-1), 2.97 (m, 1H, H-3_a), 2.88 (m, 1H, H-3_b), 2.29 (m, 1H, H-2_a), 2.06 (m, 1H, H-2_b), 1.48 (s, 9H, H-4 or H-5), 1.46 (s, 9H, H-4 or H-5); $^{13}\text{C NMR APT}$ (125 MHz, CDCl_3): δ 133.8, 128.9, 126.7, 125.7, 110.2, 82.8, 54.6, 32.5, 28.5, 28.2, 21.5; IR (ATR): 3390, 2981, 2933, 1718, 1690, 1505 cm^{-1} . $^1\text{H NMR}$ data are consistent with published report.⁹³



Bis(1-O-methyl-5-deoxy-2,3-O-isopropylidene- β -D-ribofuranos-5-yl)-5,5'-disulfide (43) Formed as byproduct in synthesis of **31** (see procedure **31** above). TLC (1:3 EtOAc/hexanes): R_f 0.38; $^1\text{H NMR}$ (500 MHz, CDCl_3): δ 4.97 (s, 2H, H-1), 4.73 (d, $J = 5.9$ Hz, 2H, H-3), 4.61 (d, $J = 6.0$, 2H, H-2), 4.45 (t, $J = 7.6$ Hz, 2H, H-4), 3.35 (s, 6H, -OMe), 2.96 (m, 2H, H-5_a), 2.78 (m, 2H, H-5_b), 1.49 (s, 6H, H-6_a), 1.33 (s, 6H, H-6_b); $^{13}\text{C NMR}$ (125 MHz, CDCl_3): δ 112.7, 109.8, 85.5, 85.4, 83.3, 55.2, 42.0, 26.6, 25.1; IR (ATR): 2992, 2921, 2850, 1736, 1450, 1379 cm^{-1} . $^1\text{H NMR}$ data are consistent with published report.¹⁰²

References

1. The Infectious Diseases Society of America. Facts about Antibiotic Resistance Home Page. http://www.idsociety.org/AR_Facts/ (accessed Dec 3, 2017).
2. Centers for Disease Control and Prevention. Antibiotic / Antimicrobial Resistance Home Page. <https://www.cdc.gov/drugresistance/index.html> (accessed Dec 3, 2017).
3. National Institute of Allergy and Infectious Diseases. History, MRSA, Antimicrobial Resistance Home Page. <https://www.niaid.nih.gov/research/mrsa-antimicrobial-resistance-history> (accessed Dec 3, 2017).
4. Miller, M.B.; Bassler, B.L. *Annu. Rev. Microbiol.* **2001**, *55*, 165-199.
5. Xavier, K.B.; Bassler, B.L. *Curr. Opin. Microbiol.* **2003**, *6*, 191-197.
6. Fuqua, W.; Winans, S.; Greenberg, E. *J. Bacteriol.*, **1994**, *176*, 269-275.
7. LaSarre, B.; Federle, M.J. *Microbiol. Mol. Biol. Rev.* **2013**, *77*, 73-111.
8. Rocha, J.; Flores, V.; Cabrera, R.; Soto-Guzman, A.; Granados, G.; Juaristi, E.; Guarneros, G.; de la Torre, M. *Appl. Microbiol. Biotechnol.* **2012**, *94*, 1069-1078.
9. Rocha-Estrada, J.; Aceves-Diez, A.E.; Guarneros, G.; de la Torre, M. *Appl. Microbiol. Biotechnol.* **2010**, *87*, 913-923.
10. Soares, J.A.; Ahmer, B.M. *Curr. Opin. Microbiol.* **2011**, *14*, 188-193.
11. Von Bodman, S.B.; Bauer, W.D.; Coplin, D.L. *Annu. Rev. Phytopathol.* **2003**, *41*, 455-482.
12. Moreira, C.G.; Weinshenker, D.; Sperandio, V. *Infect. Immun.* **2010**, *78*, 914-926.
13. Thoendel, M.; Kavanaugh, J.S.; Flack, C.E.; Horswill, A.R. *Chem. Rev.* **2011**, *111*, 117-151.
14. Havarstein, L.S.; Coomaraswamy, G.; Morrison, D.A. *Proc. Natl. Acad. Sci. U.S.A.* **1995**, *92*, 11140-11144.
15. Ng, W.L.; Bassler, B.L. *Annu. Rev. Genet.* **2009**, *43*, 197-222.
16. Bassler, B.L. *Mol. Microbiol.* **1994**, *13*(2), 273-286.
17. Tay, S.B.; Yew, W.S. *Int. J. Mol. Sci.* **2013**, *14*, 16570-16599.
18. André, J.-B.; Godelle, B. *Ecol. Lett.* **2005**, *8*, 800-810.
19. Schauder, S.; Shokat, K.; Surette, M.G.; Bassler, B.L. *Mol. Microbiol.* **2001**, *41*, 463-476.
20. Pereira, C.S.; Thompson, J.A.; Xavier, K.B. *FEMS Microbiol. Rev.* **2013**, *37*, 156-181.
21. (a) Bassler, B.L.; Wright, M.; Silverman, M.R. *Mol. Microbiol.* **1994**, *13*, 273-286; (b) Henke, J.M.; Bassler, B.L. *J. Bacteriol.* **2004**, *186*, 6902-6914.

22. Li, L.; Xu, Z.; Zhou, Y.; Li, T.; Sun, L.; Chen, H.; Zhou, R. *Microb. Pathog.* **2011**, *50*, 293-302.
23. Babb, K.; von Lackum, K.; Wattier, R.L.; Riley, S.P.; Stevenson, B. *J. Bacteriol.* **2005**, *187*, 3079-3087.
24. Ohtani, K.; Hayashi, H.; Shimuzu, T. *Mol. Microbiol.* **2002**, *44*, 171-179.
25. (a) Bansal, T.; Jesudhasan, P.; Pillai, S.; Wood, T.K.; Jayaraman, A. *Appl. Microbiol. Biotechnol.* **2008**, *78*, 811-819; (b) Sperandio, V.; Mellies, J.L.; Nguyen, W.; Shin, S.; Kaper, J.B. *Proc. Natl. Acad. Sci. USA.* **1999**, *96*, 15196-15201; (c) Sperandio, V.; Torres, A.G.; Kaper, J.B. *Mol. Microbiol.* **2002**, *43*, 809-821; (d) Sperandio, V.; Li, C.C.; Kaper, J.B. *Infect. Immun.* **2002**, *70*, 3085-3093.
26. Rader, B.A.; Campagna, S.R.; Semmelhack, M.F.; Bassler, B.L.; Guillemin, K. *J. Bacteriol.* **2007**, *189*, 6109-6117.
27. Duan, K.; Dammel, C.; Stein, J.; Rabin, H.; Surette, M.G. *Mol. Microbiol.* **2003**, *50*, 1477-1491.
28. (a) Choi, J.; Shin, D.; Ryu, S. *Infect. Immun.* **2007**, *75*, 4885-4890; (b) Choi, J.; Shin, D.; Kim, M.; Park, J.; Lim, S.; Ryu, S. *PLoS ONE.* **2012**, *7*, e37059.
29. Zhao, L.; Xue, T.; Shang, F.; Sun, H.; Sun, B. *Infect. Immun.* **2010**, *78*, 3506-3515.
30. (a) Ahmed, N.A.; Petersen, F.C.; Scheie, A.A. *Oral. Microbiol. Immunol.* **2008**, *23*, 492-497; (b) Ahmed, N.A.; Petersen, F.C.; Scheie, A.A. *Antimicrob. Agents Chemother.* **2009**, *53*, 4258-4263.
31. (a) Miller, M.B.; Skorupski, K.; Lenz, D.H.; Taylor, R.K.; Bassler, B.L. *Cell.* **2002**, *110*, 303-314; (b) Zhu, J.; Miller, M.B.; Vance, R.E.; Dziejman, M.; Bassler, B.L.; Mekalanos, J.J. *P. Natl. Acad. Sci. USA.* **2002**, *99*, 3129-3134; (c) Hammer, B.K.; Bassler, B.L. *Mol. Microbiol.* **2003**, *50*, 101-104; (d) Antonova, E.S.; Hammer, B.K. *FEMS Microbiol. Lett.* **2011**, *322*, 68-76.
32. Chen, X.; Schauder, S.; Potier, N.; Van Dorsselaer, A.; Pelczer, I.; Bassler, B.L.; Hughson, F.M. *Nature* **2002**, *415*, 545-549.
33. Miller, S.T.; Xavier, K.B.; Capagne, S.R.; Taga, M.E.; Semmelhack, M.F.; Bassler, B.L.; Hughson, F.M. *Mol. Cell* **2004**, *15*, 677-687.
34. Federle, M.J. *Contrib. Microbiol.* **2009**, *16*, 18-32.
35. Winzer, K.; Hardie, K.R.; Burgess, N.; Doherty, N.; Kirke, D.; Holden, M.T.; Linfoth, R.; Cornell, K.A.; Taylor, A.J.; Hill, P.J.; Williams, P. *Microbiology* **2002**, *148*, 909-922.
36. Vendeville, A.; Winzer, K.; Heurlier, K.; Tang, C.M.; Hardie, K.R. *Nat. Rev. Microbiol.* **2005**, *3*, 383-396.
37. Nibras, A.A.M.A.; Petersen, F.C.; Scheie, A.A. *J. Antimicrob. Chemother.* **2007**, *60*, 49-53.
38. Roy, V.; Meyer, M.T.; Smith, J.A.I.; Gamby, S.; Sintim, H.O.; Ghodssi, R.; Bentley, W.E. *Appl. Microbiol. Biotechnol.* **2013**, *97*, 2627-2638.

39. Centers for Disease Control and Prevention. About Antimicrobial Resistance Home Page. <https://www.cdc.gov/drugresistance/about.html> (accessed Dec 3, 2017).
40. Alfaro, J.F.; Zhang, T.; Wynn, D.P.; Karschner, E.L.; Zhou, Z.S. *Org. Lett.* **2004**, *6*(18), 3043-3046.
41. Wnuk, S.F.; Robert, J.; Sobczak, A.J.; Meyers, B.P.; Malladi, V.L.A.; Zhu, J.; Gopishetty, B.; Pei, D. *Bioorg. Med. Chem.* **2009**, *17*, 6699-6706.
42. Shen, G.; Rajan, R.; Zhu, J.; Bell, C.E.; Pei, D. *J. Med. Chem.* **2006**, *49*, 3003-3011.
43. Malladi, V.L.A.; Sobczak, A.J.; Meyer, T.M.; Pei, D.; Wnuk, S.F. *Bioorg. Med. Chem.* **2011**, *19*, 5507-5519.
44. Gopishetty, B.; Zhu, J.; Rajan, R.; Sobczak, A.J.; Wnuk, S.F.; Bell, C.E.; Pei, D. *J. Am. Chem. Soc.* **2009**, *131*, 1243-1250.
45. (a) Hilgers, M.T.; Ludwig, M.L. *P. Natl. Acad. Sci. USA.* **2001**, *98*, 11169-11174; (b) Ruzheinikov, S.N.; Das, S.K.; Sedelnikova, S.E.; Hartley, A.; Foster, S.J.; Horsburgh, M.J.; Cox, A.G.; McCleod, C.W.; Mekhalfia, A.; Blackburn, G.M.; Rice, D.W.; Baker, P.J. *J. Mol. Biol.* **2001**, *313*, 111-122; (c) Lewis, H.A.; Furlong, E.B.; Laubert, B.; Eroshkina, G.A.; Batiyenko, Y.; Adams, J.M.; Bergseid, M.G.; Marsh, C.D.; Peat, T.S.; Sanderson, W.E. et al. *Structure* **2001**, *9*, 527-537.
46. Pei, D.; Zhu, J. *Curr. Opin. Chem. Biol.* **2004**, *8*, 492-497.
47. Zhu, J.; Xubo, H.; Dizin, E.; Pei, D. *J. Am. Chem. Soc.* **2003**, *125*, 13379-13381.
48. Huang, W.J.; Gherib, R.; Gauld, J.W. *J. Phys. Chem. B.* **2012**, *116*, 8916-8929.
49. Wnuk, S.F.; Lalama, J.; Garmendia, C.A.; Robert, J.; Zhu, J.; Pei, D. *Bioorg. Med. Chem.* **2008**, *16*, 5090-5102.
50. Zhu, J.; Dizin, E.; Hu, X.; Wavreille, A.-S.; Park, J.; Pei, D. *Biochemistry.* **2003**, *42*, 4717-4726.
51. ThermoFisher Scientific. DTNB (Ellman's Reagent) Description Page. <https://www.thermofisher.com/order/catalog/product/22582> (accessed Dec 3, 2017).
52. Cheng, J.H.; Ramesh, C.; Kao, H.L.; Wang, Y.J.; Chan, C.C.; Lee, C.F. *J. Org. Chem.* **2012**, *77*, 10369-10374.
53. Tabor, A.B. *Org. Biomol. Chem.* **2011**, *9*, 7606-7628.
54. Probert, J.M.; Rennex, D.; Bradley, M. *Tetrahedron Lett.* **1996**, *37*, 1101-1104.
55. Olsen, R.K.; Kini, G.D.; Hennen, W.J. *J. Org. Chem.* **1985**, *50*, 4332-4336.
56. Zhu, X.; Schmidt, R.R. *Eur. J. Org. Chem.* **2003**, 4069-4072.
57. Triola, G.; Brunsveld L.; Waldmann, H. *J. Org. Chem.* **2008**, *73*, 3646-3649.

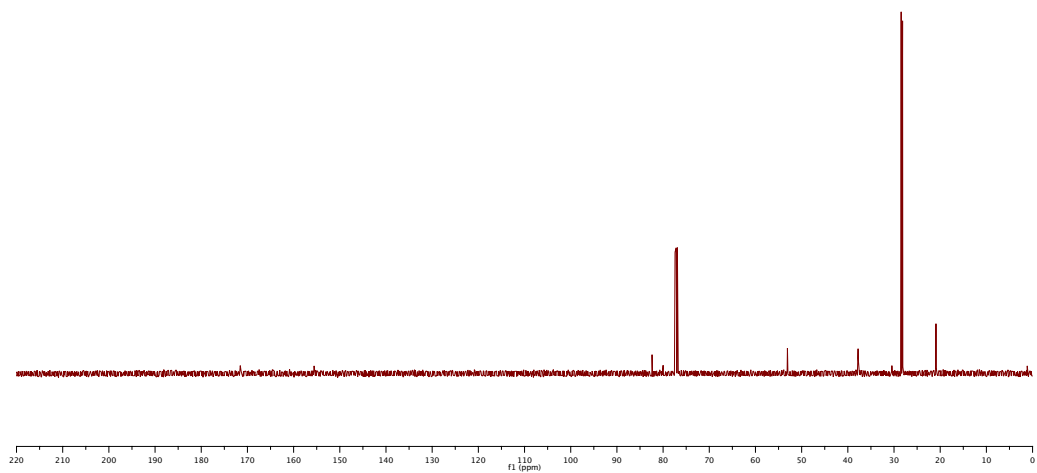
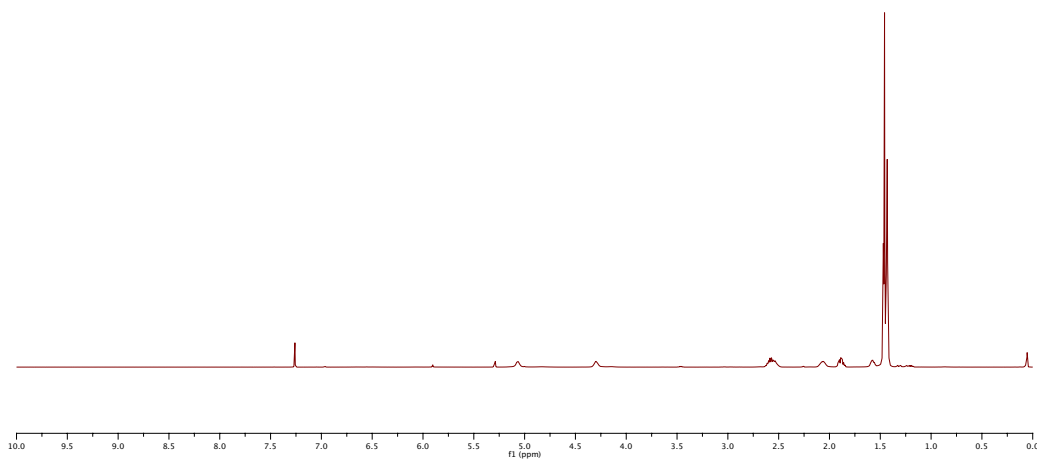
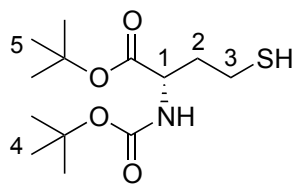
58. Guillerme, G.; Allart, B. *J. Labelled Compd. Radiopharm.* **1991**, *29*, 1027-1032.
59. Zhao, G.; Wan, W.; Mansouri, S.; Alfaro, J.F.; Bassler, B.L.; Cornell, K.A.; Zhou, Z.S. *Bioorg. Med. Chem. Lett.* **2003**, *13*, 3897-3900.
60. Liu, Ruoyi. Synthesis of *S*-Ribosyl-L-Homocysteine and Analogs Modified at the Homocysteine-C3 Position. M.S. Thesis, University of San Francisco, San Francisco, CA, 2012.
61. Lowe, A.B. *Polym. Chem.* **2010**, *1*, 17-36.
62. Dondoni, A.; Massi, A.; Nanni, P.; Roda, A. *Chem. Eur. J.* **2009**, *15*, 11444-11449.
63. Fiore, M.; Marra, A.; Dondoni, A. *J. Org. Chem.* **2009**, *74*, 4422-4425.
64. Fiore, M.; Lo Conte, M.; Pacifico, S.; Marra, A.; Dondoni, A. *Tetrahedron Lett.* **2011**, *52*, 444-447.
65. Carey, Francis A. *Organic Chemistry*; 5th Ed; McGraw-Hill: New York, 2003; 330-338.
66. Smith, Michael B.; March, J. *March's Advanced Organic Chemistry: Reactions, Mechanisms, and Structure*; 5th Ed.; Wiley: New York, 2001; 431-454.
67. Klein, D. *Organic Chemistry*; 2nd Ed.; Wiley: New York, 2015; 325.
68. Bourdier, T.; Fookes, C.J.R.; Pham, T.Q.; Gerguric, I.; Katsifis, A. *J. Labelled Compd. Radiopharm.* **2008**, *51*, 369-373.
69. Bolitho, M.E.; Corcoran, B.J.; Showell-Rouse, E.I.; Wang, K.Q. *Carbohydr. Res.* **2014**, *394*, 32-38.
70. Albinia, P.A. Small Molecule Modulation of Biological Systems. Ph.D. Dissertation, Princeton University, Princeton, NJ, 2008.
71. Wartchow, C.A.; Wang, P.; Bednarski, M.D.; Callstrom, M.R. *J. Org. Chem.* **1995**, *60*, 2216-2226.
72. McCartney, J.L.; Meta, C.T.; Cicchillo, R.M.; Bernardina, M.D.; Wagner, T.R.; Norris, P. *J. Org. Chem.* **2003**, *68*(26), 10152-10155.
73. Gyepes, A.; Schäffer, R.; Bajor, G.; Woller, A.; Fodor, P. *Polyhedron* **2008**, *27*, 2655-2661.
74. Kissman, H.M.; Baker, B.R. *J. Am. Chem. Soc.* **1957**, *79*, 5534-5540.
75. Showell-Rouse, E.I. M.S. Thesis, University of San Francisco, San Francisco, CA, 2017.
76. Green, W. *Protective Groups in Organic Synthesis*; 3rd Ed.; Wiley: New York, 1999.
77. Carey, Francis A. *Organic Chemistry*; 5th Ed; McGraw-Hill: New York, 2003; 348-349.
78. Cudia, D.L. University of San Francisco, San Francisco, CA. Undergraduate Research Report, 2015.

79. Ramalingam, K.; Woodard, R.W. *J. Org. Chem.* **1988**, *53*, 1900-1903.
80. Dörr, A.; Lubell, W.D. *Biopolymers* **2007**, *88*, 290-299.
81. May, A.L.; Eisenhauer, M.E.; Coulston, K.S.; Campagna, S.R. *Anal. Chem.* **2012**, *84*, 1243-1252.
82. Qu, W.; Zha, Z.; Ploessel, K.; Lieberman, B.P.; Zhu, L.; Wise, D.; Thompson, C.; Kung, H.F. *J. Am. Chem. Soc.* **2011**, *133*, 1122-1133.
83. Hughes, N.A.; Munkombwe, N.M. *Carbohydr. Res.* **1985**, *136*, 397-409.
84. Almendros, M.; Danalev, D.; François-Heude, M.; Loyer, P.; Legentil, L.; Nugier-Chauvin, C.; Daniellou, R.; Ferrières, V. *Org. Biomol. Chem.* **2011**, *9*, 8371-8378.
85. Nair, D.P.; Podgórski, M.; Chantani, S.; Gong, T.; Xi, W.; Fenoli, C.R.; Bowman, C.N. *Chem. Mater.* **2014**, *26*, 724-744.
86. Dénès, F.; Pichowicz, M.; Povie, G.; Renaud, P. *Chem Rev.* **2014**, *114*, 2587-2693.
87. Carey, Francis A. *Organic Chemistry*; 5th Ed; McGraw-Hill: New York, 2003; 172.
88. Ivanova, N.A.; Valiullina, Z.R.; Shitikova, O.V.; Mifakhov, M.S. *Russ J. Org. Chem.* **2007**, *43*, 742-746.
89. Fischer, H.; Baer, R.; Hany, R.; Verhoolen, I.; Walbiner, M. *J. Chem. Soc., Perkin Trans. 2.* **1990**, 787-798.
90. Serianni, A.S.; Barker, R. *J. Org. Chem.* **1984**, *49*, 3292-3300.
91. Stenutz, R. Conformation Analyses of Carbohydrates, NMR Page. <http://www.stenutz.eu/conf/index.html> (accessed Dec 3, 2017).
92. Napolitano, J.G.; Gavín, J.A.; García, C.; Norte, M.; Fernández, J.J.; Hernández Daranas, A. *Chem. Eur. J.* **2011**, *17*, 6338-6347.
93. Siebum, A.H.G.; Woo, W.S.; Raap, J.; Lugtenburg, J. *Eur. J. Org. Chem.* **2004**, 2905-2913.
94. Cai, X.; Ng, K.; Panesar, H.; Moon, S.J.; Paredes, M.; Ishida, K.; Hertweck, C.; Minehan, T.G. *Org. Lett.* **2014**, *16*, 2962-2965.
95. Aïssa, C. *J. Org. Chem.* **2006**, *71*, 360-363.
96. Burtin, G.; Corringier, P.; Young, D.W. *J. Chem. Soc., Perkin Trans. 1.* **2000**, 3451-3459.
97. Kumar, J.D.K.; Baskaran, S. *J. Org. Chem.* **2005**, *70*, 4520-4523.
98. Lherbet, C.; Keillor, J.W. *Org. Biomol. Chem.* **2004**, *2*, 238-245.
99. Ferreira, S.B.; Soderó, A.C.R.; Cardoso, M.F.C.; Lima, E.S.; Kaiser, C.R.; Silva, F.P.; Ferreira, V.F. *J. Med. Chem.* **2010**, *53*, 2364-2375.

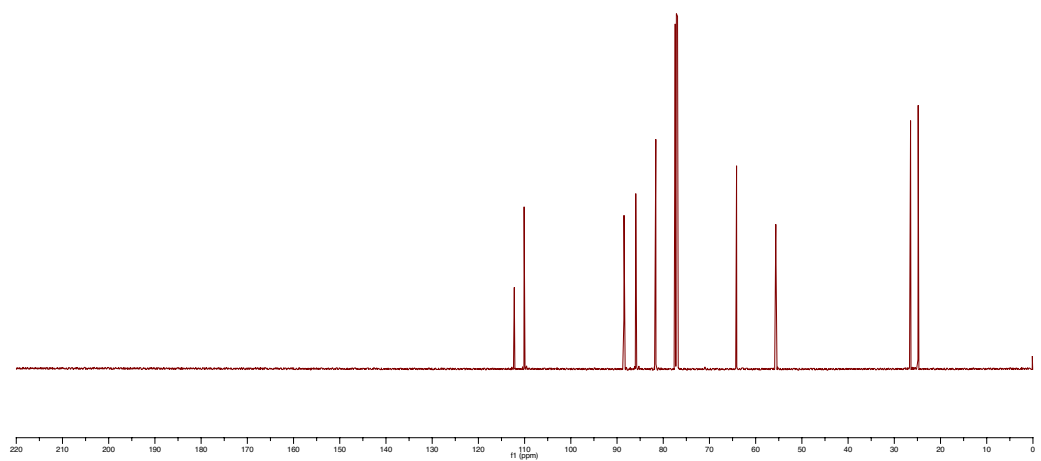
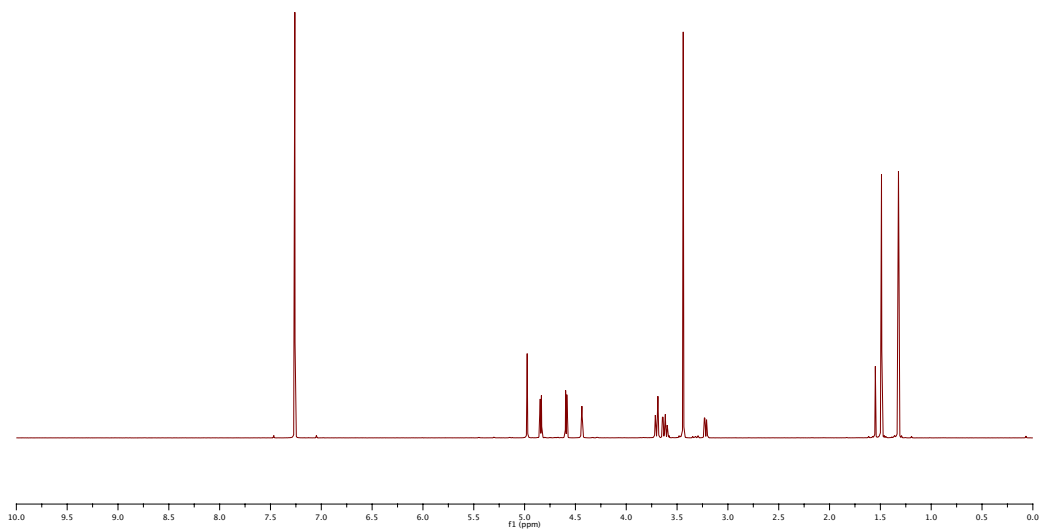
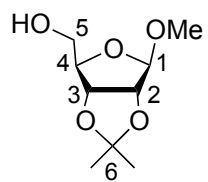
100. Palmer, A.M.; Jäger, V. *Eur. J. Org. Chem.* **2001**, 1293-1308.
101. Flohr, A.; Aemissegger, A.; Hilvert, D. *J. Med Chem.* **1999**, *42*, 2633-2640.
102. Pakulski, Z.; Pierożyński, D.; Zamojski, A. *Tetrahedron* **1994**, *50*, 2975-2992.

Supporting Information: ¹H and ¹³C NMR Spectra

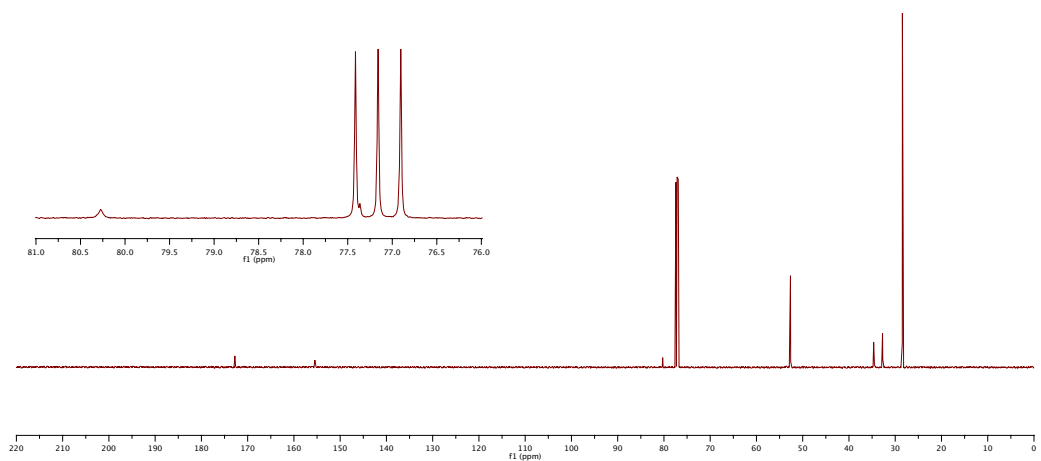
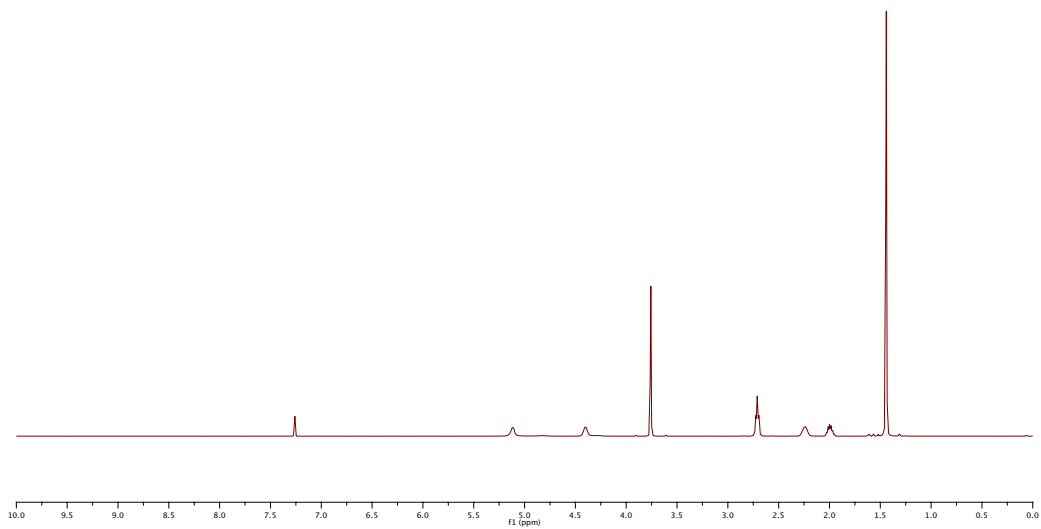
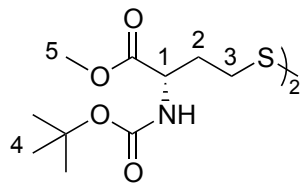
<i>N</i> - <i>tert</i> -butoxycarbonyl-L-homocysteine, <i>tert</i> -butyl ester (7)	84
1- <i>O</i> -methyl-2,3- <i>O</i> -isopropylidene-D-ribofuranoside (17)	85
<i>N,N'</i> -Di(<i>tert</i> -butoxycarbonyl)-L,L-homocystine, bis(methyl) ester (18)	86
<i>N</i> - <i>tert</i> -butoxycarbonyl- <i>S</i> -(5-deoxy-1- <i>O</i> -methyl-2,3- <i>O</i> -isopropylidene-D-ribofuranos-5-yl)-L-homocysteine, methyl ester (19a)	87
<i>N</i> - <i>tert</i> -butoxycarbonyl- <i>S</i> -(5-deoxy-1- <i>O</i> -methyl-2,3- <i>O</i> -isopropylidene-D-ribofuranos-5-yl)-L-homocysteine, <i>tert</i> -butyl ester (19b)	89
1- <i>O</i> -methyl-2,3- <i>O</i> -isopropylidene-5- <i>O</i> -(methanesulfonyl)-β-D-ribofuranoside (20a)	91
1- <i>O</i> -methyl-2,3- <i>O</i> -isopropylidene-5- <i>O</i> -(<i>p</i> -toluenesulfonyl)-β-D-ribofuranoside (20b)	92
1- <i>O</i> -methyl-2,3- <i>O</i> -isopropylidene-5- <i>O</i> -(trifluoromethanesulfonyl)-β-D-ribofuranoside (20c)	93
1- <i>O</i> -methyl-2,3- <i>O</i> -isopropylidene-5-chloro-5-deoxy-D-ribofuranoside (20d)	94
1- <i>O</i> -methyl-2,3- <i>O</i> -isopropylidene-5-bromo-5-deoxy-D-ribofuranoside (20e)	95
1- <i>O</i> -methyl-2,3- <i>O</i> -isopropylidene-5-iodo-5-deoxy-D-ribofuranoside (20f)	96
<i>N</i> - <i>tert</i> -butoxycarbonyl-L-homocysteine, methyl ester (22)	97
1- <i>O</i> -methyl-2,3- <i>O</i> -isopropylidene-4-methylene-β-D-erythrofuranoside (26)	98
<i>N</i> -(<i>tert</i> -butoxycarbonyl)- <i>O</i> -(methanesulfonyl)-L-homoserine, 1- <i>tert</i> -butyl ester (30)	99
1- <i>O</i> -methyl-2,3- <i>O</i> -isopropylidene-5-thio-β-D-ribofuranoside (31)	100
<i>N</i> -(<i>tert</i> -butoxycarbonyl)-L-vinylglycine, <i>tert</i> -butyl ester (32)	101
<i>N,N'</i> -Di(<i>tert</i> -butoxycarbonyl)-L,L-homocystine, bis(<i>tert</i> -butyl) ester (34)	102
<i>N</i> -(<i>tert</i> -butoxycarbonyl)-L-aspartic acid, 4-methyl ester, 1- <i>tert</i> -butyl ester (37)	103
<i>N</i> -(<i>tert</i> -butoxycarbonyl)-L-aspartic acid, 1- <i>tert</i> -butyl ester (38)	104
<i>N</i> -(<i>tert</i> -butoxycarbonyl)-L-homoserine, 1- <i>tert</i> -butyl ester (39)	105
<i>S</i> -acetyl-1- <i>O</i> -methyl-2,3- <i>O</i> -isopropylidene-5-thio-β-D-ribofuranoside (40)	106
<i>N</i> - <i>tert</i> -butoxycarbonyl- <i>S</i> -(5-deoxy-1- <i>O</i> -methyl-2,3- <i>O</i> -isopropylidene-L-lyxofuranos-5-yl)-L-homocysteine, methyl ester (41)	107
<i>tert</i> -butyl, 2- <i>tert</i> -butoxycarbonylamino-4-(2-nitrophenylselenyl)butanoate (42)	109
Bis(1- <i>O</i> -methyl-5-deoxy-2,3- <i>O</i> -isopropylidene-β-D-ribofuranos-5-yl)-5,5'-disulfide (43)	110



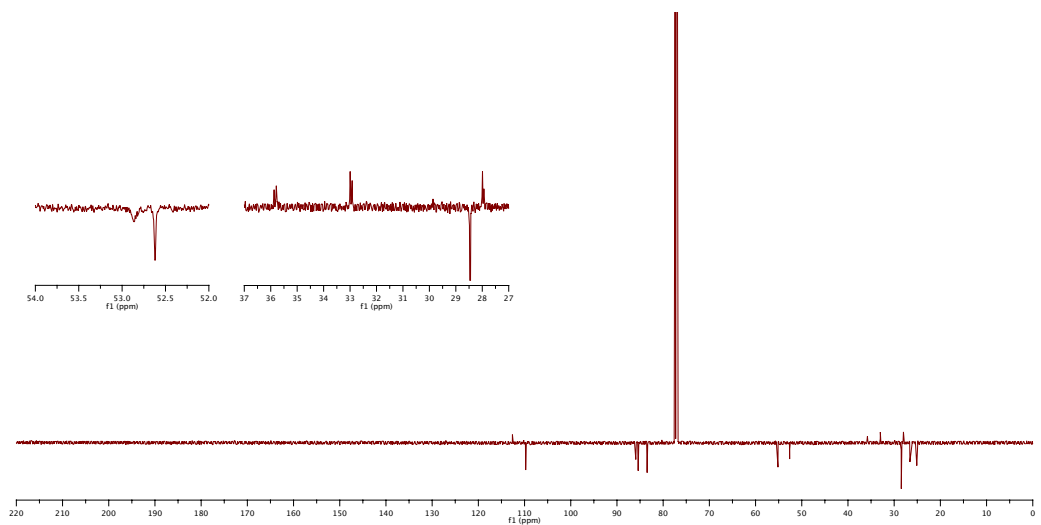
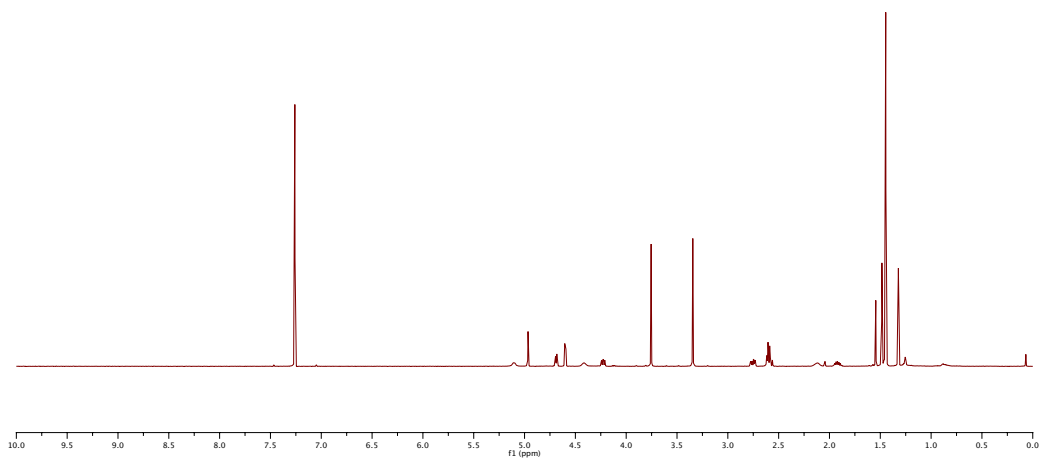
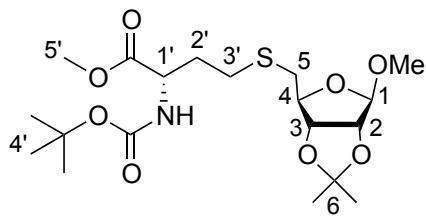
Compound (7)



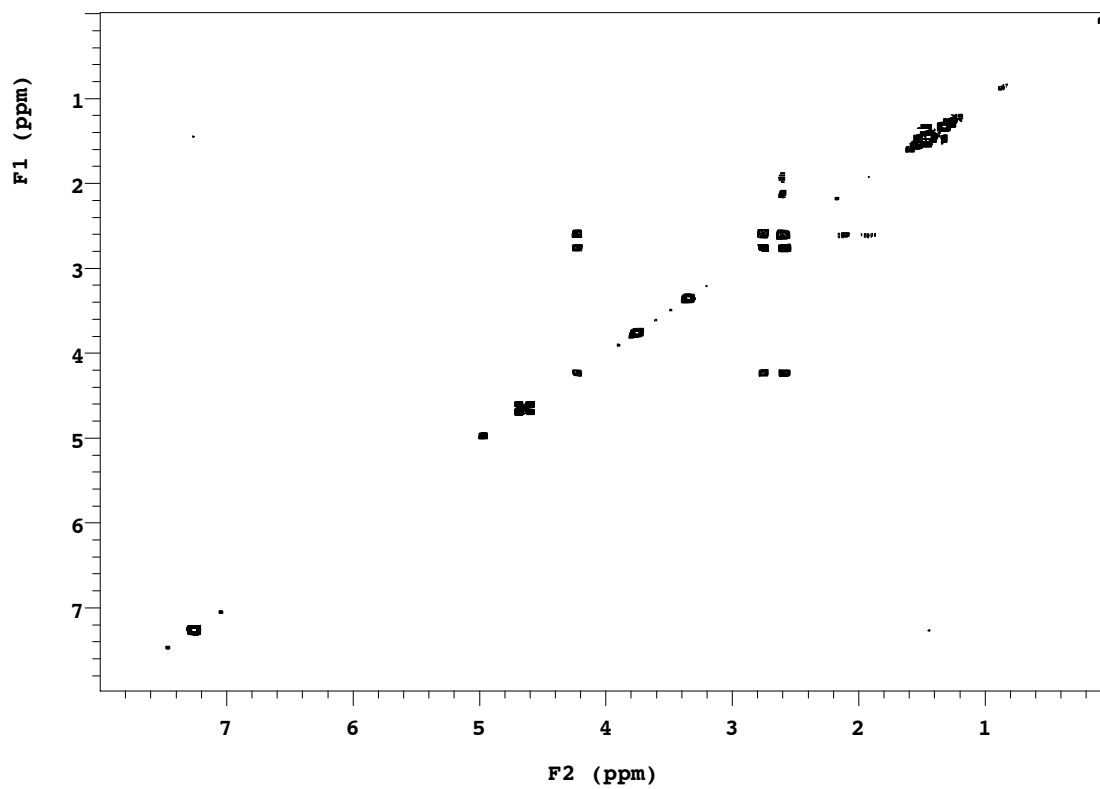
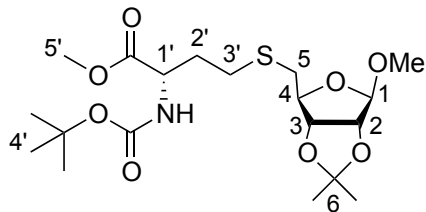
Compound (17)



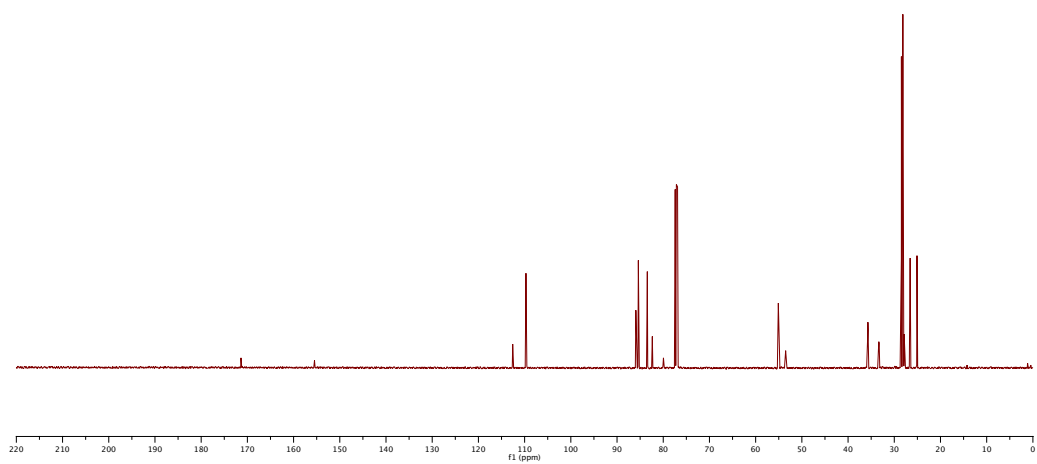
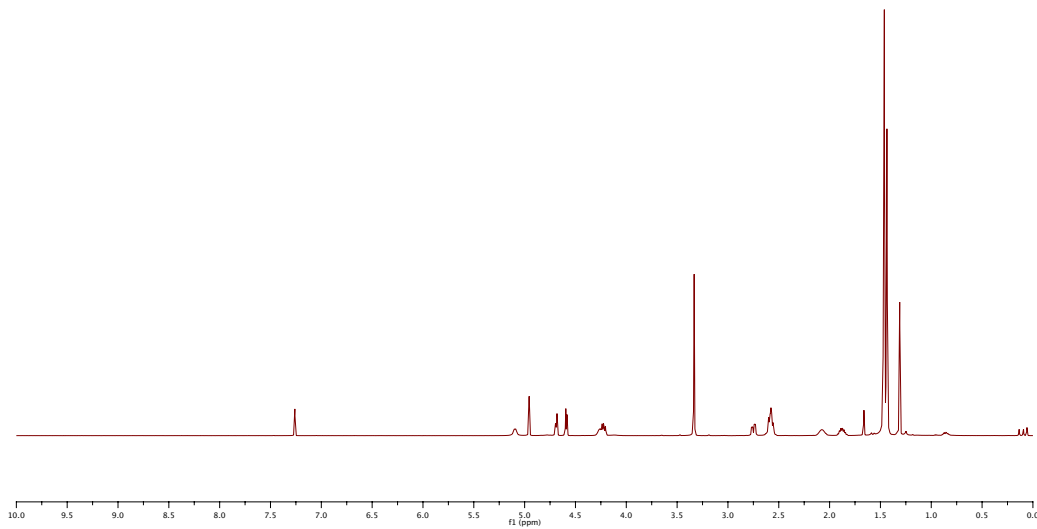
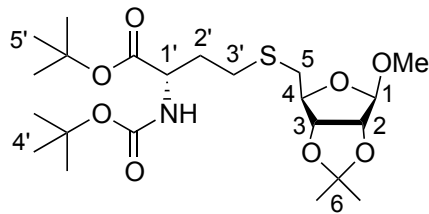
Compound (18)



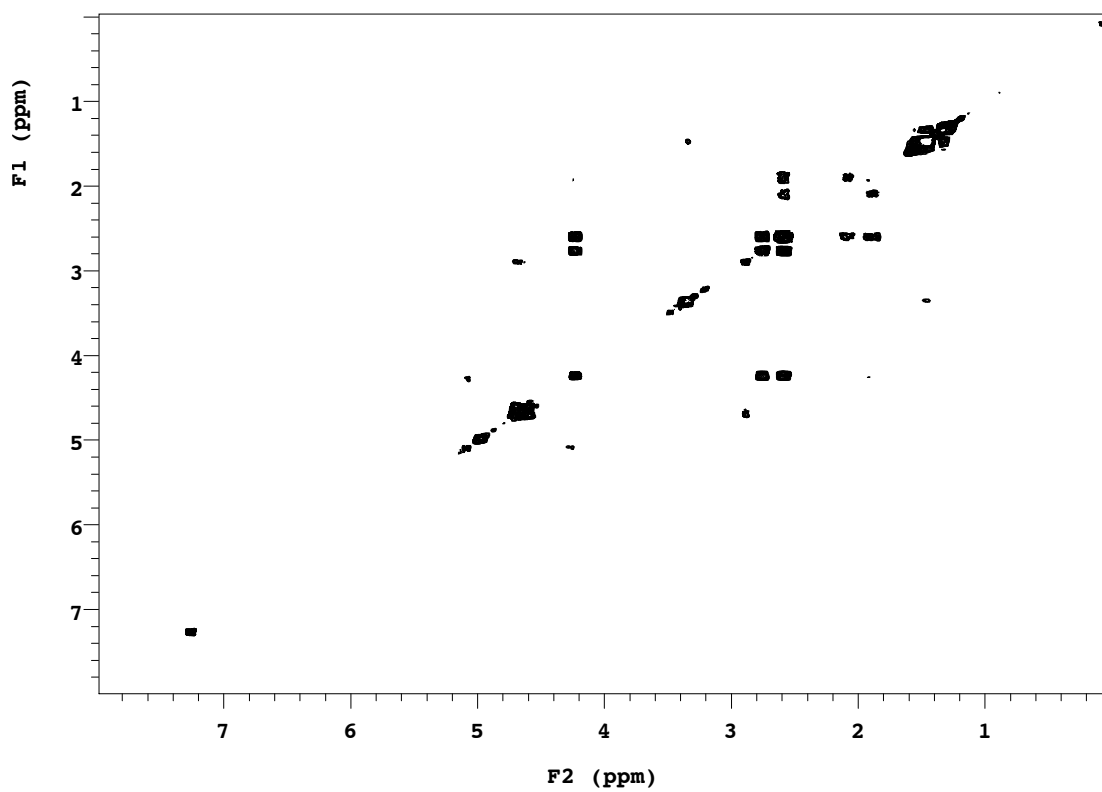
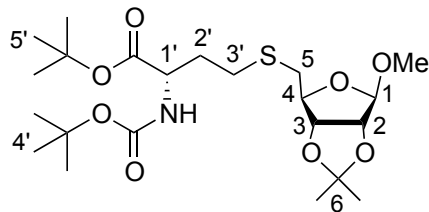
Compound (19a)



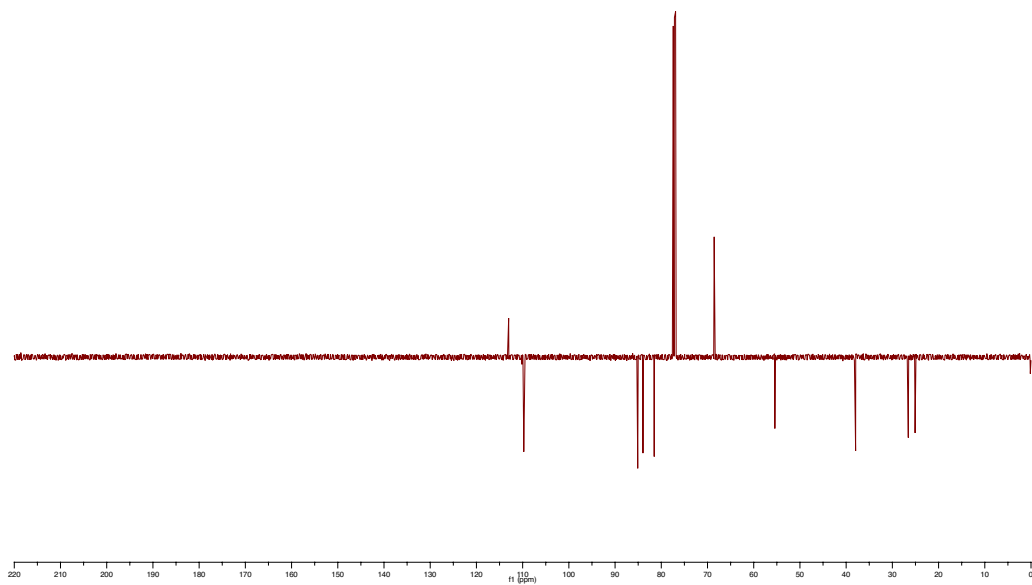
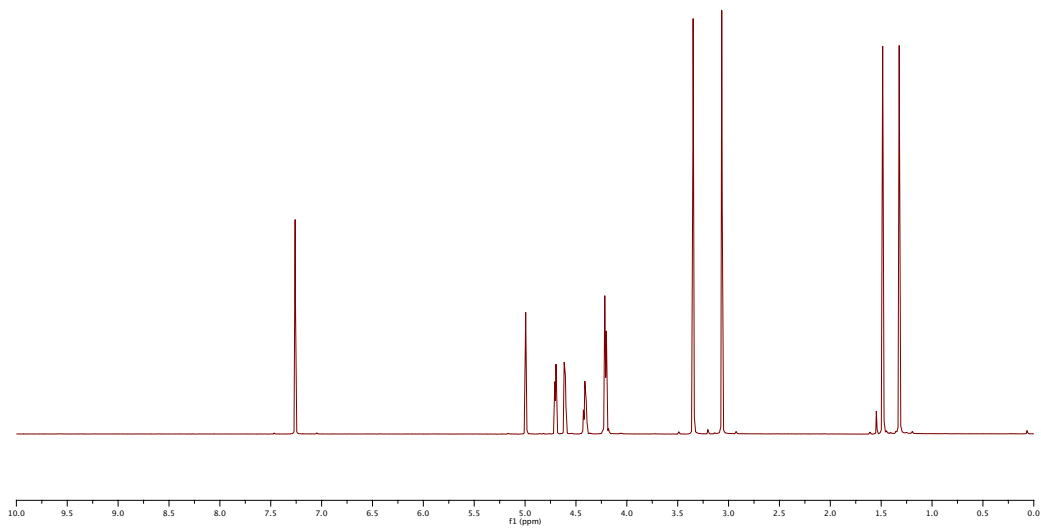
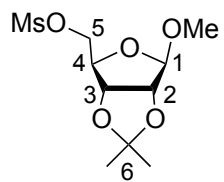
Compound (19a)



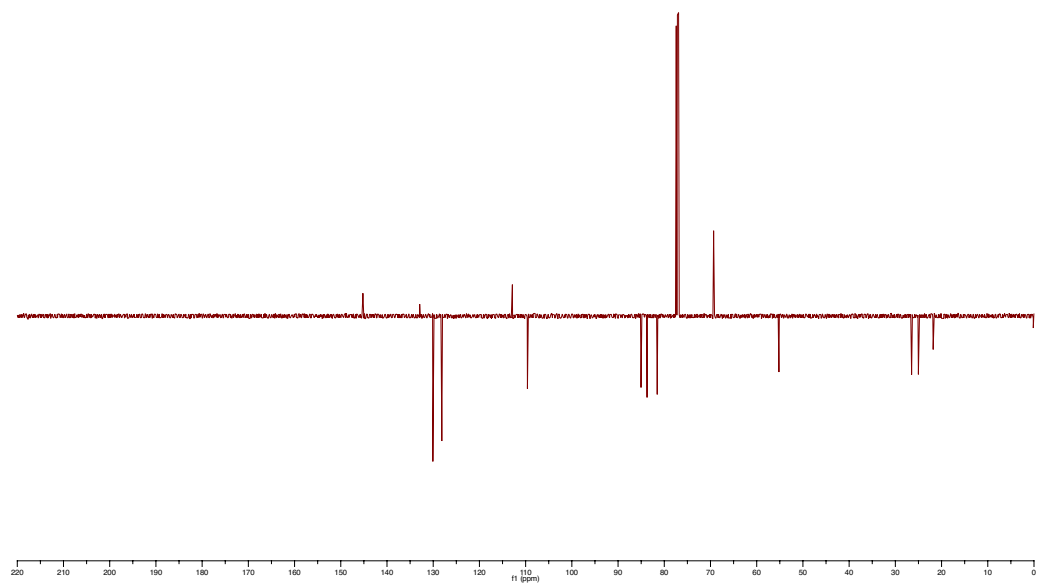
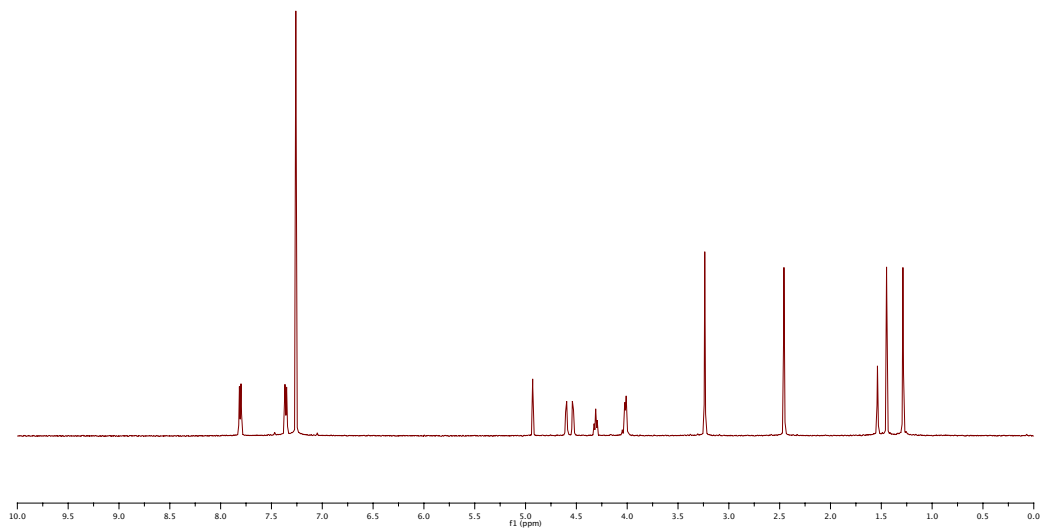
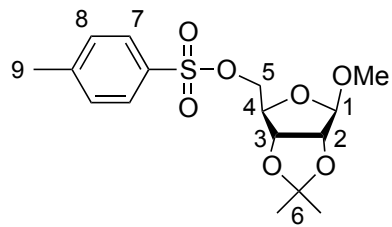
Compound (19b)



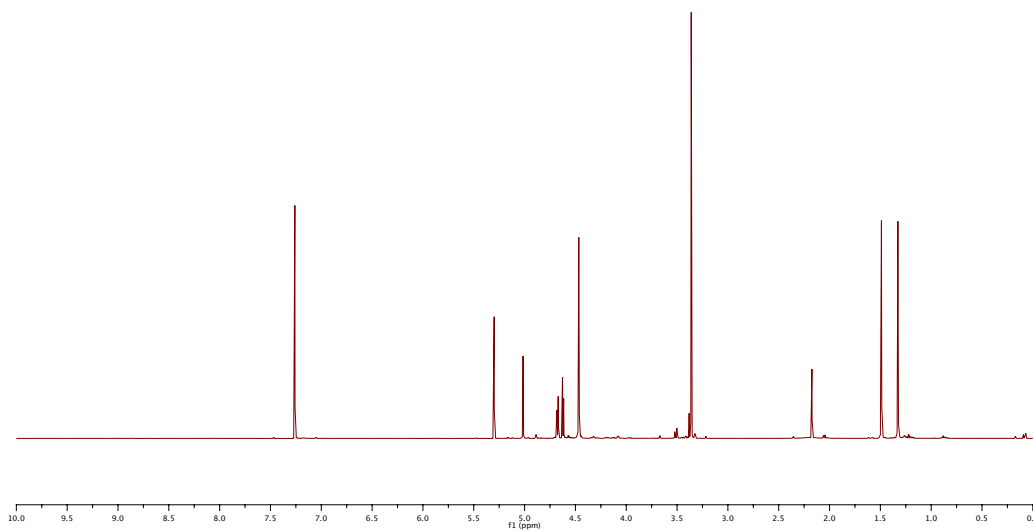
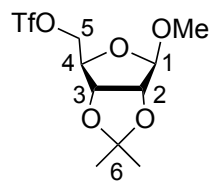
Compound (19b)



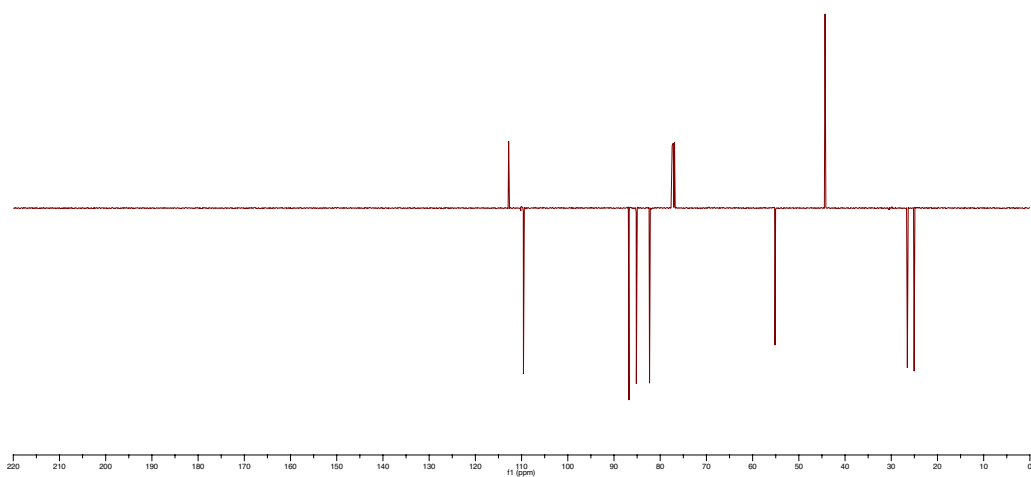
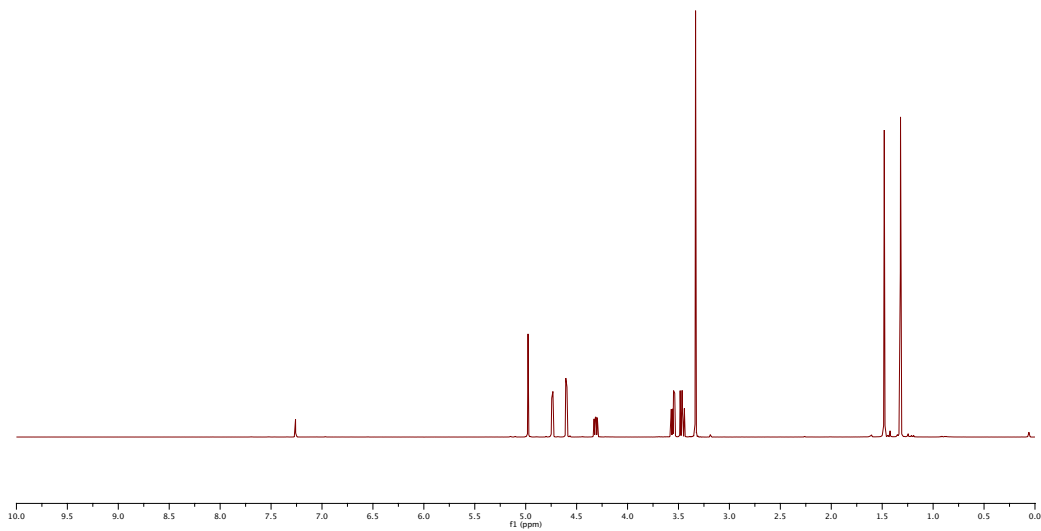
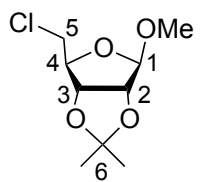
Compound (20a)



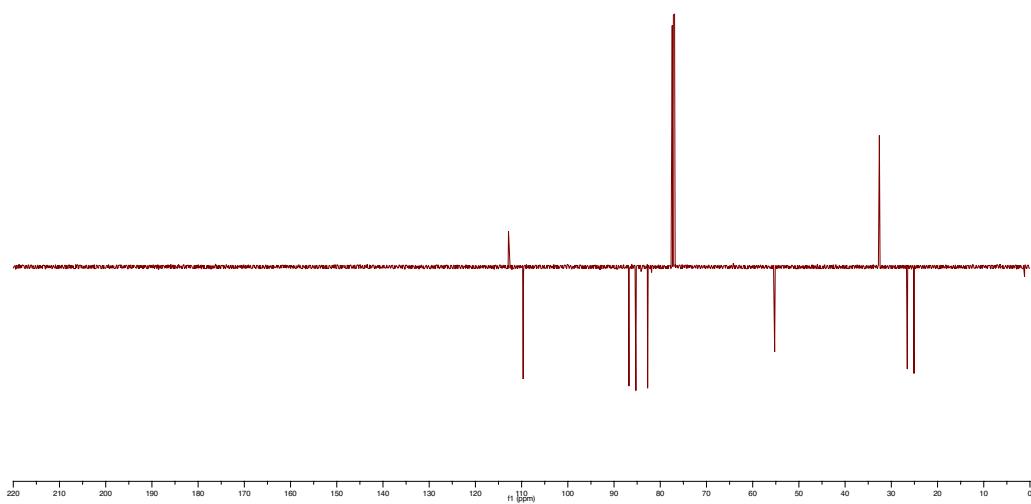
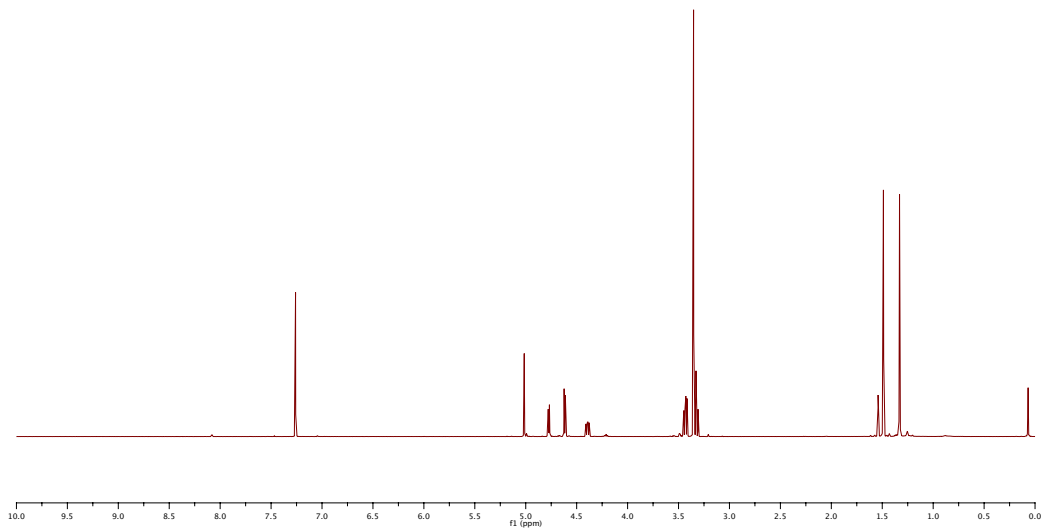
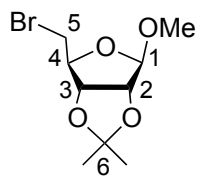
Compound (20b)



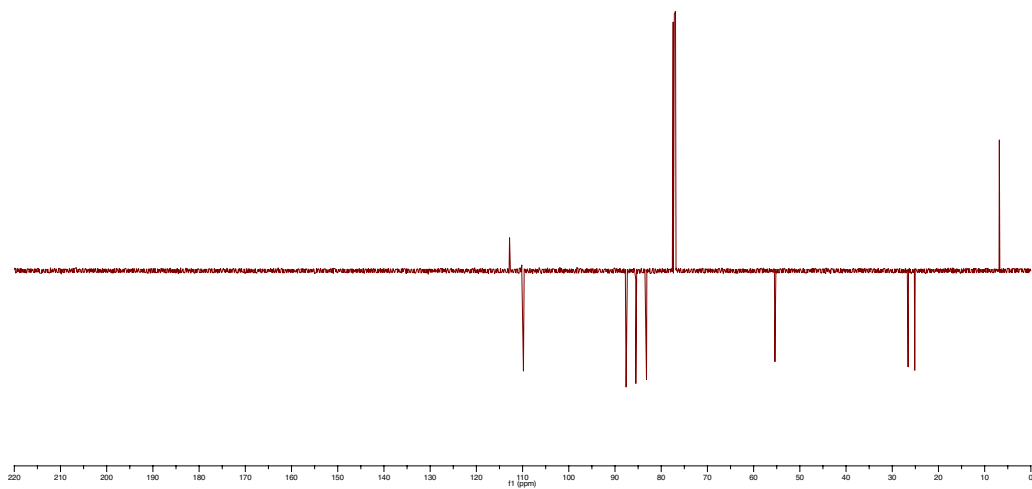
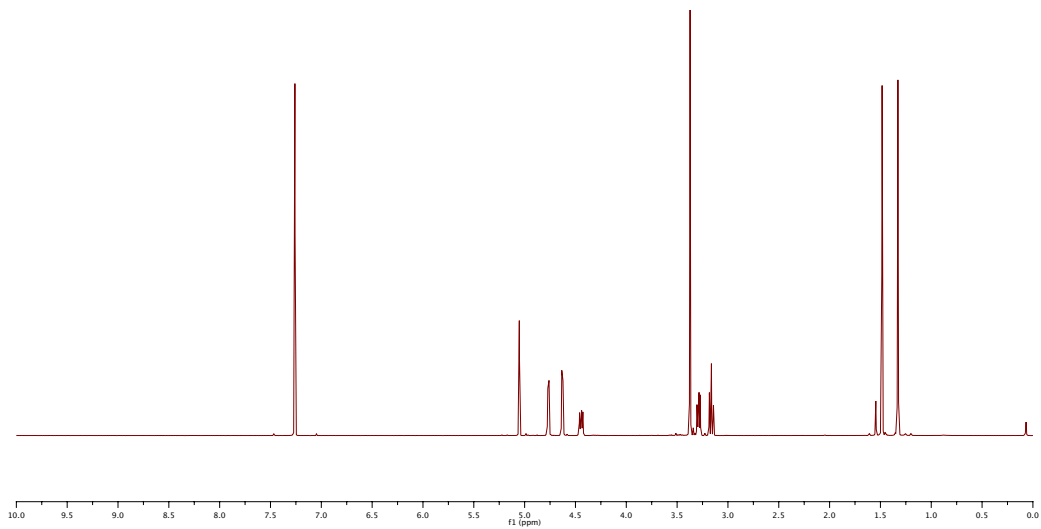
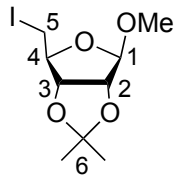
Compound (20c)



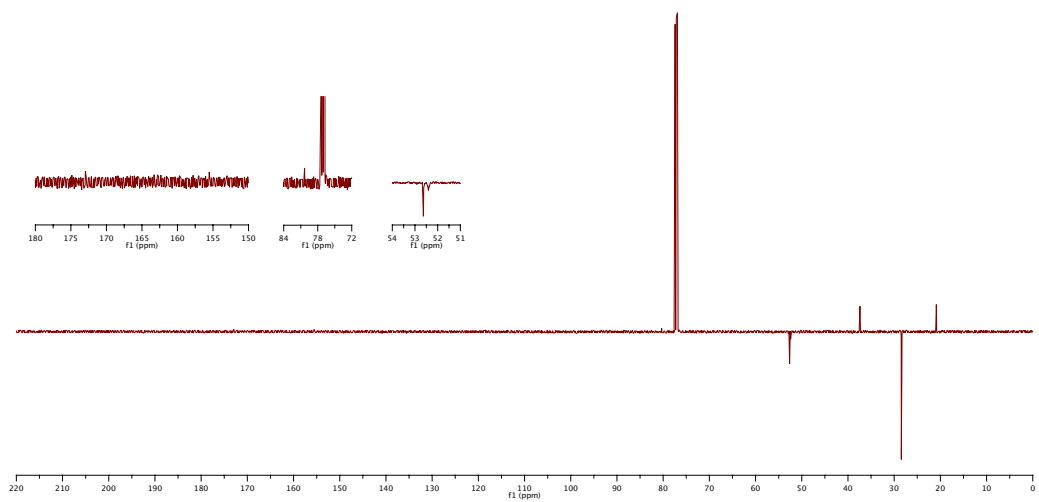
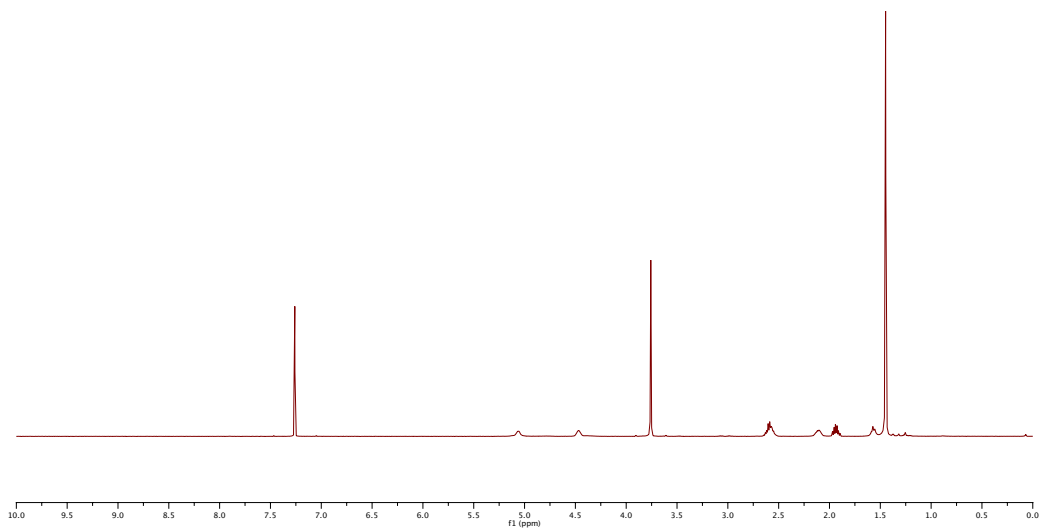
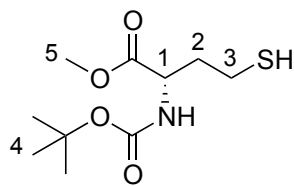
Compound (20d)



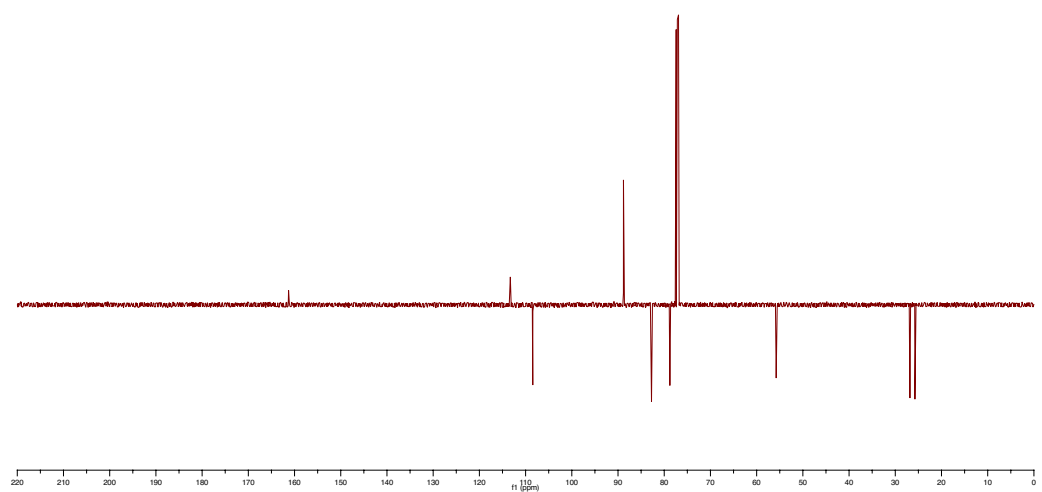
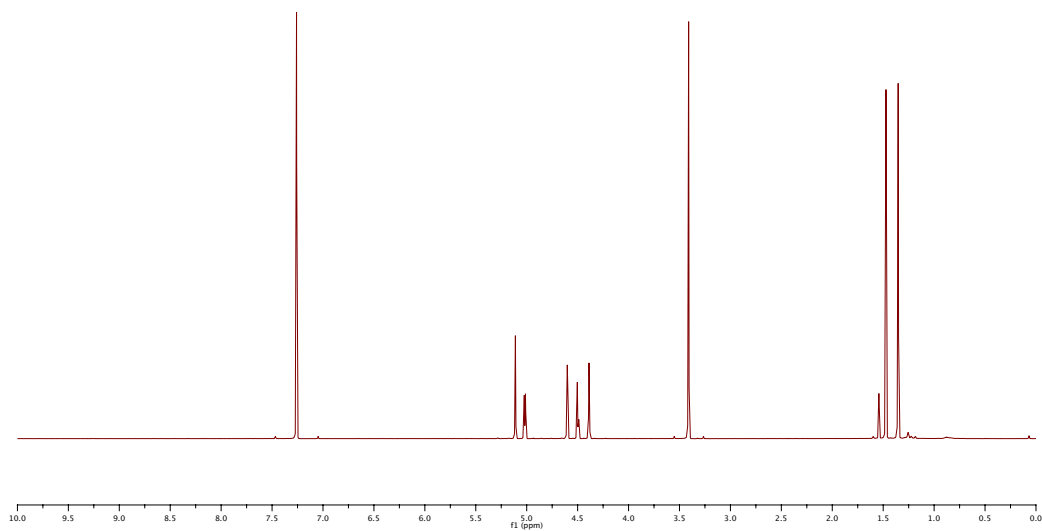
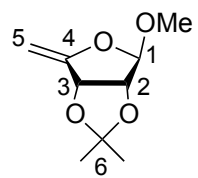
Compound (20e)



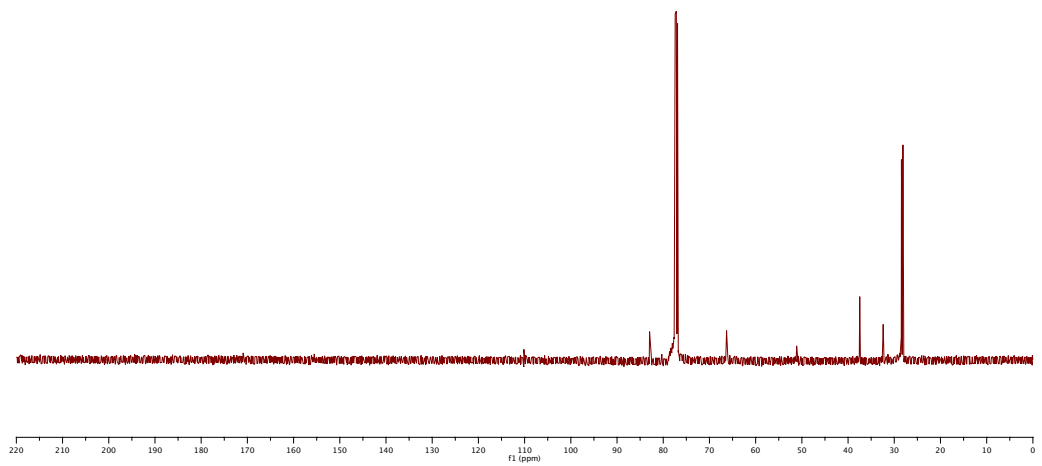
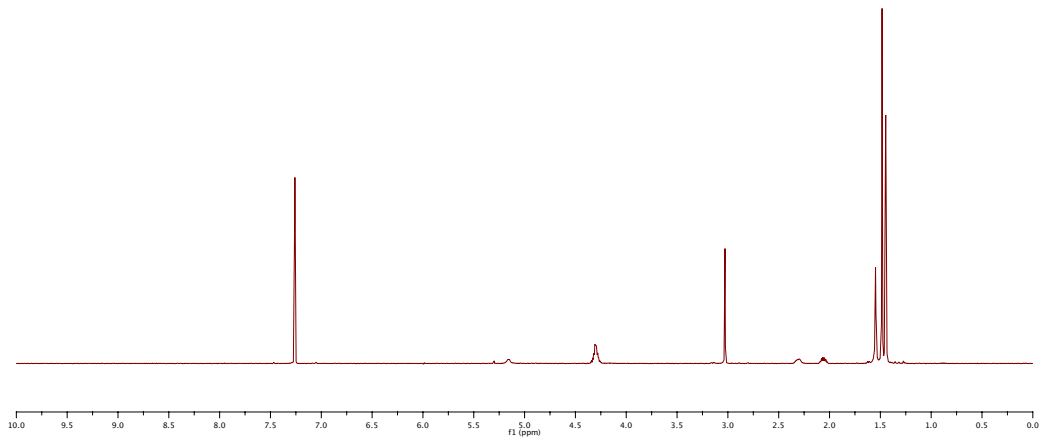
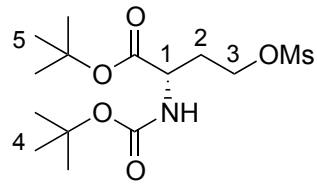
Compound (20f)



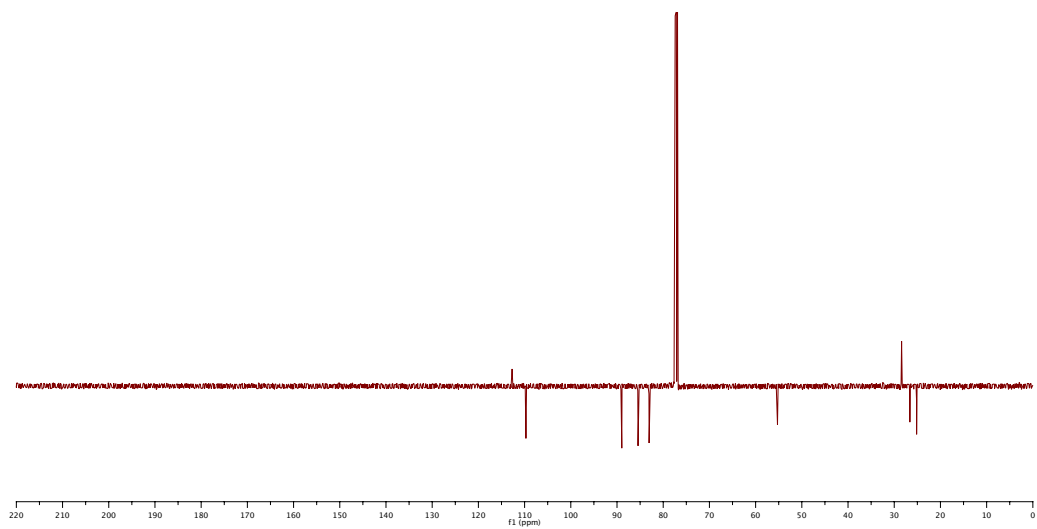
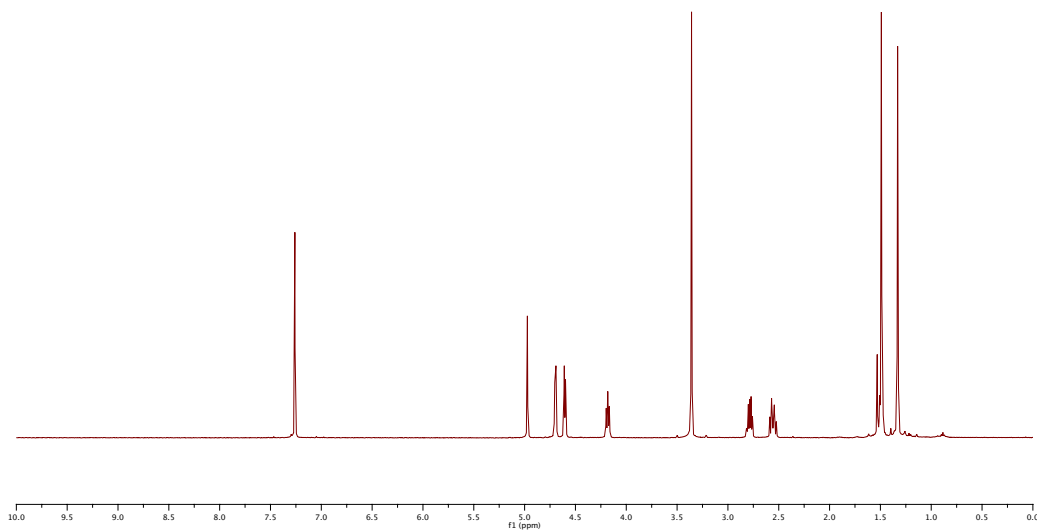
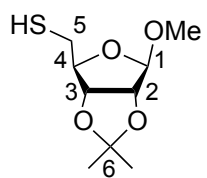
Compound (22)



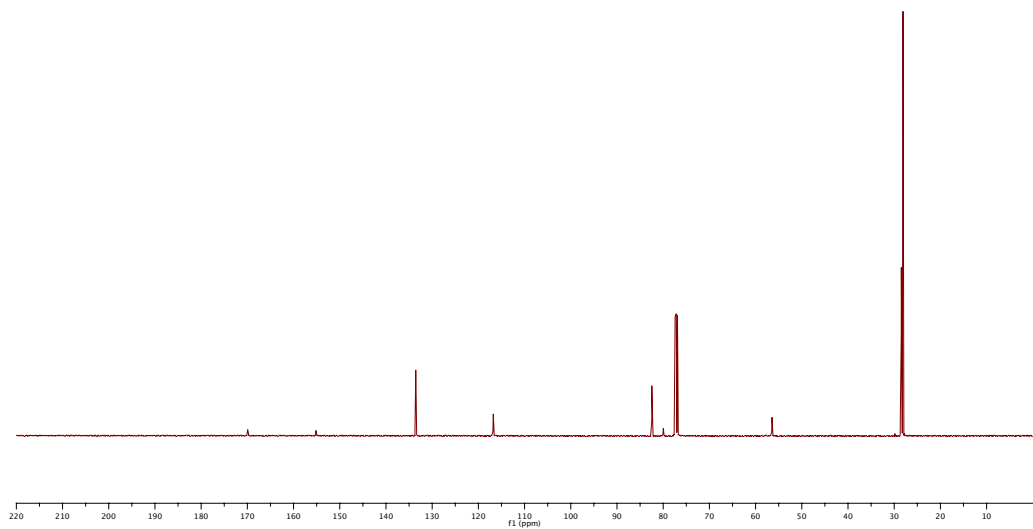
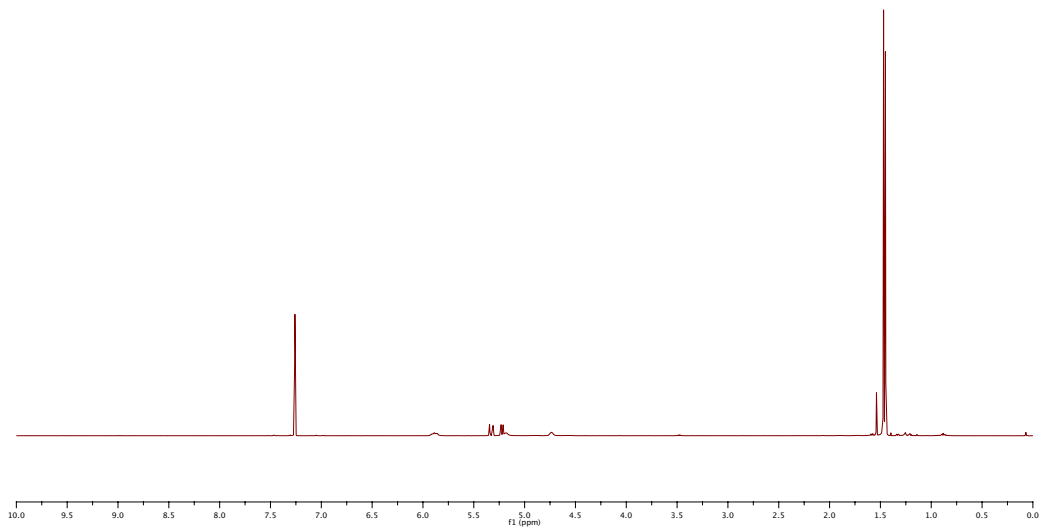
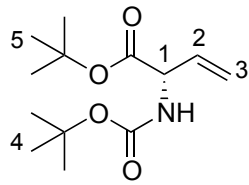
Compound (26)



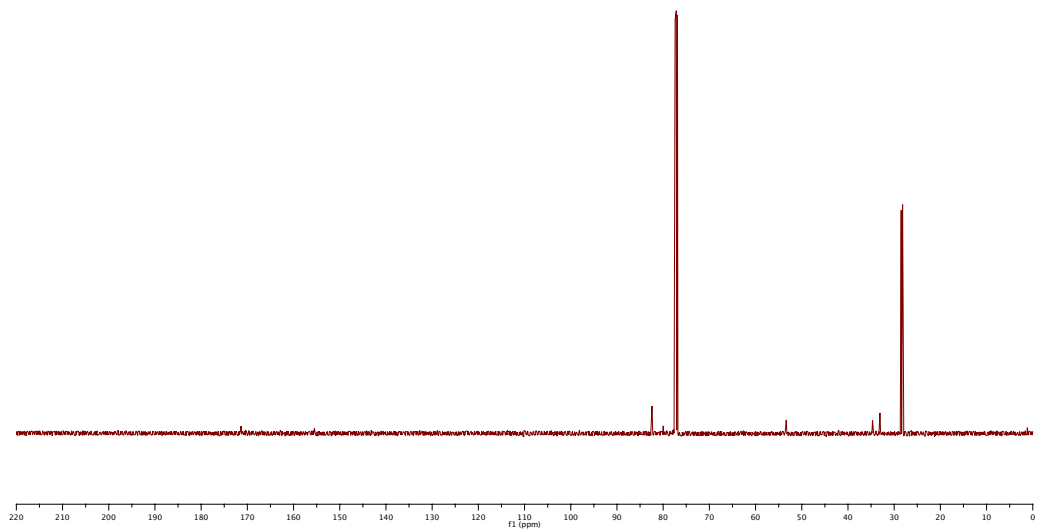
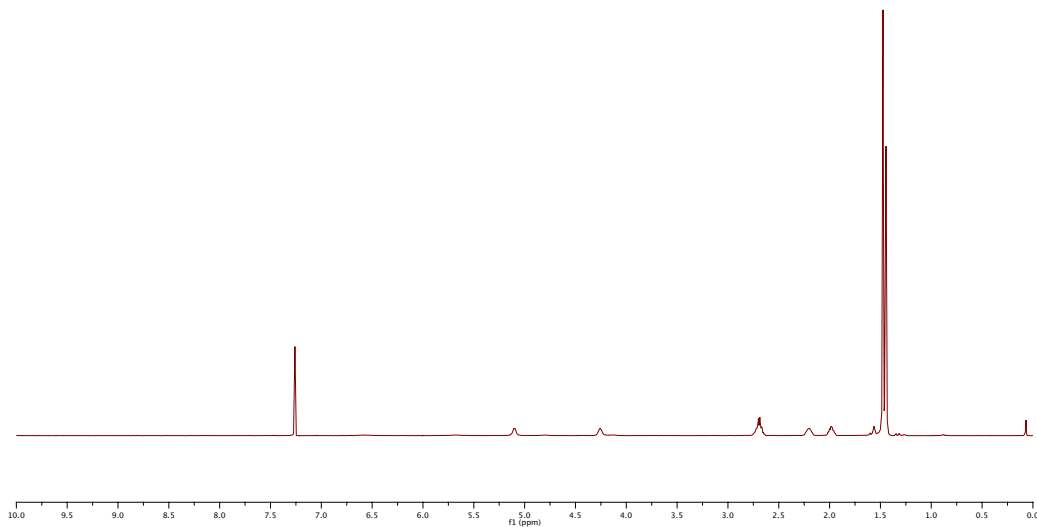
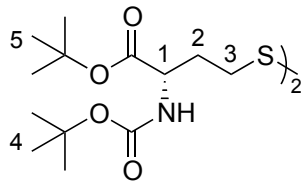
Compound (30)



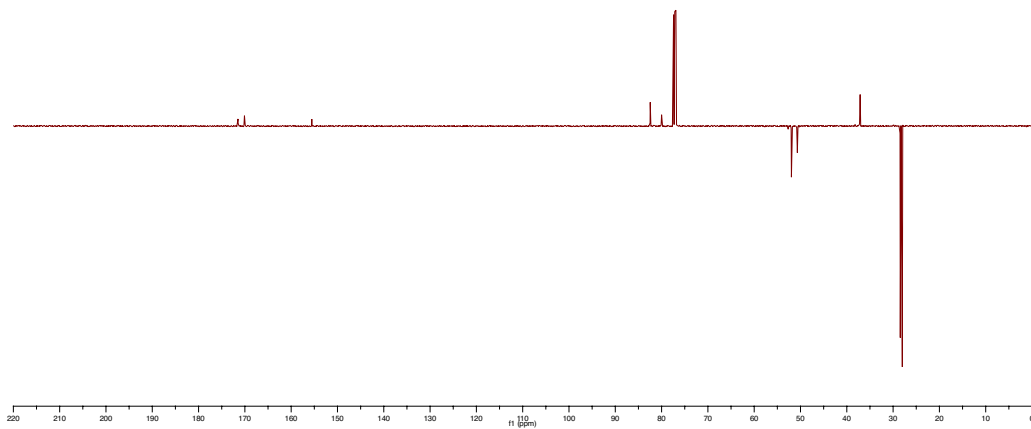
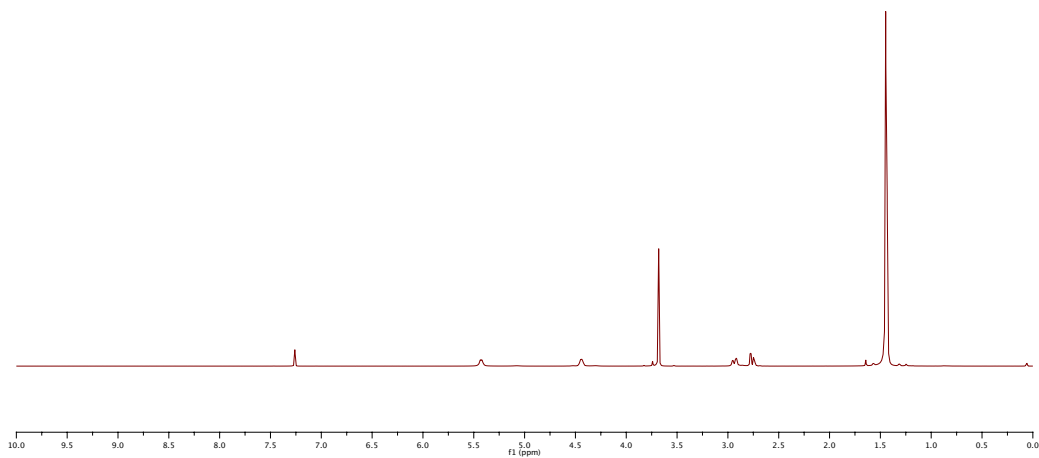
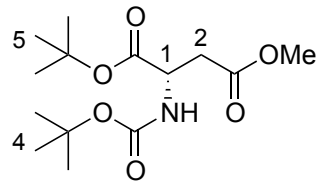
Compound (31)



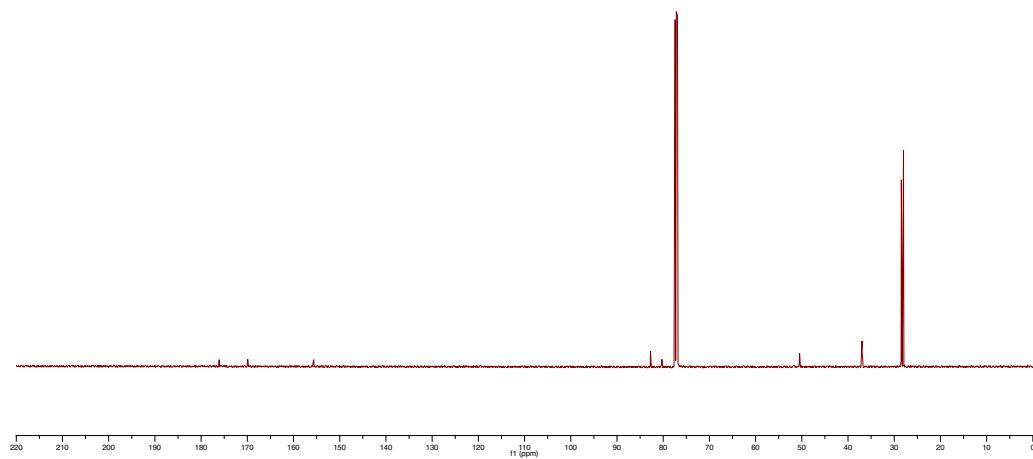
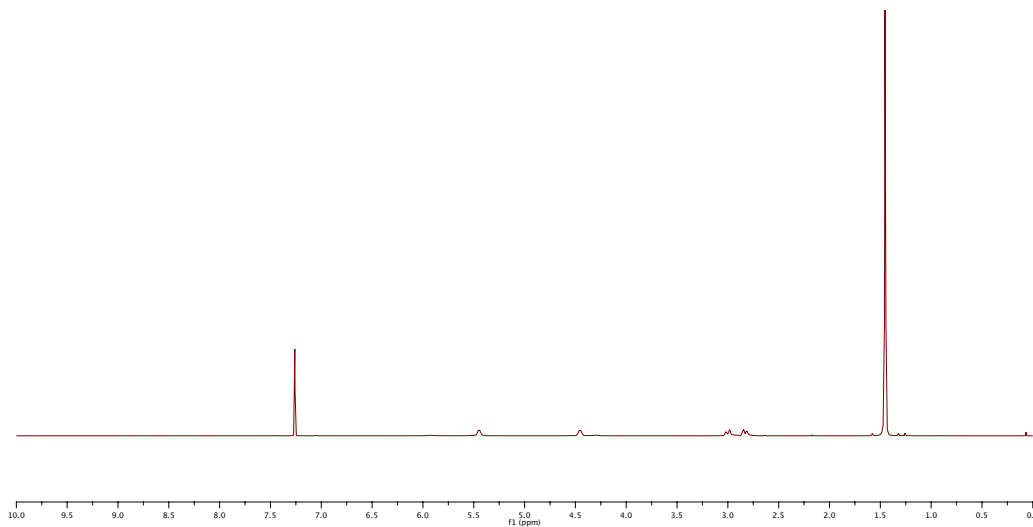
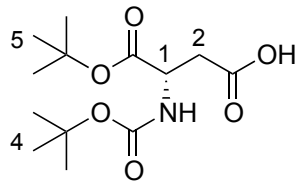
Compound (32)



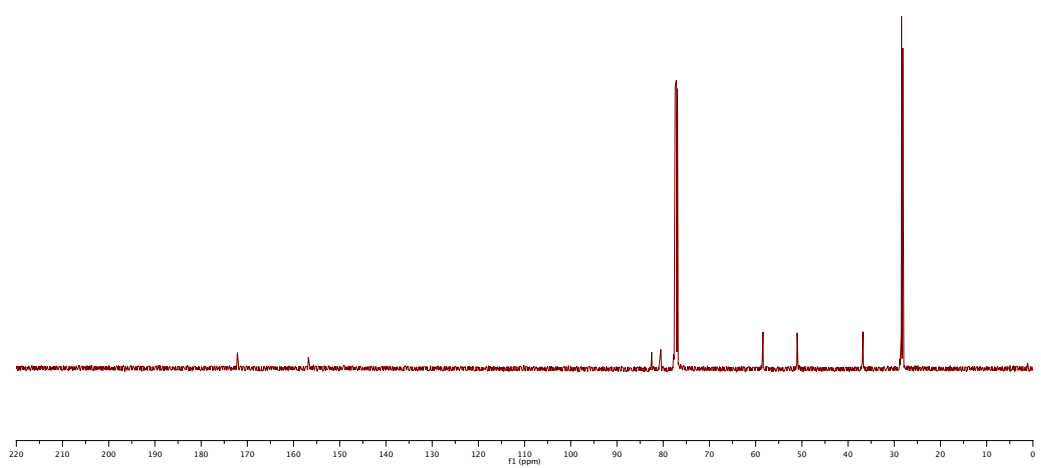
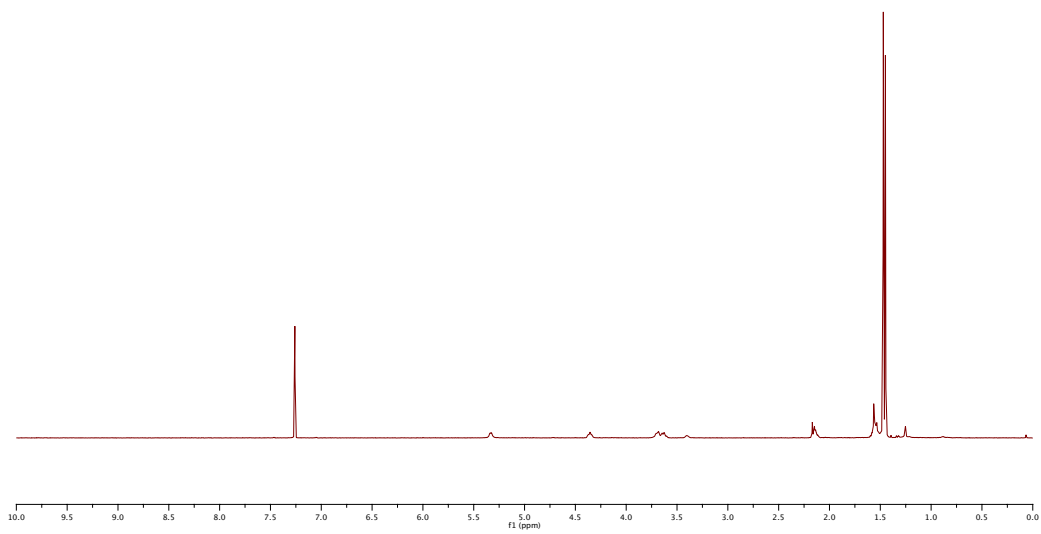
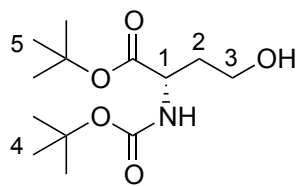
Compound (34)



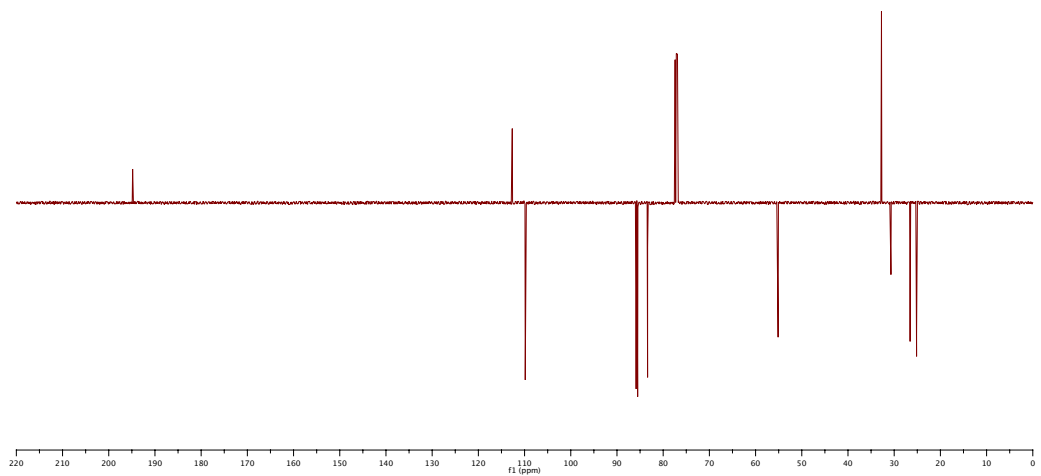
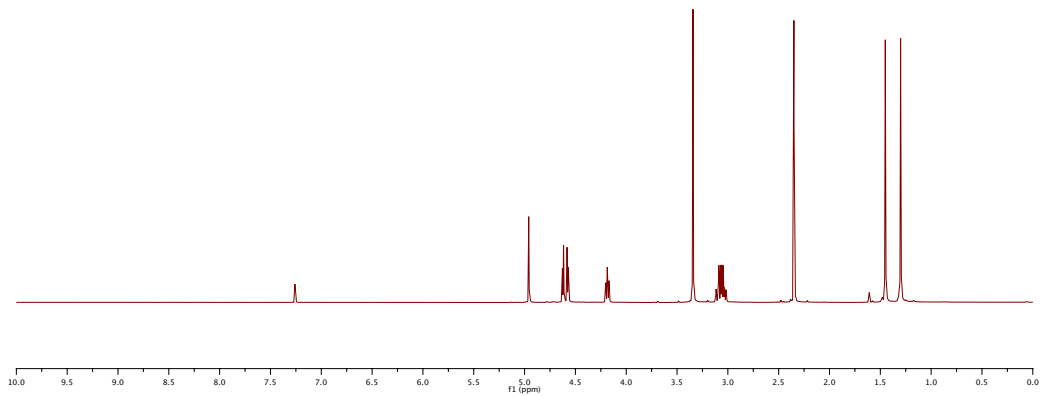
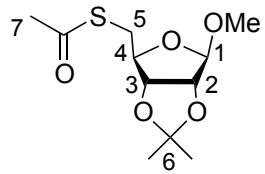
Compound (37)



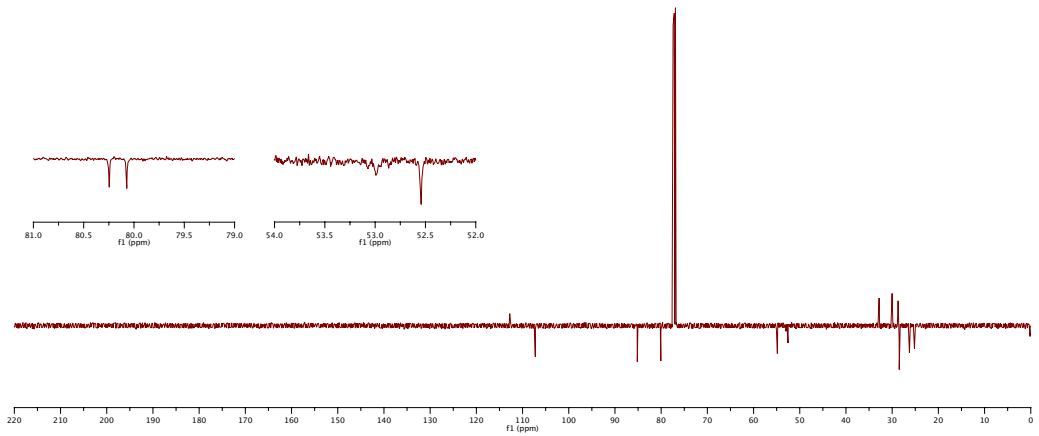
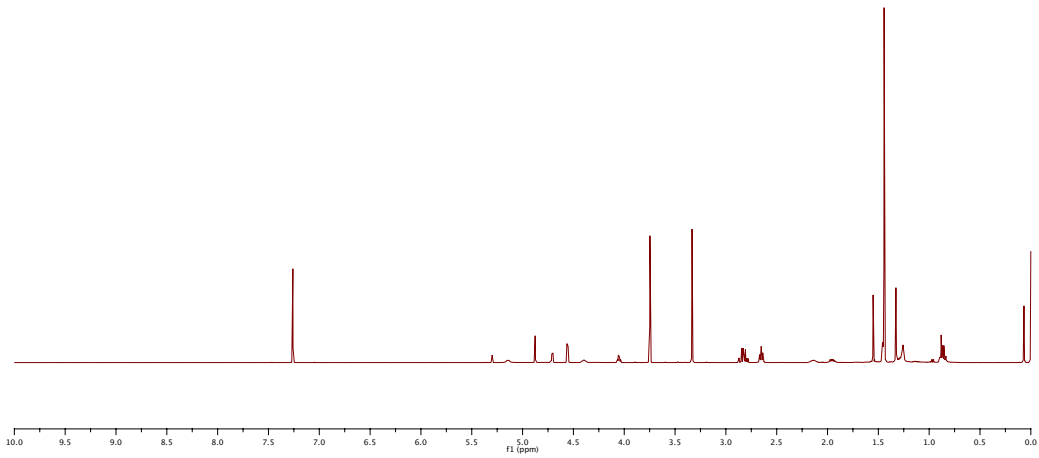
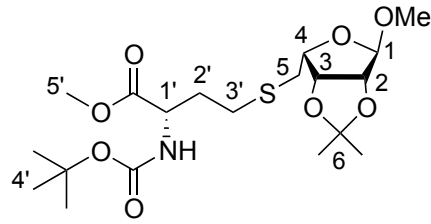
Compound (38)



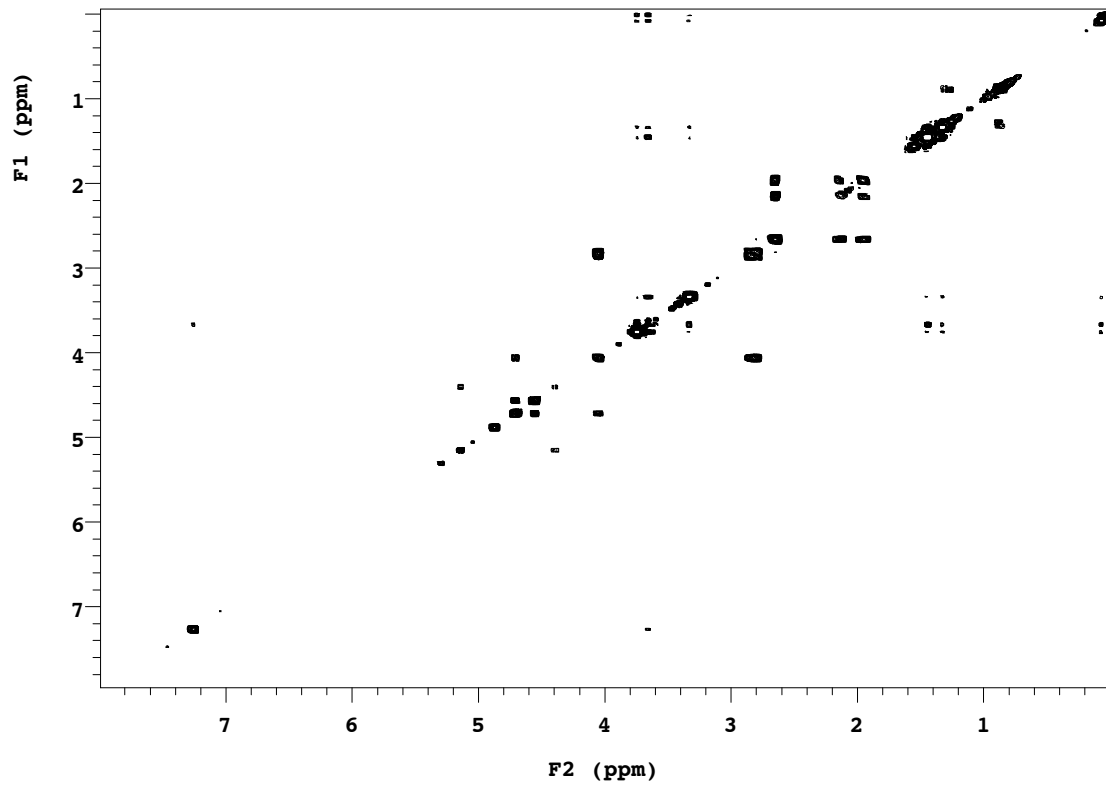
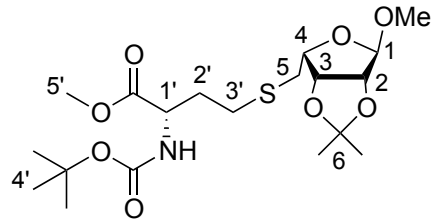
Compound (39)



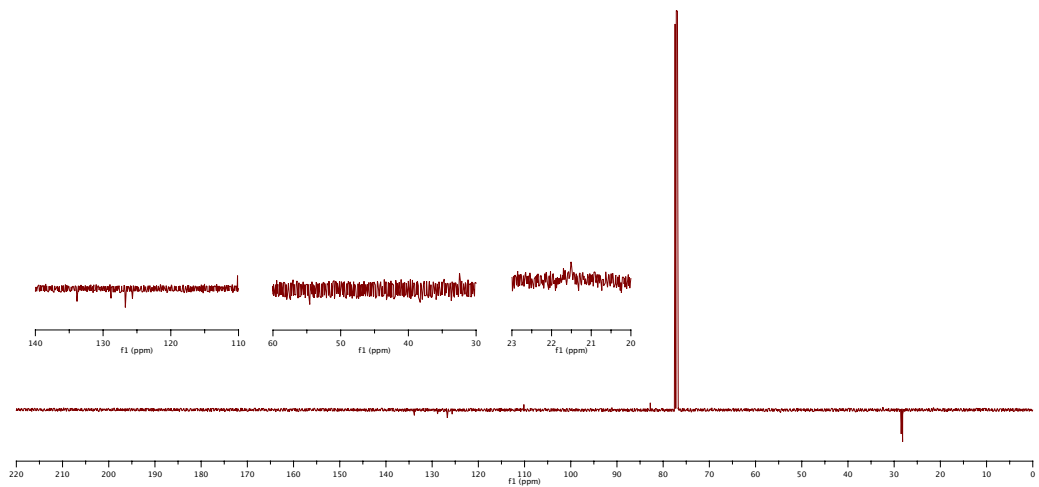
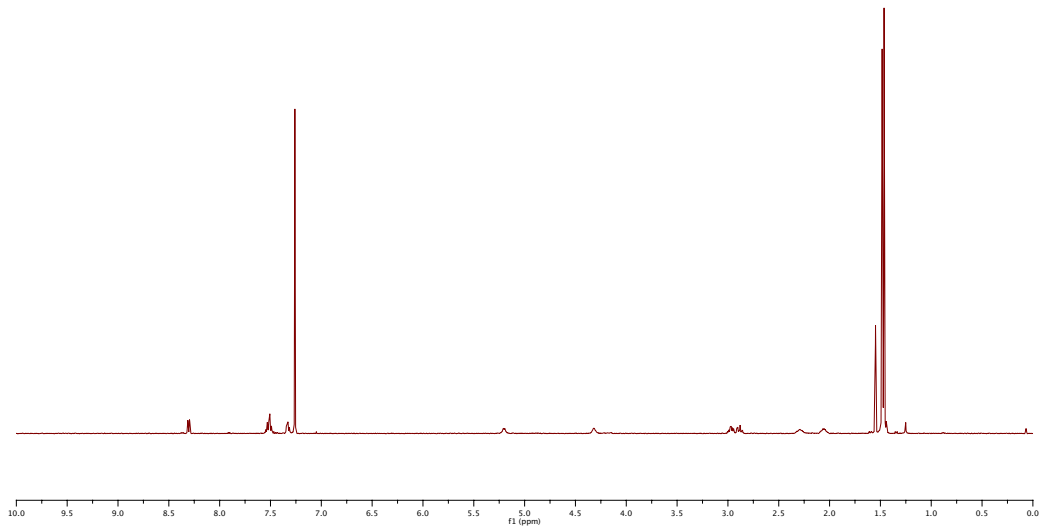
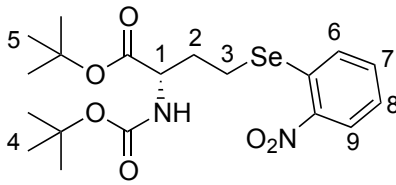
Compound (40)



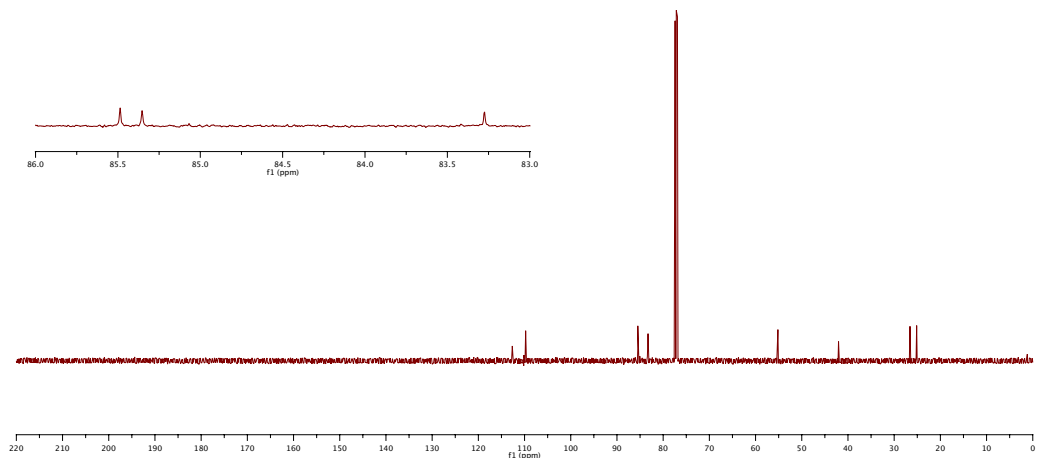
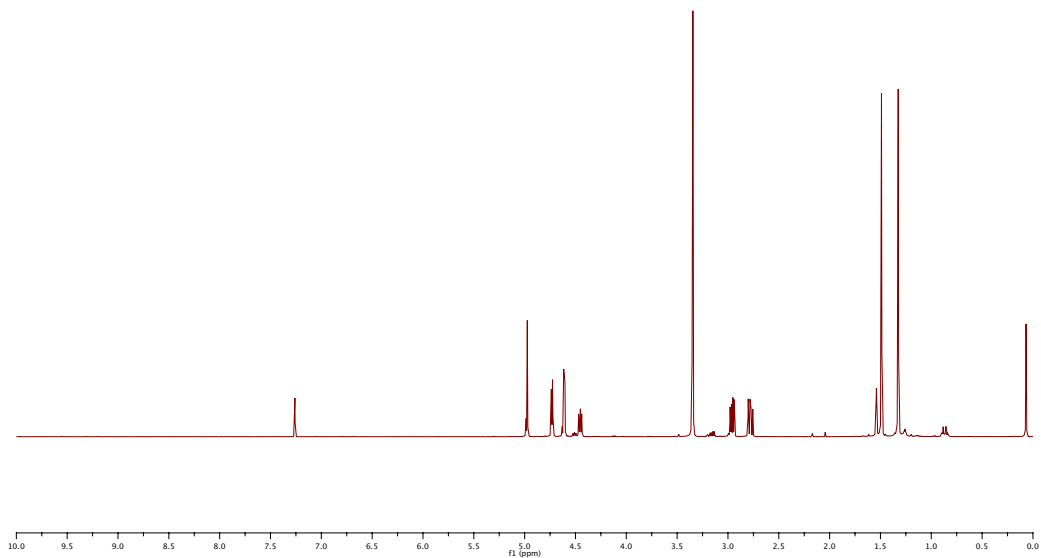
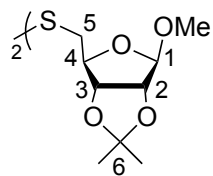
Compound (41)



Compound (41)



Compound (42)



Compound (43)